No. 306
February 1987

TIME-DOMAIN ANALYSIS OF WAVE EXCITING FORCES ON SHIPS AND BODIES

Bradley King

THE DEPARTMENT OF NAVAL ARCHITECTURE AND MARINE ENGINEERING

THE UNIVERSITY OF MICHIGAN
COLLEGE OF ENGINEERING

TIME-DOMAIN ANALYSIS OF WAVE EXCITING FORCES ON SHIPS AND BODIES

by
Bradley K. King

A dissertation submitted in partial fulfillment
of the requirements for the degree of
Doctor of Philosophy
(Naval Architecture and Marine Engineering)
in The University of Michigan
1987

Doctoral Committee:

Professor Robert F. Beck, Chairperson
Assistant Professor William W. Schultz
Associate Professor Armin W. Troesch
Professor William S. Vorus

There are three things that are too amazing for me,
four that I do not understand:
the way of an eagle in the sky,
the way of a snake on a rock,
the way of a ship on the high seas,
and the way of a man with a maiden.

Proverbs 30:18-19

To Ann

ACKNOWLEDGEMENTS

This dissertation is the result of research sponsored by the Office of Naval Research, Accelerated Research Initiative Contract No. N14-85-K-0118, along with a generous grant of computer time from the Cray Grant, University Research and Development Program at the San Diego Supercomputer Center.

In addition, I am grateful to my dissertation committee for their helpful suggestions. I would especially like to thank Professor Robert Beck, whose helpful criticism, interest, and personal involvement were largely responsible for the success of this endeavor.

Finally, I would like to thank my wife, who not only gave her moral support throughout, but is responsible for the typing and appearance of this dissertation.

TABLE OF CONTENTS

LIST OF FIGURES

Figure

LIST OF APPENDICES

Appendix

CHAPTER I

INTRODUCTION

The problem considered here is the determination of the forces and fluid motions due to waves coming in contact with a ship or a body that is either fixed or moving on an infinite sea. The approach employed is direct three-dimensional calculation of the fluid motion treated as an initial value problem in time. The work is referred to as taking place in the time domain to contrast it with more traditional frequency-domain calculations. Frequency-domain methods are very difficult when a body has a steady forward speed, and it is hoped that time-domain methods will prove advantageous in those problems.

The second half of this century has seen growing interest in and rapid development of the study of ship motions due to waves. The pioneering work of Haskind (1946) introduced the concept of dividing the problem into components that could be considered individually. This decomposition separated the fluid flow into three distinct components: the steady flow due to translation, the flow caused by the body's motions, and the flow due to the diffraction of the incident wave. Each component offered a simpler problem to address.

The earliest attempts at determining the force due to waves were restricted to simple hydrostatics. The approximation of the force due to waves as the buoyant force due to still water taking the shape of a wave is still used by some to determine the bending moments on a ship due to waves (Comstock 1967).

The first significant improvement is credited to both William Froude (1861) and Krylov, a Russian naval officer (Kriloff 1896). Their approximation of the force due to a wave is simply a surface integration of the pressure due to a sinusoidal wave that is assumed not to be diffracted. The pressure is given by the linearization of Bernoulli's equation. The force determined by this method is referred to as the Froude-Krylov force. In the range of wavelengths where the waves are much longer than the body dimensions, this approximation is accurate enough. The Froude-Krylov force represents the force due to the incident wave in the absence of the body, and it is corrected by the force due to the diffracted wave system. In general, the Froude-Krylov force is much the larger of the two.

Haskind first showed that the exciting force on a fixed body due to sinusoidal waves may be determined by the solution of the radiated wave problem, that is, the wave system

due to the sinusoidal oscillation of the body about its mean position. These results have been extended by Newman (1965) to the case of a moving ship. The relation between the radiated wave potential and the exciting force is referred to as the Haskind relation.

By using the Haskind relation, it is possible to determine the ship motions using only the solution to the radiation problems. Because of this fact, greater effort has been given to the solution of the forced oscillation radiation problem than the diffraction problem. The Haskind relation can only give forces on an entire body and cannot be used to determine sectional force. It also cannot be used for the determination of relative motion where the wave elevation for the diffracted wave is required. Thus, the solution of the diffraction problem has practical application as well as scientific interest.

Historically, as has been the case for the radiation problem, solutions have been pursued for regular sinusoidal waves. As is the case for solution of the radiated wave problem, solutions have been pursued that employ an asymptotic approximation. Newman (1964) showed that a long wave approximation gave the trivial result that the first-order solution was simply hydrostatics. Much work was done with a short wave approximation, with some success. See, for example, Faltinsen (1971), Maruo and Sasaki (1974), and Troesch (1976).

The most recent theory is the unified theory by Sclavounos (1984), which is valid for a broad range of wavelengths. Until now there has been no known, fully three-dimensional approach to the solution of the diffraction problem at forward speed. Inglis and Price (1981) and Chang (1977) developed three-dimensional solutions using an integral equation for the radiation problem. Their approach could have been employed for a three-dimensional diffraction solution, but no such results are known.

It should be noted that the fully three-dimensional theories referred to here are three dimensional in the sense that body boundary conditions are met on the body surface. Any of the theories thus far, including the one developed here, require simplifications and approximations that are only valid for ships or bodies whose shapes produce small disturbances. Any body that produces large waves must be considered in terms of many nonlinear effects, which greatly complicate any practical analysis.

The consideration of using time-domain methods was first discussed by Cummins (1962) and Ogilvie (1964). Most such solutions to radiation problems have been two-dimensional. They have been accomplished by several researchers, such as Adachi and Ohmatsu (1980), Yeung (1982), and Newman (1985). The most recent work is that of Liapis and Beck (1985), who performed fully three-dimensional calculations on ship shapes with steady forward speed.

The success of these attempts has led to the consideration of a direct solution to the diffraction problem by using time-domain methods. An important aspect of this solution is the determination of a suitable body boundary condition for an initial value problem. Traditional regular wave boundary conditions as employed in the frequency domain have the unacceptable property of being nonzero for all time with no suitable initial condition.

The choice of an appropriate incident wave boundary condition is developed in Chapter 3. The concept of considering ship waves as the input to a linear system directly in the time domain was first discussed by Davis and Zarnick (1964) and Breslin, Savitsky, and Tsakonos (1964). They were primarily interested in experimental ship motions determinations, but first introduced the concept of an impulsive wave, which is used here also.

The work here builds on that of Liapis and Beck, who succeeded in solving a three-dimensional solution to an integral equation similar to that of Ogilvie (1964). The approach employed generalizes the integral equation to one that is valid for an arbitrary body boundary condition. This allows the same integral equation to be solved for both radiation and diffraction problems. Liapis and Beck considered an impulsive displacement of the body. Here the option of solving the radiation problem for a nonimpulsive motion is considered in Chapter 4.

The work of Liapis and Beck confirmed that of Adachi and Ohmatsu (1979), which indicated that an integral equation solving for an unknown potential rather than an unknown source strength gave better results. As in the frequency domain, irregular frequencies were shown to exist. The approach used here follows their conclusions, and an integral formulation that has the fluid potential as its unknown function is the only approach considered.

Wehausen (1967) developed Haskind relations for the initial value problem, relating the impulsive radiation solution to the wave exciting forces. His results were for a fixed body only, and no analagous relationship for a steady translating body is known. The results from the Haskind relation may be compared with those from the direct computation of the diffraction potential. Both experimental and theoretical results from frequency-domain calculations can be compared by Fourier transformation. Results from all of these methods are compared in Chapter 6.

CHAPTER II

MATHEMATICAL PROBLEM FORMULATION

2.1 Boundary Value Problem

The problem under consideration is discussed with reference to the coordinate system shown in Figure 2.1. The solution is developed using a linear formulation. The domain consists of the fluid bounded by the free surface, which is linearized to the plane $z = 0$; the body surface; and an enclosing contour at infinity denoted by S_f, S_0, and S_∞, respectively. The surface normal is taken with the positive sense out of the fluid domain. The body is advancing with steady forward speed U_0 in the $+x$ direction.

The fluid is treated as incompressible, inviscid, and irrotational, implying the existence of a velocity potential. The body shape is considered as arbitrary. It must be assumed, however, that the body shape is such that a small disturbance results. The velocities produced by the body's presence in the fluid may be separated into three distinctive parts written as:

$$\underline{V}_T(x, y, z, t) = \nabla \Phi_T(x, y, z, t)$$

where

$$\Phi_T(x, y, z, t) = -U_0 x + \Phi_0(x, y, z) + \phi_0(x, y, z, t) + \Phi(x, y, z, t)$$

and

$-U_0 x + \Phi_0$ represents the potential due to steady translation

ϕ_0 represents the incident wave

$$\Phi(x, y, z, t) = \sum_{k=1}^{7} \phi_k(x, y, z, t) \tag{2.1}$$

$k = 7$ is the diffracted wave

$k = 1, 2, \ldots, 6$ are the potentials due to the body motions

surge, sway, heave, roll, pitch, and yaw, respectively.

This decomposition of the potential into separate components greatly simplifies the analysis that follows. The decomposition was first performed by Haskind (1946) and is

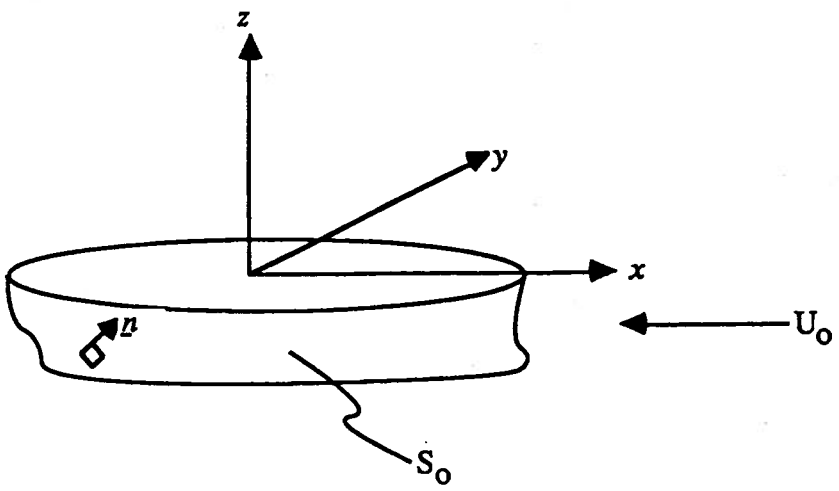

Figure 2.1 — Reference Coordinate System

consistent with the linearization of the governing equations. Physically, the decomposition ignores the interaction of the waves produced by the individual components.

The potential must meet the following conditions:

$$\nabla^2 \Phi_T = 0,$$

$$\frac{\partial \Phi_T}{\partial n} = 0 \text{ on } S_0,$$

and the linearized free surface boundary condition for the unsteady potentials is

$$\left(\frac{\partial}{\partial t} - U_0 \frac{\partial}{\partial x}\right)^2 \phi_k + g \frac{\partial}{\partial z} \phi_k = 0 \text{ on } z = 0,$$

with g being the acceleration of gravity.

The inflow velocity was approximated as U_0 in the linearization of Bernoulli's equation. This assumption eliminates the interaction between the various potentials except an interaction of the steady flow with the body boundary condition mentioned later. In addition, Newman (1964) has shown that the appropriate free surface boundary condition for ϕ_7, the diffracted wave, is an inhomogeneous form of the boundary condition given. The additional term, which is due to the interaction of the incident wave and the steady flow, has been neglected in this development, as it was by Newman (1965) when he developed the Haskind relations for steady forward speed.

The unsteady potentials will be considered as initial value problems with the conditions that

$$\phi_k(x, y, z, t) \to 0 \quad t \to -\infty \qquad k = 1, 2, \ldots, 7$$

and

$$\nabla\phi_k(x,y,z,t) \to 0 \quad \text{on } S_\infty \qquad k = 1,2,\ldots,7.$$

The body boundary conditions for the various potentials on S_0 are

$$\begin{aligned} \frac{\partial \Phi_0}{\partial n} &= U_0 n_1 \\ \frac{\partial \phi_7}{\partial n} &= -\frac{\partial \phi_0}{\partial n} \\ \frac{\partial \phi_k}{\partial n} &= n_k \dot{\varsigma}_k + m_k \varsigma_k \qquad k = 1,2,\ldots,6 \end{aligned} \tag{2.2}$$

where n_k represents the generalized unit normal defined as

$$(n_1, n_2, n_3) = \underline{n}$$

$$(n_4, n_5, n_6) = \underline{r} \times \underline{n}$$

$$\underline{r} = (x, y, z)$$

$$(m_1, m_2, m_3) = -(\underline{n} \cdot \nabla)\underline{W}$$

$$(m_4, m_5, m_6) = -(\underline{n} \cdot \nabla)(\underline{r} \times \underline{W})$$

$$\underline{W} = \nabla(-U_0 x + \Phi_0).$$

ς_k represents the displacement in the kth mode of motion, and the overdot represents the derivative with respect to time. The m_j terms represent the only interaction with the steady flow.

The conditions on the radiated wave potentials ($k = 1,2,\ldots,6$) as given result from the linearization of the complete normal body boundary condition on the instantaneous body surface to the mean underwater body surface S_0. The development for this form was first discussed in Timman and Newman (1962) and described fully in Newman (1977). This linear approximation is an important consideration, because meeting the correct body boundary condition on the instantaneous body surface would be extremely difficult.

2.2 Formulation of an Integral Equation

Liapis (1986) has shown that an integral equation may be derived for an unsteady potential with the initial conditions that $\phi=0 \quad t < 0$ and $\partial\phi/\partial t=0 \quad t < 0$. The development here is analagous.

Applying Green's theorem to the fluid domain,

$$\iiint_V dV\left(\phi\nabla^2 G - G\nabla^2\phi\right) = \iint_S dS\left(\phi\frac{\partial G}{\partial n} - G\frac{\partial \phi}{\partial n}\right). \tag{2.3}$$

The volume V is bounded by S where $S = S_0 \cup S_f \cup S_\infty$ and

$$G(P,Q,t-\tau) = \left(\frac{1}{r} - \frac{1}{r'}\right)\delta(t-\tau) + H(t-\tau)\tilde{G}(P,Q,t-\tau)$$

$$\tilde{G}(P,Q,t-\tau) = \int_0^\infty dk\sqrt{kg}\sin\left(\sqrt{kg}(t-\tau)\right)e^{k(z+\zeta)}J_0(kR)$$

$$P = (x,y,z)$$

$$Q = (\xi,\eta,\zeta)$$

$$r = \left((x-\xi)^2 + (y-\eta)^2 + (z-\zeta)^2\right)^{1/2}$$

$$r' = \left((x-\xi)^2 + (y-\eta)^2 + (z+\zeta)^2\right)^{1/2} \qquad (2.4)$$

$$R = \left((x-\xi+U_0(t-\tau))^2 + (y-\eta)^2\right)^{1/2}$$

$$\delta(t) = \text{delta function where } \int_{-\infty}^{\infty}\delta(t)f(t)\,dt = f(0)$$

$$H(t) = \text{unit step function}$$

$$= 0 \quad t < 0$$

$$= 1 \quad t \geq 0$$

with the properties that

$$\nabla^2 G = -4\pi\delta(P-Q)\delta(t-\tau)$$

$$\left(\frac{\partial}{\partial t} - U_0\frac{\partial}{\partial x}\right)^2 G + g\frac{\partial}{\partial z}G = 0 \qquad \text{on } z = 0$$

$$G, \frac{\partial G}{\partial t} = 0 \qquad t-\tau < 0$$

$$\nabla G \to 0 \qquad r \to \infty.$$

The Green's function G represents the potential at point P and time t due to an impulsive disturbance at point Q and time τ. The integral form was derived by Wehausen and Laitone (1960), and the form as given was employed by Liapis.

Integrating (2.3) with respect to τ from $-\infty$ to ∞ and employing the properties of G yields

$$\phi(P,t) = -\frac{1}{4\pi}\int_{-\infty}^{t} d\tau \iint_S dS\left[\phi(Q,\tau)\frac{\partial}{\partial n}G(P,Q,t-\tau) - G(P,Q,t-\tau)\frac{\partial}{\partial n}\phi(Q,\tau)\right].$$

The contribution to the integral on S_∞ is zero since $\nabla\phi$ and ∇G go to zero at infinity.

The contribution from S_f may be reduced to a line integral about the waterline of the body. From (2.1),

$$\frac{\partial}{\partial n} = \frac{\partial}{\partial \zeta} = -\frac{1}{g}\left(\frac{\partial}{\partial \tau} - U_0\frac{\partial}{\partial \xi}\right)^2 \text{ on } S_f.$$

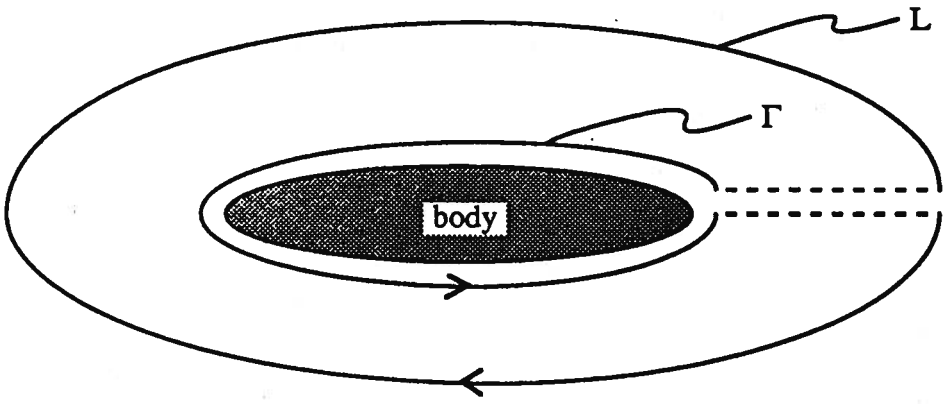

Figure 2.2 — Free Surface Bounding Contour

The free surface contribution is then

$$\phi_f = \frac{1}{4\pi g}\int_{-\infty}^{t} d\tau \iint_{S_f} dS\left[\phi\left(-\frac{1}{g}\frac{\partial}{\partial\tau} - U_0\frac{\partial}{\partial\xi}\right)^2 G - G\left(-\frac{1}{g}\frac{\partial}{\partial\tau} - U_0\frac{\partial}{\partial\xi}\right)^2\phi\right].$$

Liapis has shown that this contribution may be reduced to

$$\phi_f = -\frac{1}{4\pi g}\int_{-\infty}^{t} d\tau \oint_{\Gamma} d\eta\left[U_0^2(\phi G_\xi - \phi_\xi G) - U_0(\phi G_\tau - \phi_\tau G)\right]$$

where Γ is the intersection of the body surface S_0 and the free surface S_f and represents the only nonzero contribution from the contour L enclosing S_f as seen in Figure 2.2.

The complete integral equation may now be written as

$$\begin{aligned}\phi(P,t) = &-\frac{1}{4\pi}\int_{-\infty}^{t} d\tau \iint_{S_0} dS\left[\phi(Q,\tau)\frac{\partial}{\partial n}G(P,Q,t-\tau) - G(P,Q,t-\tau)\frac{\partial}{\partial n}\phi(Q,\tau)\right]\\ &-\frac{1}{4\pi g}\int_{-\infty}^{t} d\tau \oint_{\Gamma} d\eta\Big[U_0^2\big(\phi(Q,\tau)G_\xi(P,Q,t-\tau) - \phi_\xi(Q,\tau)G(P,Q,t-\tau)\big)\\ &-U_0\big(\phi(Q,\tau)G_\tau(P,Q,t-\tau) - \phi_\tau(Q,\tau)G(P,Q,t-\tau)\big)\Big]. \qquad (2.5)\end{aligned}$$

This integral equation gives the potential at any point P in the fluid as the integral of the potential over S_0 and Γ, the intersecting line between the body and the free surface. Liapis has shown that this formulation is equivalent to the traditional frequency-domain formulation if $\partial\phi/\partial n$ is sinusoidal.

Taking the limit as $P \to S_0$ and integrating the part of G involving $\delta(\tau)$ with respect to τ, the integral equation becomes

$$\begin{aligned}
&\phi(P,t) + \frac{1}{2\pi}\iint_{S_0} dS\,\phi(Q,t)\frac{\partial}{\partial n_Q}\left(\frac{1}{r}-\frac{1}{r'}\right) = \frac{1}{2\pi}\iint_{S_0} dS\left(\frac{1}{r}-\frac{1}{r'}\right)\frac{\partial}{\partial n}\phi(Q,t) \\
&-\frac{1}{2\pi}\int_{-\infty}^{t} d\tau \iint_{S_0} dS\left[\phi(Q,\tau)\frac{\partial}{\partial n_Q}\tilde{G}(P,Q,t-\tau) - \tilde{G}(P,Q,t-\tau)\frac{\partial}{\partial n}\phi(Q,\tau)\right] \\
&\quad -\frac{1}{2\pi g}\int_{-\infty}^{t} d\tau \oint_{\Gamma} d\eta\Big[U_0^2\big(\phi(Q,\tau)\tilde{G}_\xi(P,Q,t-\tau) - \phi_\xi(Q,\tau)\tilde{G}(P,Q,t-\tau)\big) \\
&\qquad - U_0\big(\phi(Q,\tau)\tilde{G}_\tau(P,Q,t-\tau) - \phi_\tau(Q,\tau)\tilde{G}(P,Q,t-\tau)\big)\Big] \qquad P \in S_0.
\end{aligned} \tag{2.6}$$

It is implied that the singular contribution to the surface integral on the left-hand side has been removed.

This integral equation is a Fredholm integral equation of the second kind in space and a Volterra integral equation in time. The unknown potential ϕ may be determined numerically as discussed in Chapter 5.

2.3 Consideration of Body Boundary Conditions

The integral equation as formulated in (2.6) is applicable for any arbitrary motion provided $\partial\phi/\partial n \to 0$ as $t \to -\infty$. The integral equation might thus be used to determine the potential, from which the forces or other pertinent information for some specific motion may be computed. The cost of numerical computation makes it prohibitive to consider this calculation for an arbitrary motion. Therefore, it is advantageous to choose a motion for solution of the integral equation that will give as much information as possible about the system response.

The choice by Liapis of an impulsive body boundary condition is a natural choice since it represents an input of constant amplitude at all frequencies simultaneously. However, it does include infinite velocities at the initial time, which must be handled by generalized functions. Since it is often not pertinent to know the response at very high frequencies, it might be desirable to consider inputs to the system that contain only lower frequencies of excitation. Included in this work is the consideration of that particular option and its effect on the results of radiation potential calculations. Chapter 4 explains how a nonimpulsive input is used to derive useful information about the system.

The choice of a boundary condition for $\partial\phi_7/\partial n$ is an important consideration. A steady sinusoidal input would not only provide little information, it would also not allow the potential ϕ_7 to satisfy the condition that $\phi \to 0 \quad t \to -\infty$. The most desirable boundary condition is one that will provide information at all frequencies of incident waves. This suggests that the velocity due to a wave of impulsive elevation is an appropriate choice. The derivation and discussion of the physical nature of such an incident wave is discussed in Chapter 3.

2.4 Determination of Forces

Of primary interest in this problem is the determination of the forces produced by the wave-body interactions of the incident, radiated, and diffracted wave systems. The force in any of the six modes of motion is given as

$$F_j(t) = \iint_{S_0} dS\, p(P,t) n_j \qquad j = 1,2,\ldots,6 \tag{2.7}$$

where $p(P,t)$ = the pressure that may be computed in keeping with the linear formulation as

$$p(P,t) = -\rho \frac{\partial \phi}{\partial t} - \rho \underline{W} \cdot \nabla \phi \tag{2.8}$$

and

$$F_j(t) = -\rho \iint_{S_0} dS \left[\frac{\partial \phi}{\partial t} + \underline{W} \cdot \nabla \phi \right] n_j. \tag{2.9}$$

If sectional forces are desired, it becomes essential to determine $\nabla \phi$. This may be done by taking the gradient of (2.5), but this is difficult and may be avoided if total forces are the only results desired.

Employing the theorem derived by Ogilvie and Tuck (1969) and explained in Ogilvie (1977):

$$\iint_{S_0} dS\, [m_j \phi + n_j (\underline{W} \cdot \nabla \phi)] = - \oint_{\Gamma} d\ell \phi n_j (\underline{\ell} \times \underline{n}) \cdot \underline{W}. \tag{2.10}$$

Combining (2.8), (2.9), and (2.10) yields

$$F_j(t) = -\rho \iint_{S_0} dS\, \frac{\partial \phi}{\partial t} n_j + \rho \iint_{S_0} dS\, \phi m_j + \rho \oint_{\Gamma} d\ell \phi n_j (\underline{\ell} \times \underline{n}) \cdot \underline{W}.$$

Defining

$$\begin{aligned} g_{jk}(t) &\equiv \rho \iint_{S_0} dS\, \phi_k n_j \qquad && j = 1,2,\ldots,6 \\ h_{jk}(t) &\equiv -\rho \iint_{S_0} dS\, \phi_k m_j - \rho \oint_{\Gamma} d\ell \phi_k n_j (\underline{\ell} \times \underline{n}) \cdot \underline{W} && k = 1,2,\ldots,7, \end{aligned} \tag{2.11}$$

we may write the force in mode j due to excitation in mode k as

$$F_{jk}(t) = -\frac{\partial}{\partial t} g_{jk}(t) - h_{jk}(t). \tag{2.12}$$

The force determined here is then the force due to the motion $\varsigma_k(t)$ chosen to determine $\partial \phi_k / \partial n$.

CHAPTER III

DETERMINATION OF TIME-DOMAIN WAVE PRESSURE AND VELOCITY

3.1 Determination of Velocities and Pressures Due to an Impulsive Wave at Zero Forward Speed

The time-domain response to a linear system may be written in the form

$$f(t) = \int_{-\infty}^{\infty} K(t-\tau)A(\tau)\,d\tau \tag{3.1}$$

where

$A(t)$ is an arbitrary input

$K(t)$ is the impulse response function

$f(t)$ is the system output.

Consider such an operator for the velocity due to an arbitrary long crested incident wave, that is, the vector function $\underline{K}(P,t)$ with the property that

$$\nabla\phi_0(P,t) = \int_{-\infty}^{\infty} \underline{K}(P,t-\tau)\varsigma_0(\tau)\,d\tau \tag{3.2}$$

where $\varsigma_0(t)$ is the arbitrary wave elevation measured at the origin of the coordinate system in Figure 2.1.

To determine $\underline{K}(P,t)$, consider the input $\varsigma_0(t) = e^{i\omega t}$. For this example, ϕ_0 is known and given as

$$\phi_0(P,t) = \frac{ig}{\omega} e^{k(z-i\varpi)} e^{i\omega t}$$

where

$$\varpi = x\cos\beta + y\sin\beta$$

$$k = \omega^2/g.$$

The angle of the wave propagation direction with the positive x axis (π represents headseas) is represented by β.

This may be easily seen since the linearized wave elevation is given as

$$\begin{aligned} \varsigma_0(P,t) &= -\frac{1}{g}\frac{\partial \phi_0}{\partial t} \qquad \text{on } z=0 \\ &= e^{-ik\varpi}\, e^{i\omega t}. \end{aligned} \tag{3.3}$$

For the origin $x, z, y = 0$,

$$\varsigma_0(P,t) = \varsigma_0(t) = e^{i\omega t}.$$

In this case,

$$\nabla\phi_0(P,t) = \begin{bmatrix} \hat{\imath}\cos\beta \\ \hat{\jmath}\sin\beta \\ \hat{k}i \end{bmatrix} \omega e^{k(z-i\varpi)}\, e^{i\omega t}. \tag{3.4}$$

Substituting $\varsigma_0(t) = e^{i\omega t}$ into (3.2) yields

$$\nabla\phi_0(P,t) = \int_{-\infty}^{\infty} \underline{K}(P, t-\tau) e^{i\omega\tau}\, d\tau = e^{i\omega t} \int_{-\infty}^{\infty} \underline{K}(P,\tau) e^{-i\omega\tau}\, d\tau.$$

Equating (3.3) and (3.4) and dividing by $e^{i\omega t}$ yields

$$\int_{-\infty}^{\infty} \underline{K}(P,\tau) e^{-i\omega\tau}\, d\tau = \begin{bmatrix} \hat{\imath}\cos\beta \\ \hat{\jmath}\sin\beta \\ \hat{k}i \end{bmatrix} \omega e^{k(z-i\varpi)}. \tag{3.5}$$

Defining the Fourier transform pair

$$\begin{aligned} \bar{f}(\omega) &= \mathcal{F} f(t) = \int_{-\infty}^{\infty} f(t) e^{-i\omega t}\, dt \\ f(t) &= \mathcal{F}^{-1}\bar{f}(\omega) = \frac{1}{2\pi}\int_{-\infty}^{\infty} \bar{f}(\omega) e^{i\omega t}\, d\omega \end{aligned} \tag{3.6}$$

with the property that $\mathcal{F}^{-1}\mathcal{F} f(t) = f(t)$, we may apply $\mathcal{F}^{-1}$ to (3.5) giving

$$\underline{K}(P,t) = \mathcal{F}^{-1}\left\{ \begin{bmatrix} \hat{\imath}\cos\beta \\ \hat{\jmath}\sin\beta \\ \hat{k}i \end{bmatrix} \omega e^{k(z-i\varpi)} \right\}. \tag{3.7}$$

Because $\underline{K}(P,t)$ must be real, it must be noted that (3.5) requires the right-hand side to be complex conjugate symmetric with respect to ω. This means that the right-hand side must be artificially extended to be complex conjugate symmetric in the negative frequency range. The physical implication is that $\underline{K}(P,t)$ is only valid for waves with positive ω, that is, waves traveling in the $+\beta$ direction. When the right-hand side of (3.7) is extended to be complex conjugate symmetric, it may be rewritten succinctly as

$$\underline{K}(P,t) = \frac{1}{\pi}\,\mathrm{Re}\left\{ \begin{bmatrix} \hat{\imath}\cos\beta \\ \hat{\jmath}\sin\beta \\ \hat{k}i \end{bmatrix} \int_0^{\infty} \omega e^{k(z-i\varpi)}\, e^{i\omega t}\, d\omega \right\} \tag{3.8}$$

where Re implies taking the real part of the expression.

The pressure due to an arbitrary wave may be derived in an analagous fashion where

$$p(P,t) = \int_{-\infty}^{\infty} \widehat{p}(P, t-\tau)\varsigma_0(\tau)\, d\tau. \tag{3.9}$$

Substituting $\varsigma_0(t) = e^{i\omega t}$ with the linearized pressure given as

$$p(P,t) = -\rho\frac{\partial \phi_0}{\partial t} = \rho g e^{k(z-i\varpi)}\, e^{i\omega t}$$

yields

$$\int_{-\infty}^{\infty} \widehat{p}(P,t) e^{-i\omega\tau}\, d\tau = \rho g e^{k(z-i\varpi)}.$$

Extending the right-hand side to be complex conjugate symmetric and Fourier transforming gives

$$\widehat{p}(P,t) = \frac{\rho g}{\pi}\,\mathrm{Re}\left\{\int_0^{\infty} e^{k(z-i\varpi)}\, e^{i\omega t}\, d\omega\right\}. \tag{3.10}$$

The characteristics and physical significance of $\underline{K}(P,t)$ and $\widehat{p}(P,t)$ should be considered. These functions represent impulse response functions as the term $K(t)$ in (3.1). The impulse is an impulse in wave elevation at the origin of the coordinate system at $t = 0$. The response is the velocity or pressure due to this wave.

The integrals in (3.8) and (3.10) may be calculated analytically. The details of their derivation are given in Appendix A. Values of $\widehat{p}(P,t)$ have been plotted in nondimensional form in Figure 3.1. It may be noted that $\widehat{p}$ and $\underline{K}$ are not causal in the traditional sense, that is, $\underline{K}$ and $\widehat{p}$ are not $= 0$ for $t < 0$. This condition is a result of the fact that water waves are dispersive.

The development here is very similar to the Cauchy-Poisson problem as discussed in Lamb (1932). The Cauchy-Poisson problem deals with an initial disturbance of impulsive nature at the origin, while a propagating disturbance with the property that the wave elevation becomes impulsive at the origin is derived here. While it would seem that the velocity and pressure should go to zero at large distances in the direction of wave propagation, this is not the case. This was explained in Lamb:

> One noteworthy feature in the above problems is that the disturbance is propagated ***instantaneously*** to all distances from the origin, however great. Analytically, this might be accounted for by the fact that we have to deal with a synthesis of waves of all possible lengths, and that for infinite lengths the wave-velocity is infinite. It has been shewn, however, by Rayleigh that the instantaneous character is preserved even when the water is of finite depth, in which case there is an upper limit to the wave-velocity. The physical reason of the peculiarity is that the fluid is treated as incompressible, so that changes of pressure are propagated with infinite velocity. ... When compressibility is taken into

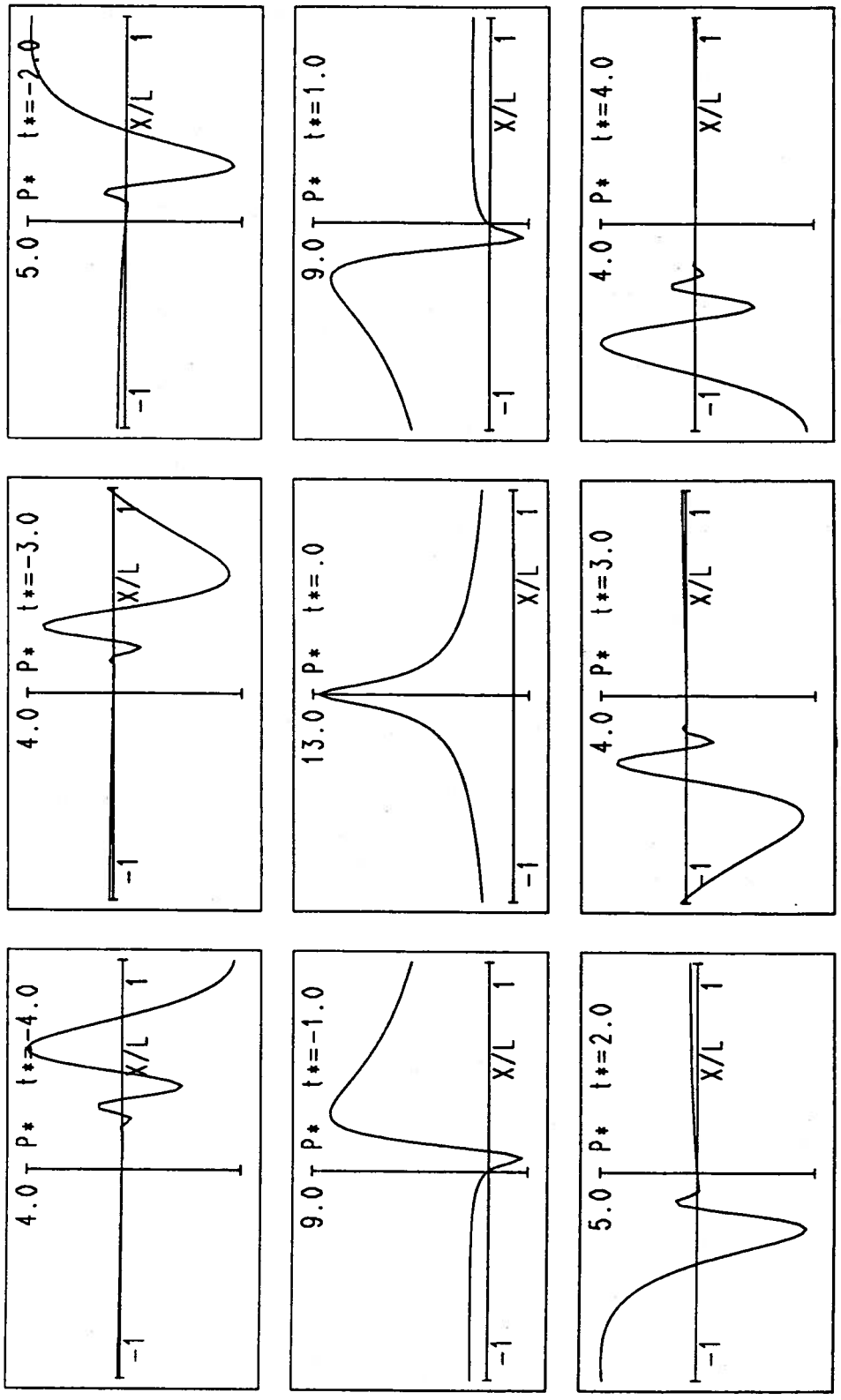

$$p(x,t)=\rho g\sqrt{g/L}\int_{-\infty}^{\infty}\dot{p}\,(x/L,t-\tau)\chi_0(\tau)d\tau$$

Figure 3.1 — Nondimensional Pressure Impulse Response Function

account a finite, though it may be very short, interval elapses before the disturbance manifests itself at any point.[1]

For traditional linear systems a noncausal system could be considered physically unrealistic. In this case, the implication of noncausality is simply that the effect of this disturbance is felt throughout the fluid before the wave elevation at the origin is affected.

3.2 Determination of the Froude-Krylov Impulse Response Function

We may integrate the pressure given by (3.9) over the body to determine a Froude-Krylov impulse response function. Writing the Froude-Krylov force for a body at zero speed with surface S_0 in mode j as

$$\begin{aligned} F_{j0}(t) &= \iint_{S_0} dS\, p(P,t) n_j \\ &= \iint_{S_0} dS \int_{-\infty}^{\infty} d\tau \widehat{p}(P, t-\tau) \varsigma_0(\tau) n_j \\ &= \int_{-\infty}^{\infty} d\tau \varsigma_0(\tau) \iint_{S_0} dS\, \widehat{p}(P, t-\tau) n_j \end{aligned}$$

and defining K_{j0} as

$$K_{j0}(t) \equiv \iint_{S_0} dS\, \widehat{p}(P,t) n_j,$$

the force becomes

$$F_{j0}(t) = \int_{-\infty}^{\infty} K_{j0}(t-\tau) \varsigma_0(\tau)\, d\tau.$$

As an example, Figure 3.2 is a plot of the nondimensional Froude-Krylov impulse response function in heave, $K_{30}(t)$, and sway, $K_{20}(t)$, for a half-submerged sphere with $\varsigma_0(t)$ measured at the sphere center.

3.3 The Use of $\underline{K}$ As a Boundary Condition for the Diffraction Problem

Since (3.2) gives $\nabla\phi_0(P,t)$ for an arbitrary wave $\varsigma_0(t)$, it is worthwhile to consider the use of $\underline{K}$ in the boundary condition for the diffracted wave. That is,

$$\frac{\partial \phi_7}{\partial n} = -\frac{\partial \phi_0}{\partial n} = -\underline{n} \cdot \nabla \phi_0 = -\underline{n} \cdot \int_{-\infty}^{\infty} \underline{K}(P, t-\tau) \varsigma_0(t)\, d\tau.$$

Now let $\varsigma_0(t) = \delta(t)$. For this case:

$$\frac{\partial \widehat{\phi}_7}{\partial n} = -\underline{n} \cdot \underline{K}(P,t).$$

The integral equation (2.6) may then be used to determine the potential due to this incident wave. Thus determined, $\widehat{\phi}_7$ represents the diffracted wave potential due to an impulsive incident wave as discussed in the previous section, and the diffracted wave potential due to an arbitrary incident wave measured from the origin is

$$\phi_7(P,t) = \int_{-\infty}^{\infty} \widehat{\phi}_7(P, t-\tau) \varsigma_0(\tau)\, d\tau.$$

---

[1] Lamb (1932: 394)

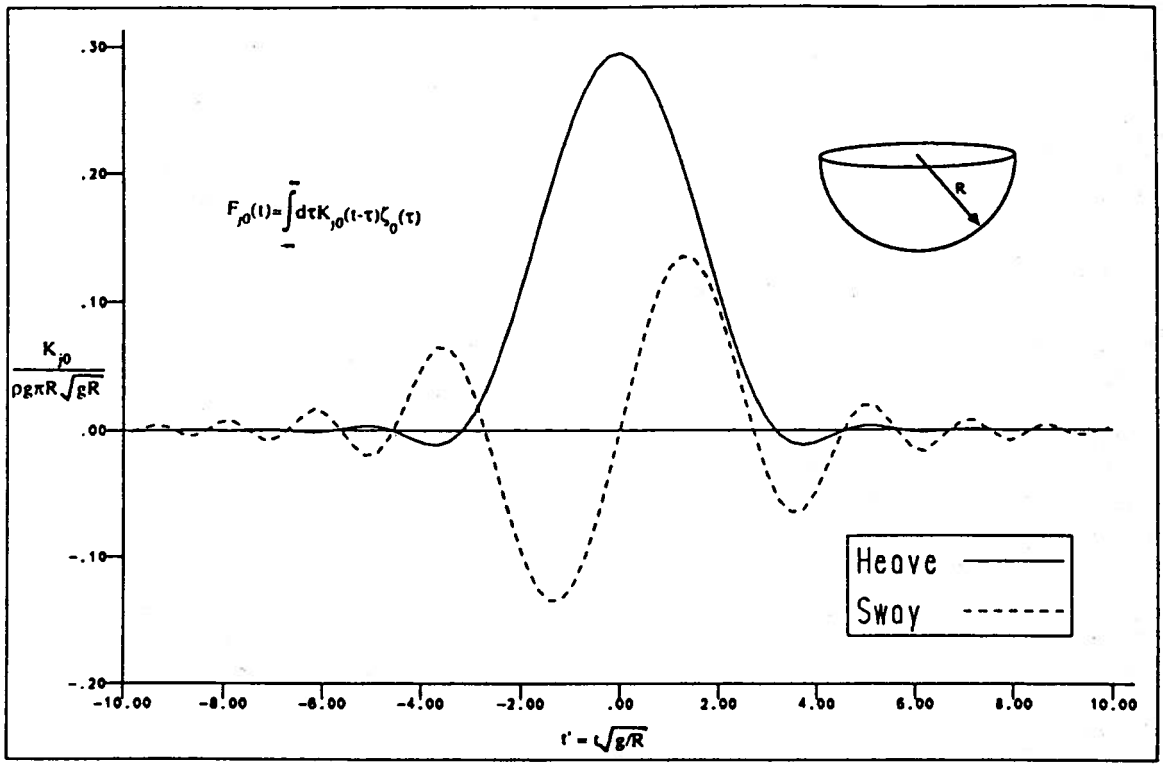

Figure 3.2 — Nondimensional Froude-Krylov Impulse Response Functions

To determine the diffraction forces, (2.12) may be employed with $U_0 = 0$;

$$F_{j7}(t) = -\frac{\partial}{\partial t} g_{j7}(t)$$

where

$$\begin{aligned} g_{j7}(t) &= \rho \iint_{S_0} dS\, \phi_7(P,t) n_j \\ &= \rho \iint_{S_0} dS\, n_j \int_{-\infty}^{\infty} d\tau \widehat{\phi}_7(P, t-\tau) \varsigma_0(\tau) \\ &= \rho \int_{-\infty}^{\infty} d\tau\, \varsigma_0(\tau) \iint_{S_0} dS\, \widehat{\phi}_7(P, t-\tau) n_j. \end{aligned}$$

Or, defining K_{j7} as the diffraction force impulse response function,

$$K_{j7}(t) \equiv -\rho \frac{\partial}{\partial t} \iint_{S_0} dS\, \widehat{\phi}_7(P,t) n_j.$$

The force may be written as

$$F_{j7}(t) = \int_{-\infty}^{\infty} d\tau\, K_{j7}(t-\tau) \varsigma_0(\tau). \tag{3.11}$$

The total force due to the incident wave may now be written as

$$F_{Ij}(t) = \int_{-\infty}^{\infty} d\tau \left[K_{j7}(t-\tau) + K_{j0}(t-\tau)\right]\varsigma_0(\tau). \tag{3.12}$$

3.4 The Determination of the Spatial Shift of Wave Elevation

Pursuing the same approach used in the previous sections for determining pressure and velocity due to the incident wave $\varsigma_0(t)$, consider $\widehat{\varsigma}(x, y, t)$ with the property that

$$\varsigma(x, y, t) = \int_{-\infty}^{\infty} \widehat{\varsigma}(x, y, t-\tau)\varsigma_0(\tau)\, d\tau. \tag{3.13}$$

Let $\varsigma_0(t) = e^{i\omega t}$, and, substituting into (3.13),

$$\int_{-\infty}^{\infty} \widehat{\varsigma}(x, y, t-\tau)e^{i\omega\tau}\, d\tau = e^{i\omega t}\mathcal{F}\widehat{\varsigma}(x, y, \tau) = \varsigma(x, y, t)$$

$$\varsigma(x, y, t) = e^{-ik\varpi}e^{i\omega t}$$

$$\varpi = x\cos\beta + y\sin\beta.$$

Substituting and cancelling the term $e^{i\omega t}$ yields

$$\mathcal{F}\widehat{\varsigma}(x, y, t) = e^{-ik\varpi}$$

$$\widehat{\varsigma}(x, y, t) = \frac{1}{\pi}\,\mathrm{Re}\left\{\int_0^{\infty} e^{-ik\varpi}e^{i\omega t}\, d\omega\right\},$$

with the restriction that $\varsigma_0(t)$ represents a wave traveling in the $+\beta$ direction as in the case of the velocity and pressure determinations.

Alternatively, the elevation at the origin may be written as

$$\begin{aligned} \varsigma_0(t) &= \int_{-\infty}^{\infty} \widehat{\varsigma}^{-1}(x, y, t-\tau)\varsigma(x, y, \tau)\, d\tau \\ \widehat{\varsigma}^{-1}(x, y, t) &= \frac{1}{\pi}\,\mathrm{Re}\left\{\int_0^{\infty} e^{ik\varpi}e^{i\omega t}\, d\omega\right\} \end{aligned} \tag{3.14}$$

where $\widehat{\varsigma}^{-1}$ represents the transformation of the wave elevation at an arbitrary point back to the origin.

In practice, (3.13) may be more easily determined using the property of Fourier transforms that

$$\varsigma(x, y, t) = \mathcal{F}^{-1}\{\mathcal{F}\widehat{\varsigma}\mathcal{F}\varsigma_0\}.$$

We may thus write

$$\varsigma(x, y, t) = \mathcal{F}^{-1}\{e^{-ik\varpi}\mathcal{F}\varsigma_0\}$$

with $e^{-ik\varpi}$ extended to be complex conjugate symmetric in ω.

Figure 3.3 shows a plot of the Froude-Krylov impulse response function for a sphere in heave with the coordinate shift $x_0 = x - 5R$, $y_0 = y$, and $z_0 = z$. Plotted on the same graph is the Froude-Krylov impulse response function calculated for ς_0 at the origin of the original coordinate system, with $\varsigma_0(t)$ shifted to the point $x = 5R$ by (3.14). Thus, it is possible to determine the Froude-Krylov force on the body due to the wave elevation at any point as

$$F_{j0}(t) = \int_{-\infty}^{\infty} K_{j0}(t-\tau)\varsigma_0(\tau)\, d\tau$$

$$\varsigma_0(\tau) = \int_{-\infty}^{\infty} \widehat{\varsigma}^{-1}(x,y,t-\tau)\varsigma(x,y,\tau)\, d\tau$$

$$F_{j0}(t) = \int_{-\infty}^{\infty} d\tau \int_{-\infty}^{\infty} d\theta\, K_{j0}(t-\tau)\widehat{\varsigma}^{-1}(x,y,\tau-\theta)\varsigma(x,y,\theta),$$

defining

$$K_{j0}(x,y,t) \equiv \int_{-\infty}^{\infty} K_{j0}(t-\theta)\widehat{\varsigma}^{-1}(x,y,\theta)\, d\theta$$

$$F_{j0}(t) = \int_{-\infty}^{\infty} K_{j0}(x,y,t-\tau)\varsigma(x,y,\tau)\, d\tau.$$

The same technique may be used for any impulse response function based on wave elevation at the origin to shift the input to a different point on the free surface.

3.5 The Determination of an Impulsive Incident Wave for Steady Forward Speed

Impulse response functions for the pressure and velocity due to an incident wave in a steady translating coordinate system may be derived in a manner similar to those derived for zero forward speed in the previous sections. There are several important considerations that are unique to the case of a translating body and must be considered.

The first consideration is that of the input wave elevation $\varsigma_0(t)$. For the previous case we considered $\varsigma_0(t)$ as the arbitrary wave elevation at the coordinate system origin. For a body with forward speed, the wave elevation measured at the body fixed origin differs from the wave elevation measured from a fixed point in space. The wave elevation as measured from the ship fixed origin will be denoted by $\varsigma_0(t)$. The wave elevation at a fixed point will be denoted by a prime when it differs from $\varsigma_0(t)$. The notation for the forward speed case will then be the same as for the previously derived zero speed case. The zero speed results may be considered a special case of the forward speed results, with $U_0 = 0$. For a body with steady speed U_0 and waves traveling in the $+\beta$ direction, the two elevations are

$$\varsigma_0'(t) = \mathrm{Re}\{e^{i\omega t}\}$$

$$\varsigma_0(t) = \mathrm{Re}\{e^{-ikU_0 t\cos\beta}e^{i\omega t}\},$$

which may also be written as

$$\varsigma_0(t) = \mathrm{Re}\{e^{i\omega_e t}\}$$

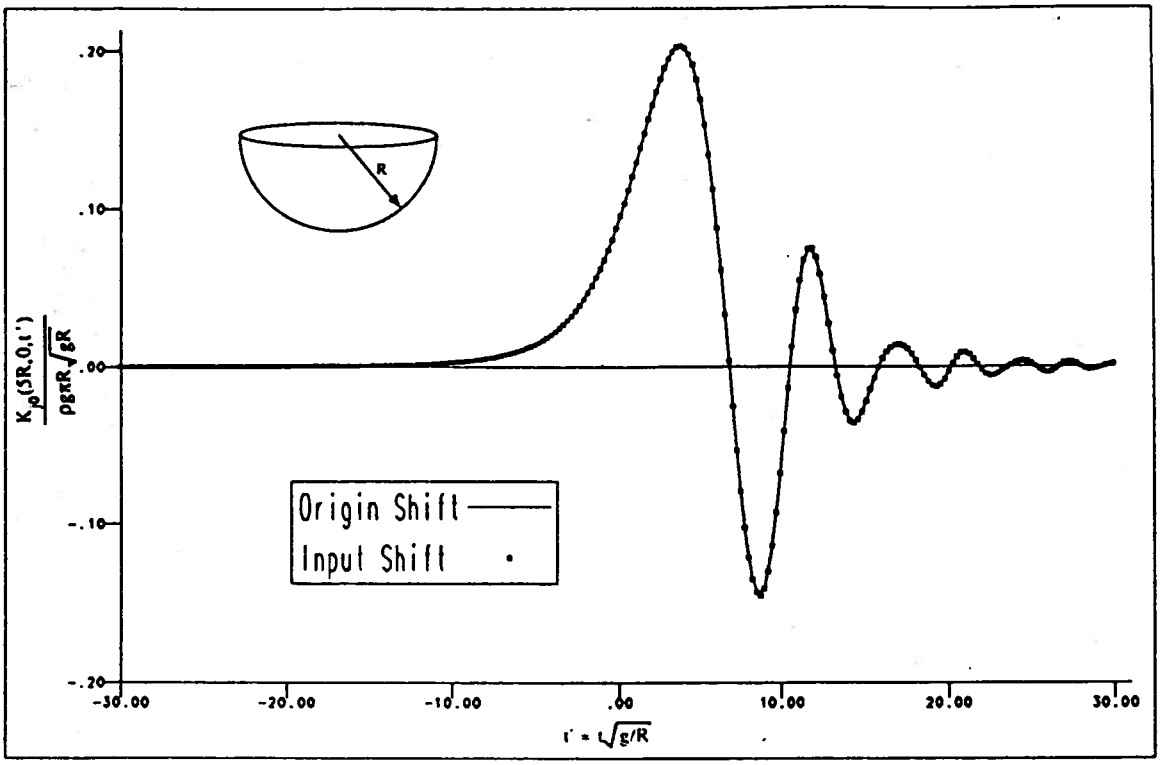

Figure 3.3 — Nondimensional Froude-Krylov Impulse Response Function for a Spatially Shifted Input

where

$$\omega_e = \omega - kU_0 \cos\beta.$$

For a time invariant linear system, the response to an input at frequency ω is an output at frequency ω_e, with phase and amplitude changed by the system. Because of the shift in frequency caused by the forward speed, it is essential to deal with a time varying system if $\varsigma_0'(t)$ is chosen for input. The determination of $\varsigma_0(t)$ from $\varsigma_0'(t)$ is discussed in Section 3.7, but for the current discussion it will be assumed that $\varsigma_0(t)$ is known, so that the frequency of the input is ω_e.

Following a development similar to that in Section 3.1, consider $\underline{K}(P,t)$ such that

$$\nabla\phi_0(P,t) = \int_{-\infty}^{\infty} \underline{K}(P,t-\tau)\varsigma_0(\tau)\, d\tau. \tag{3.15}$$

Considering an input $\varsigma_0(t) = e^{i\omega_e t}$, (3.15) may be written

$$\nabla\phi_0(P,t) = e^{i\omega_e t} \int_{-\infty}^{\infty} \underline{K}(P,\tau) e^{-i\omega_e \tau}\, d\tau. \tag{3.16}$$

For this case, $\nabla\phi_0(P,t)$ is given by

$$\nabla\phi_0(P,t) = \omega e^{k(z-i\varpi)} e^{i\omega_e t}. \tag{3.17}$$

Equating (3.16) and (3.17),

$$\omega e^{k(z-i\varpi)} = \int_{-\infty}^{\infty} \underline{K}(P,\tau) e^{-i\omega_e \tau}\, d\tau.$$

Making the same extensions of the left-hand side in the negative encounter frequency range as were made for the zero speed case in the previous section and Fourier transforming with respect to ω_e yields

$$\underline{K}(P,t) = \frac{1}{\pi} \mathrm{Re} \left\{ \begin{bmatrix} \hat{\imath}\cos\beta \\ \hat{\jmath}\sin\beta \\ \hat{k}i \end{bmatrix} \int_0^{\infty} \omega e^{k(z-i\varpi)} e^{i\omega_e t}\, d\omega_e \right\}. \tag{3.18}$$

This integral may be calculated analytically. The results are given in Appendix A.

The impulse response function for pressure may be derived in an analagous manner with the result given as

$$\hat{p}(P,t) = \frac{1}{\pi} \mathrm{Re} \left\{ \int_0^{\infty} e^{k(z-i\varpi)} e^{i\omega_e t}\, d\omega_e \right\}. \tag{3.19}$$

The evaluation of this integral is also given in Appendix A.

3.6 The Consideration of Following Seas with Steady Forward Speed

An important consideration in regard to the input $\varsigma_0(t)$ is the distinction between head seas ($\pi/2 < \beta < 3\pi/2$) and following seas ($-\pi/2 < \beta < \pi/2$). The plots of frequency of encounter versus wave frequency (Figure 3.4) show that for head seas the wave frequency ω is a single valued function of ω_e, while it is a multiple valued function of ω_e for following seas. Physically this ambiguity arises from the fact that with following seas there are two wavelengths that are overtaking the ship and one wavelength that the ship is overtaking, all having the same frequency of encounter. The frequency of encounter for the wave being overtaken is negative. However, the Fourier transform of $\varsigma_0(t)$ distinguishes between negative and positive frequency only by a change in phase. The point measurement of the wave elevation from the moving coordinate system in following seas does not contain complete information about the wave system.

A viable method of dealing with this problem is to divide the input into three different parts written as

$$\varsigma_0(t) = \sum_{m=1}^{3} \varsigma_{0m}(t)$$

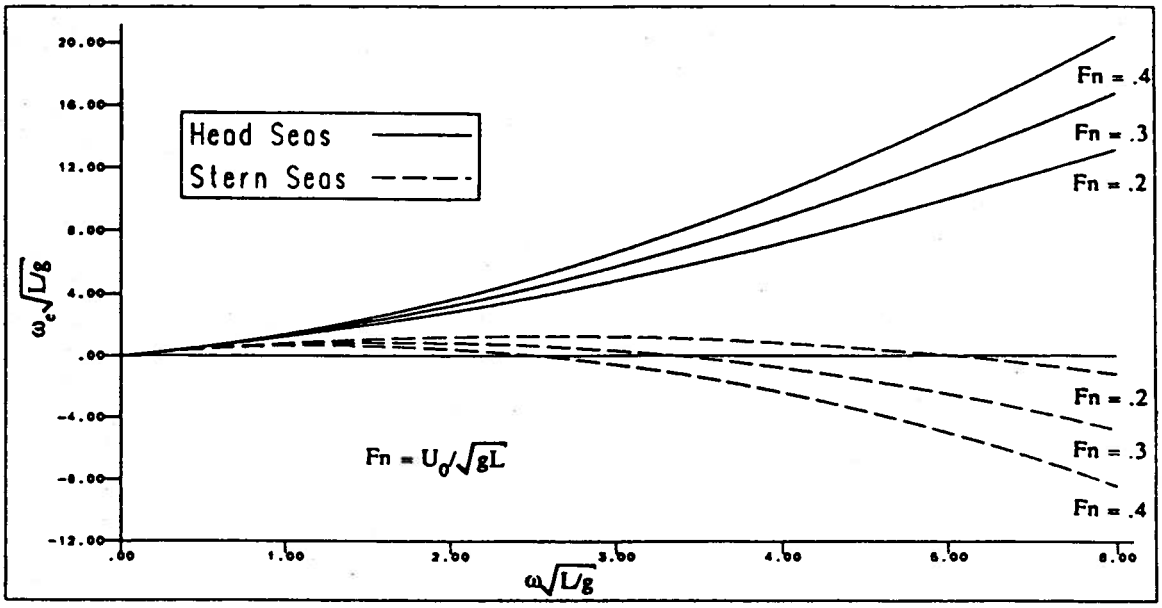

Figure 3.4 — Nondimensional Encounter Frequency Versus Wave Frequency

where $\varsigma_{0m}(t)$ represents the incident wave due to a restricted range of wavelengths,

$$\lambda_m = 2\pi/k_m$$

$$0 < k_1 < \frac{g}{4U_0^2 \cos^2\beta}$$

$$\frac{g}{4U_0^2 \cos^2\beta} < k_2 < \frac{g}{U_0^2 \cos^2\beta}$$

$$\frac{g}{U_0^2 \cos^2\beta} < k_3 < \infty.$$

Each of the inputs $\varsigma_{0m}(t)$ contains no waves outside the range prescribed above. This approach is also used in frequency-domain approaches; see, for example, Price and Bishop (1974).

Three separate impulse response functions may now be written for the velocity and pressure. The total velocity and pressure may then be written as the sum of the three components and is

$$\nabla\phi_0(P,t) = \sum_{m=1}^{3} \int_{-\infty}^{\infty} \underline{K}_m(P, t-\tau)\varsigma_{0m}(\tau)\, d\tau \tag{3.20}$$

$$p(P,t) = \sum_{m=1}^{3} \int_{-\infty}^{\infty} \hat{p}_m(P, t-\tau)\varsigma_{0m}(\tau)\, d\tau. \tag{3.21}$$

To determine the impulse response functions, consider

$$\begin{aligned}
\varsigma_{0m} &= e^{i\omega_e t} \qquad 0 < \omega_e < \frac{g}{4U_0 \cos\beta} \qquad m = 1,2 \\
\varsigma_{0m} &= 0 \qquad \omega_e > \frac{g}{4U_0 \cos\beta} \qquad m = 1,2 \\
\varsigma_{0m} &= e^{-i\omega_e t} \qquad 0 < \omega_e < \infty \qquad m = 3
\end{aligned} \tag{3.22}$$

for this input

$$\begin{aligned}
\nabla\phi_{0m} &= \begin{bmatrix} \hat{\imath}\cos\beta \\ \hat{\jmath}\sin\beta \\ \hat{k}i \end{bmatrix} \omega_m e^{k_m(z-i\varpi)} e^{i\omega_e t} \qquad m = 1,2 \\
&= \begin{bmatrix} \hat{\imath}\cos\beta \\ \hat{\jmath}\sin\beta \\ \hat{k}i \end{bmatrix} \omega_m e^{k_m(z-i\varpi)} e^{-i\omega_e t} \qquad m = 3 \\
p_m &= \rho g e^{k_m(z-i\varpi)} e^{i\omega_e t} \qquad m = 1,2 \\
&= \rho g e^{k_m(z-i\varpi)} e^{-i\omega_e t} \qquad m = 3
\end{aligned} \tag{3.23}$$

$$\begin{aligned}
\omega_1 &= \frac{g}{2U_0\cos\beta}\left(1 - \sqrt{1 - \frac{4U_0\cos\beta}{g}\omega_e}\right) \\
\omega_2 &= \frac{g}{2U_0\cos\beta}\left(1 + \sqrt{1 - \frac{4U_0\cos\beta}{g}\omega_e}\right) \\
\omega_3 &= \frac{g}{2U_0\cos\beta}\left(1 + \sqrt{1 + \frac{4U_0\cos\beta}{g}\omega_e}\right) \\
k_m &= \omega_m^2/g.
\end{aligned} \tag{3.24}$$

Substituting (3.22) into (3.20) and (3.21), equating with (3.23), and Fourier transforming yields

$$\begin{aligned}
\underline{K}_m(P,t) &= \frac{1}{\pi}\,\mathrm{Re}\left\{\begin{bmatrix} \hat{\imath}\cos\beta \\ \hat{\jmath}\sin\beta \\ \hat{k}i \end{bmatrix} \int_0^{g/4U_0\cos\beta} \omega_m e^{k_m(z-i\varpi)} e^{i\omega_e t}\, d\omega_e \right\} \qquad m = 1,2 \\
&= \frac{1}{\pi}\,\mathrm{Re}\left\{\begin{bmatrix} \hat{\imath}\cos\beta \\ \hat{\jmath}\sin\beta \\ \hat{k}i \end{bmatrix} \int_0^{\infty} \omega_m e^{k_m(z+i\varpi)} e^{i\omega_e t}\, d\omega_e \right\} \qquad m = 3 \\
\widehat{p}_m(P,t) &= \frac{\rho g}{\pi}\,\mathrm{Re}\left\{\int_0^{g/4U_0\cos\beta} e^{k_m(z-i\varpi)} e^{i\omega_e t}\, d\omega_e \right\} \qquad m = 1,2 \\
&= \frac{\rho g}{\pi}\,\mathrm{Re}\left\{\int_0^{\infty} e^{k_m(z+i\varpi)} e^{i\omega_e t}\, d\omega_e \right\} \qquad m = 3
\end{aligned}$$

where ω_m and k_m are given by (3.24).

It is important to note that for whatever quantity is the output of a following seas input, the three parts of the input must remain separate until the quantity is calculated for each of the three parts. Only then may the parts be summed to give the total. While

there are three wavelengths with the same encounter frequency, the problem is that their spatial variations of potential, elevation, velocity, and pressure are entirely different. For this approach it is necessary to solve three separate integral equations to determine the diffracted wave for the case of following seas.

3.7 The Transformation of Wave Elevation from the Fixed to the Moving Coordinate System

An important question that arises is the determination of $\varsigma_0(t)$ given $\varsigma_0'(t)$, which are the most commonly available data. The linear transformation may be written

$$\varsigma_0(t) = \int_{-\infty}^{\infty} h(t-\tau,\tau)\varsigma_0'(\tau)\, d\tau, \tag{3.25}$$

letting $\varsigma_0'(t) = e^{i\omega t}$ and substituting

$$\varsigma_0(t) = e^{i\omega t}\int_{-\infty}^{\infty} h(\tau, t-\tau)e^{-i\omega\tau}\, d\tau. \tag{3.26}$$

For this case, $\varsigma_0(t)$ is given by

$$\varsigma_0(t) = e^{-ikU_0 t\cos\beta}e^{i\omega t}.$$

Equating (3.25) and (3.26) gives

$$e^{-ikU_0 t\cos\beta} = \int_{-\infty}^{\infty} h(\tau, t-\tau)e^{-i\omega\tau}\, d\tau. \tag{3.27}$$

Fourier transforming both sides and extending the left-hand side to be complex conjugate symmetric as required by (3.27) yields

$$h(t-\tau,\tau) = \frac{1}{\pi}\,\mathrm{Re}\left\{\int_0^{\infty} e^{-ikU_0\tau\cos\beta}e^{i\omega(t-\tau)}\, d\omega\right\}. \tag{3.28}$$

The shift of the wave elevation from the fixed to the moving coordinate system is thus analytically possible, but in practice (3.25) may be very difficult to compute. Using the properties of the Fourier transform, (3.25) may be rewritten as

$$\varsigma_0(t) = \mathcal{F}^{-1}\{\mathcal{F}h\mathcal{F}\varsigma_0'\},$$

with the Fourier transforms taken with respect to ω.

From (3.27),

$$\mathcal{F}h = e^{-ikU_0 t\cos\beta}.$$

Therefore, (3.28) may be rewritten as

$$\begin{aligned}\varsigma_0(t) &= \frac{1}{\pi}\,\mathrm{Re}\left\{\int_0^{\infty}\overline{\varsigma_0'}(\omega)e^{-ikU_0 t\cos\beta}e^{i\omega t}\, d\omega\right\}\\ &= \frac{1}{\pi}\,\mathrm{Re}\left\{\overline{\varsigma_0'}(\omega)e^{i\omega_e t}\, d\omega\right\}.\end{aligned} \tag{3.29}$$

For head seas,

$$\omega_e = \omega - kU_0 \cos\beta$$

$$\omega = \frac{g}{2U_0 \cos\beta}\left(1 - \sqrt{1 + \frac{4U_0 \cos\beta}{g}\omega_e}\right)$$

$$d\omega_e = \left(1 - \frac{2U_0}{g}\omega \cos\beta\right) d\omega.$$

Substituting (3.29) gives

$$\varsigma_0(t) = \frac{1}{\pi}\,\mathrm{Re}\left\{\int_0^\infty \frac{\bar{\varsigma}_0'(\omega)}{1 - \frac{2U_0}{g}\omega\cos\beta} e^{i\omega_e t}\, d\omega_e\right\}.$$

For following seas,

$$\begin{aligned}\varsigma_{0_m}(t) &= \frac{1}{\pi}\,\mathrm{Re}\left\{\int_0^{g/4U_0\cos\beta} \frac{\bar{\varsigma}_0'(\omega_m)}{1 - \frac{2U_0}{g}\omega_m\cos\beta} e^{i\omega_e t}\, d\omega_e\right\} \quad m = 1,2 \\ &= \frac{1}{\pi}\,\mathrm{Re}\left\{\int_0^\infty \frac{\bar{\varsigma}_0'(\omega_m)}{1 - \frac{2U_0}{g}\omega_m\cos\beta} e^{-i\omega_e t}\, d\omega_e\right\} \quad m = 3\end{aligned} \tag{3.30}$$

where ω_m is given by (3.24).

It may be noted that (3.30) is singular at the upper limit of integration for the $m = 1,2$ cases. The sum of $\bar{\varsigma}_{0_1}(t) + \bar{\varsigma}_{0_2}(t)$ is not singular at $\omega_e = g/4U_0\cos\beta$. Consider

$$\sum_{m=1}^{2} \varsigma_{0_m}(t) = \frac{1}{\pi}\,\mathrm{Re}\left\{\int_0^{g/4U_0\cos\beta} \sum_{m=1}^{2} \frac{\bar{\varsigma}_0'(\omega_m)}{1 - \frac{2U_0}{g}\omega_m\cos\beta} e^{i\omega_e t}\, d\omega_e\right\}.$$

Looking at the singular terms

$$\frac{\bar{\varsigma}_0(\omega_1)}{1 - \frac{2U_0}{g}\omega_1\cos\beta} + \frac{\bar{\varsigma}_0(\omega_2)}{1 - \frac{2U_0}{g}\omega_2\cos\beta},$$

we may substitute the value of ω_1 and ω_2 from (3.23) yielding

$$\frac{\bar{\varsigma}_0(\omega_2) - \bar{\varsigma}_0(\omega_1)}{\sqrt{1 - \frac{4U_0\cos\beta}{g}\omega_e}}.$$

Since the limit as $\omega_e \to g/4U_0\cos\beta$ of $\omega_1 - \omega_2 = 0$, $\bar{\varsigma}_0(\omega_2) - \bar{\varsigma}_0(\omega_1) \to 0$. L'Hôpital's rule may be applied to find the limit. That is,

$$\lim_{\omega_e \to g/4U_0\cos\beta} \frac{\bar{\varsigma}_0(\omega_2) - \bar{\varsigma}_0(\omega_1)}{\sqrt{1 - \frac{4U_0\cos\beta}{g}\omega_e}} = \lim_{\omega_e \to g/4U_0\cos\beta} \frac{\frac{\partial}{\partial\omega_e}\left[\bar{\varsigma}_0(\omega_2) - \bar{\varsigma}_0(\omega_1)\right]}{\frac{\partial}{\partial\omega_e}\sqrt{1 - \frac{4U_0\cos\beta}{g}\omega_e}}$$

$$= 2\frac{d}{d\omega}\bar{\varsigma}_0(\omega) \quad \text{evaluated at} \quad \omega = \frac{g}{2U_0\cos\beta}.$$

For practical calculations the limit of each integral taken independently will be half of the limit of the two combined.

3.8 The Determination of a Spatial Shift of Wave Elevation in the Steady Translating Coordinate System

For the head seas case, a completely analagous development to Section 3.4 may be used with a transform of coordinates:

$$\varsigma(x,y,t) = \int_{-\infty}^{\infty} \widehat{\varsigma}(x,y,t-\tau)\varsigma_0(\tau)\,d\tau$$

where

$$\widehat{\varsigma}(x,y,t) = \frac{1}{\pi}\,\mathrm{Re}\left\{\int_0^{\infty} e^{-ik\varpi}\, e^{i\omega_e t}\,d\omega_e\right\}$$

$$\text{or} \qquad \varsigma(x,y,t) = \mathcal{F}_e^{-1}\left[e^{-ik\varpi}\,\mathcal{F}_e\varsigma_0\right]$$

where $\mathcal{F}_e$ denotes that the Fourier transforms are taken with respect to ω_e and $e^{-ik\varpi}$ is extended to be complex conjugate symmetric with respect to ω_e.

For the case of following seas, the nonuniqueness with encounter frequency cannot be ignored, and $\varsigma_0(t)$ may be handled in three separate parts as in the case of velocity and pressure impulse response functions.

3.9 The Use of $\underline{K}$ As a Boundary Condition for the Forward Speed Diffraction Problem

A parallel development to that in Section 3.3 can be used to determine the diffracted wave potential due to an arbitrary incident wave.

The body boundary condition is given as

$$\frac{\partial\phi_7}{\partial n} = \frac{-\partial\phi_0}{\partial n} = -\underline{n}\cdot\nabla\phi_0 = -\underline{n}\cdot\int_{-\infty}^{\infty}\underline{K}(P,t-\tau)\varsigma_0(\tau)\,d\tau;$$

letting $\varsigma_0(t) = \delta(\tau)$,

$$\begin{aligned}\frac{\partial\widehat{\phi}_7}{\partial n} &= -\underline{n}\cdot\underline{K}(P,t)\\ \phi_7(P,t) &= \int_{-\infty}^{\infty}\widehat{\phi}_7(P,t-\tau)\varsigma_0(\tau)\,d\tau.\end{aligned} \tag{3.31}$$

Employing (2.11), the diffraction force due to an arbitrary wave is

$$F_{j7}(t) = -\dot{g}_{j7}(t) - h_{j7}(t)$$

where

$$\begin{aligned}g_{j7}(t) &= \rho\iint_{S_0} dS\,\phi_7 n_j\\ h_{j7}(t) &= -\rho\iint_{S_0} dS\,\phi_7 m_j - \rho\oint_{\Gamma} d\ell\, n_j\phi_7(\underline{\ell}\times\underline{n})\cdot\underline{W}.\end{aligned} \tag{3.32}$$

Substituting (3.31) into (3.32) and interchanging orders of integration,

$$F_{j7}(t) = \int_{-\infty}^{\infty} d\tau\, K_{j7}(t-\tau)\varsigma_0(t)\,d\tau$$

where

$$K_{j7}(t) = -\rho\frac{\partial}{\partial t}\iint_{S_0} dS\,\widehat{\phi}_7 n_j + \rho\iint_{S_0} dS\,\widehat{\phi}_7 m_j + \rho\oint_{\Gamma} d\ell n_j\widehat{\phi}_7(\underline{\ell}\times\underline{n})\cdot\underline{W}. \tag{3.33}$$

Defining the Froude-Krylov impulse response function for steady forward speed as

$$K_{j0}(t) \equiv \iint_{S_0} dS\,\widehat{p}(P,t)n_j$$

where $\widehat{p}(P,t)$ is given by (3.19), the total force due to the incident wave for a body with steady forward speed may be written

$$F_{Ij}(t) = \int_{-\infty}^{\infty} d\tau\left[K_{j7}(t-\tau) + K_{j0}(t-\tau)\right]\varsigma_0(\tau).$$

3.10 Comparisons with Traditional Frequency-Domain Forces

For harmonic waves, the exciting forces due to an incident wave are typically written in the form

$$F_{Ij}(t) = \mathrm{Re}\left\{X_j(\omega)\bar{\varsigma}_0(\omega)e^{i\omega t}\right\} \tag{3.34}$$

where $X_j(\omega), \bar{\varsigma}_0(\omega)$ are complex and

$$\varsigma_0(t) = \mathrm{Re}\left\{\bar{\varsigma}_0(\omega)e^{i\omega t}\right\}. \tag{3.35}$$

Substituting (3.35) into (3.12) for the zero speed case yields

$$\begin{aligned} F_{Ij}(t) &= \mathrm{Re}\left\{\int_{-\infty}^{\infty}\left[K_{j7}(t-\tau)+K_{j0}(t-\tau)\right]\bar{\varsigma}_0(\omega)e^{i\omega\tau}\,d\tau\right\} \\ &= \mathrm{Re}\left\{\bar{\varsigma}_0(\omega)e^{i\omega t}\int_{-\infty}^{\infty}\left[K_{j7}(\tau)+K_{j0}(\tau)\right]e^{-i\omega\tau}\,d\tau\right\}. \end{aligned} \tag{3.36}$$

Equating (3.34) and (3.36) real and imaginary parts gives

$$\begin{aligned} X_j(\omega) &= \int_{-\infty}^{\infty}\left[K_{j7}(\tau)+K_{j0}(\tau)\right]e^{-i\omega\tau}\,d\tau \\ X_j(\omega) &= \mathcal{F}K_{j7} + \mathcal{F}K_{j0}. \end{aligned}$$

The forward speed case differs by the employment of ω_e throughout, giving

$$X_j(\omega_e) = \mathcal{F}_e K_{j7} + \mathcal{F}_e K_{j0}. \tag{3.37}$$

Thus, the exciting force in the frequency domain may be determined at both zero and forward speed from the Fourier transform of the impulse response functions for the Froude-Krylov and diffraction forces, based on a wave of impulsive elevation.

CHAPTER IV

THE USE OF NONIMPULSIVE METHODS IN THE DETERMINATION OF SYSTEM RESPONSE CHARACTERISTICS

4.1 Nonimpulse Methods

Liapis and Beck (1985) employed a fictitious velocity for the specified body motion in the radiation problems. The velocity was $\dot{\varsigma}_k(t) = \delta(t)$ where $\varsigma_k(t) = H(t)$. Because of the singular nature of the velocity, the responses proportional to $\dot{\varsigma}_k$ and ς_k were handled separately. A benefit of this method is that from one input the response at all frequencies is determined simultaneously. This can also prove to be a disadvantage because the resolution in time must be sufficient to determine properly the response at high frequency. This problem is common in digital signal analysis, where high frequency content is aliased to lower frequency if the sample period is too large.

The boundary condition developed in the previous chapter for the diffraction problem contains no infinite velocities, and thus there is no need to consider separately responses proportional to generalized functions as was done by Liapis and Beck. This fact suggests that if a specified motion in the radiation modes could be formed that contains a broad range of input frequencies but a finite amplitude, the radiation and diffraction problems could be solved by a consistent method. If the specified input for the radiation modes does not contain frequency content outside the range of interest for the particular problem, the results might be improved.

4.2 The Choice of a Nonimpulsive Input

An input is desired that has a finite maximum and a sufficiently broad frequency content. By considering the Fourier transform of the input, several things may be noted. Let $\dot{\varsigma}(t)$ be the specific input, with the Fourier transform given as

$$\bar{\dot{\varsigma}}(\omega) = \mathcal{F}\dot{\varsigma}(t)$$

where the definition of the Fourier transform is given by (3.6).

First note that for $\dot{\varsigma}(t) = \delta(t)$, $\bar{\dot{\varsigma}}(\omega) = 1$; that is, an input of impulsive nature contains all frequencies with equal amplitude. Conversely, a sinusoidal input in time has a Fourier transform represented as an impulse and contains frequency content at one frequency only. Finally,

$$\bar{\dot{\varsigma}}(0) = \int_{-\infty}^{\infty} \dot{\varsigma}(t)\, dt = \varsigma(\infty) - \varsigma(-\infty),$$

which is to say that the zero frequency content of the signal is given as the integral of the input. The implication of this fact is that if the chosen input has a zero final displacement there is no zero frequency content.

These facts suggest that a transient and peaked velocity with nonzero final displacement is the best choice of input. The input

$$\dot{\varsigma}(t) = \sqrt{\frac{a}{\pi}} e^{-at^2}$$

meets these qualifications. The Fourier transform is given by

$$\bar{\dot{\varsigma}}(\omega) = e^{-\omega^2/4a},$$

with

$$\bar{\dot{\varsigma}}(0) = \int_{-\infty}^{\infty} \dot{\varsigma}(t)\, dt = 1.$$

This choice of input has the useful characteristic that for $a \to \infty$ the behavior is identical to that of the input $\dot{\varsigma}(t) = \delta(t)$. It may also be seen that by variation of a the frequency content may be easily controlled.

4.3 The Determination of Frequency Domain and Impulse Response Behavior for Zero Forward Speed

First consider the solution of the integral equation (2.6) with $U_0 = 0$ and

$$\frac{\partial \phi_k}{\partial n} = n_k \dot{\varsigma}_k(t)$$

$$\dot{\varsigma}_k(t) = \sqrt{\frac{a}{\pi}} e^{-at^2}.$$

The force due to this input is given by (2.12) and may be written as

$$\begin{aligned} F_{jk}(t) &= -\dot{g}_{jk}(t) \\ g_{jk}(t) &= \rho \iint_{S_0} dS\, \phi_k n_j. \end{aligned} \tag{4.1}$$

The formulation of Cummins gives the force as

$$F_{jk}(t) = -\mu_{jk}\ddot{\varsigma}_k(t) - \int_0^t K_{jk}(t-\tau)\dot{\varsigma}_k(\tau)\, d\tau \tag{4.2}$$

where μ_{jk} represents the infinite frequency added mass and K_{jk} contains the memory of the fluid response. The impulse response function $K_{jk}(t)$ may be found by equating (4.1) and (4.2) as

$$-\mu_{jk}\ddot{\varsigma}_k(t) - \int_0^\infty K_{jk}(t-\tau)\dot{\varsigma}_k(\tau) = -\dot{g}_{jk}(t).$$

Rearranging and Fourier transforming gives

$$\mathcal{F}\{\dot{g}_{jk} - \mu_{jk}\ddot{\varsigma}_k\} = \mathcal{F}K_{jk}\mathcal{F}\dot{\varsigma}_k$$

$$i\omega\mathcal{F}\{g_{jk} - \mu_{jk}\dot{\varsigma}_k\} = \mathcal{F}K_{jk}\mathcal{F}\dot{\varsigma}_k,$$

and solving for K_{jk} produces

$$K_{jk}(t) = \mathcal{F}^{-1}\left\{\frac{i\omega\mathcal{F}\{g_{jk} - \mu_{jk}\dot{\varsigma}_k\}}{\mathcal{F}\dot{\varsigma}_k}\right\}. \tag{4.3}$$

For the input example $\dot{\varsigma}_k(t) = \sqrt{a/\pi}e^{-at^2}$,

$$K_{jk}(t) = \mathcal{F}^{-1}\quad\frac{i\omega\mathcal{F}\{g_{jk} - \mu_{jk}\sqrt{\frac{a}{\pi}}e^{-at^2}\}}{e^{-\omega^2/4a}}\quad. \tag{4.4}$$

The time-domain formulation may be compared with the traditional frequency-domain representation as follows. For $\varsigma_k(t) = e^{i\omega t}$,

$$F_{jk}(t) = \left[\omega^2 A_{jk}(\omega) - i\omega B_{jk}(\omega)\right]e^{i\omega t},$$

neglecting the hydrostatic restoring force term C_{jk}. Substituting $\varsigma_k(t) = e^{i\omega t}$ into (4.2) and taking the limit as $t \to \infty$ gives

$$[\omega^2\mu_{jk} - i\omega\mathcal{F}K_{jk}]e^{i\omega t} = F_{jk}(t).$$

Equating these two expressions gives

$$\omega^2\mu_{jk} - i\omega\mathcal{F}K_{jk} = \omega^2 A_{jk}(\omega) - i\omega B_{jk}(\omega). \tag{4.5}$$

Equating real and imaginary parts produces

$$A_{jk}(\omega) = \mu_{jk} - \frac{1}{\omega}\int_0^\infty K_{jk}(t)\sin\omega t\, d\omega$$

$$B_{jk}(\omega) = \int_0^\infty K_{jk}(t)\cos\omega t\, d\omega,$$

which is the result given by Liapis and Beck. From (4.5) and the (3.6) definition of the Fourier transform,

$$A_{jk}(\omega) = \mu_{jk} + \frac{1}{\omega}\,\mathrm{Im}\{\mathcal{F}K_{jk}\}$$

$$B_{jk}(\omega) = \mathrm{Re}\{\mathcal{F}K_{jk}\}$$

where Im implies that the imaginary part is taken.

It may be noted that in (4.4) while the term $e^{-\omega^2/4a}$ becomes exponentially small for $\omega \to \infty$, $i\omega\mathcal{F}\{g_{jk} - \mu_{jk}\sqrt{a/\pi}e^{-at^2}\}$ represents the memory response to an input with frequency content given as $e^{-\omega^2/4a}$. On physical grounds it may be argued that the term in braces is also exponentially small for large frequency. From (4.3) and (4.4) it may be seen that

$$i\omega\mathcal{F}\left\{g_{jk} - \mu_{jk}\sqrt{\frac{a}{\pi}}e^{-at^2}\right\} = \left\{i\omega\left(A_{jk}(\omega) - \mu_{jk}\right) + B_{jk}(\omega)\right\}e^{-\omega^2/4a}.$$

Substituting this form into (4.4) gives

$$K_{jk}(t) = \mathcal{F}^{-1}\left\{i\omega\left(A_{jk}(\omega) - \mu_{jk}\right) + B_{jk}(\omega)\right\}.$$

The term μ_{jk} represents the infinite frequency added mass, so the first term goes to zero for $\omega \to \infty$. It is well known that the infinite frequency limit of a body oscillation on the free surface is an infinite fluid problem with no waves, so the damping term $B_{jk}(\omega)$ goes to zero for $\omega \to \infty$. Thus, the Fourier transform in (4.5) can be computed. In practical terms, a discrete Fourier transform would not be expected to produce this limit correctly, and it becomes essential to assume that the right-hand side of (4.5) goes to zero at some maximum frequency. This fact provides insight on the determination of an appropriate value of a so that valid results are obtained at frequencies of interest.

4.4 The Use of a Nonimpulsive Input in the Diffraction Problem

It is worthwhile to consider using a nonimpulsive input for the diffraction problem in a similar fashion to the input for the radiation problem. In Chapter 3 an appropriate diffraction boundary condition was determined for $\varsigma_0(t) = \delta(t)$. Consider now a nonimpulsive input of the same form as in the previous section; that is,

$$\varsigma_0(t) = \sqrt{\frac{a}{\pi}}e^{-at^2}. \tag{4.6}$$

The velocity due to this wave may be found using (3.2):

$$\nabla\phi_0(P,t) = \int_{-\infty}^{\infty} \underline{K}(P, t-\tau)\varsigma_0(\tau)\,d\tau.$$

Fourier transforming produces

$$\mathcal{F}\nabla\phi_0 = \mathcal{F}\underline{K}\mathcal{F}\varsigma_0.$$

Substituting $\mathcal{F}K$ from (3.5) and $\mathcal{F}\varsigma_0 = e^{-\omega^2/4a}$ gives

$$\mathcal{F}\nabla\phi_0 = \begin{bmatrix} \hat{\imath}\cos\beta \\ \hat{\jmath}\sin\beta \\ \hat{k}i \end{bmatrix} e^{k(z-i\varpi)}e^{-\omega^2/4a}.$$

Extending to be complex conjugate symmetric and inverse Fourier transforming gives the result

$$\mathcal{F}^{-1}\mathcal{F}\nabla\phi_0 = \nabla\phi_0(P,t) = \frac{1}{\pi}\,\mathrm{Re}\left\{\begin{bmatrix}\hat{\imath}\cos\beta\\ \hat{\jmath}\sin\beta\\ \hat{k}i\end{bmatrix}\int_0^\infty \omega e^{k(z-i\omega)}e^{-\omega^2/4a}\,d\omega\right\}. \tag{4.7}$$

Then

$$\frac{\partial\phi_7}{\partial n} = -\frac{\partial\phi_0}{\partial n} = -n\cdot\nabla\phi_0(P,t)$$

where ϕ_7 represents the potential due to the incident wave given by $\varsigma_0(t) = \sqrt{a/\pi}e^{-at^2}$.

The force due to the diffracted wave is given by (2.12) as

$$F_{j7}(t) = -\dot{g}_{j7}(t) = -\rho\frac{\partial}{\partial t}\iint_{S_0} dS\,\phi_7 n_j.$$

Equating this expression with (3.11) gives

$$-\dot{g}_{jk}(t) = \int_{-\infty}^{\infty} K_{j7}(t-\tau)\varsigma_0(\tau)\,d\tau$$

where $\varsigma_0(t)$ is given by (4.6). Fourier transforming produces

$$-i\omega\mathcal{F}g_{j7} = \mathcal{F}K_{j7}\mathcal{F}\varsigma_0.$$

Therefore,

$$\begin{aligned}\mathcal{F}K_{j7} &= \frac{-i\omega\mathcal{F}g_{j7}}{\mathcal{F}\varsigma_0}\\ K_{j7}(t) &= \mathcal{F}^{-1}\left\{\frac{-i\omega\mathcal{F}g_{j7}}{\mathcal{F}\varsigma_0}\right\}.\end{aligned} \tag{4.7}$$

It was shown in Section 3.10 that the exciting forces were given as

$$X_j(\omega) = \mathcal{F}K_{j0} + \mathcal{F}K_{j7}$$

in the frequency domain. Therefore, the exciting forces and the impulse response function for the exciting force may be found from the determination of the forces due to a nonimpulsive input. It should be noted that as in the previous section, $\mathcal{F}\varsigma_0 = e^{-\omega^2/4a}$ so that the response must be assumed zero for some maximum frequency if the calculations of (4.7) are to be performed practically.

It may be noted that the boundary condition for the nonimpulsive diffracted wave differs from the impulsive wave only in the term $e^{-\omega^2/4a}$. Thus, in the limit as $a\to\infty$ the impulsive wave is recovered. The physical difference in the two waves is that the nonimpulsive wave does not contain the shortest wavelengths at finite amplitude. Since the shortest waves take an infinitely long time to pass the length of the body, it is probable that the integral equation may be more easily solved for the nonimpulsive input.

4.5 Nonimpulsive Inputs for the Forward Speed Radiation Problem

4.5.1 Equating of Impulsive and Nonimpulsive Forces

A nonimpulsive imposed motion may be used for the forward speed radiation problem as it was used in Section 4.3 for the zero speed problem. As in (2.2), let

$$\begin{aligned} \frac{\partial \phi_k}{\partial n} &= n_k \dot{\varsigma}_k(t) + m_k \varsigma_k(t) \\ \dot{\varsigma}_k(t) &= \sqrt{\frac{a}{\pi}} e^{-at^2} \\ \varsigma_k(t) &= \int_{-\infty}^{t} \dot{\varsigma}_k(\tau)\, d\tau. \end{aligned} \tag{4.8}$$

As for the zero speed case, the force due to this forced motion is given by (2.12) as

$$\begin{aligned} F_{jk}(t) &= -\dot{g}_{jk}(t) - h_{jk}(t) \\ g_{jk}(t) &= \rho \iint_{S_0} dS\, \phi_k n_j \\ h_{jk}(t) &= -\rho \iint_{S_0} dS\, \phi_k m_j - \rho \oint_{\Gamma} d\ell \phi_k n_j (\underline{\ell} \times \underline{n}) \cdot \underline{W}, \end{aligned} \tag{4.9}$$

and ϕ_k represents the solution to (2.6) with $U_0 \neq 0$ and $\partial \phi_k / \partial n$ given by (4.8).

Cummins shows that the force may be written

$$F_{jk}(t) = -\mu_{jk} \ddot{\varsigma}_k(t) - b_{jk} \dot{\varsigma}_k(t) - c_{jk} \varsigma_k(t) - \int_{-\infty}^{t} K_{jk}(t-\tau) \dot{\varsigma}_k(\tau)\, d\tau. \tag{4.10}$$

The function $K_{jk}(t)$ represents the memory as in the zero speed case. The constants μ_{jk} and b_{jk} were shown by Liapis and Beck to be

$$\begin{aligned} \mu_{jk} &= \rho \iint_{S_0} dS\, \psi_{1k} n_j \\ b_{jk} &= \rho \left[\iint_{S_0} dS\, \psi_{2k} n_j - \iint_{S_0} dS\, \psi_{1k} m_j - \oint_{\Gamma} d\ell \psi_{1k} n_j (\underline{\ell} \times \underline{n}) \cdot \underline{W} \right]. \end{aligned}$$

Physically, c_{jk} represents the infinite fluid Munk moment plus an additional contribution to the Munk moment due to the presence of the free surface at steady forward speed.

The potentials ψ_{1k} and ψ_{2k} meet the following boundary conditions:

$$\begin{aligned} \psi_{1k}, \psi_{2k} &= 0 \qquad \text{on } z = 0 \\ \nabla \psi_{1k}, \nabla \psi_{2k} &\to 0 \qquad \text{at } \infty \\ \frac{\partial \psi_{1k}}{\partial n} &= n_k \qquad \text{on } S_0 \\ \frac{\partial \psi_{2k}}{\partial n} &= m_k \qquad \text{on } S_0. \end{aligned} \tag{4.11}$$

These are both solutions to the integral equation

$$\psi + \frac{1}{2\pi}\iint_{S_0} dS\,\psi \frac{\partial}{\partial n_Q}\left(\frac{1}{r} - \frac{1}{r'}\right) = \frac{1}{2\pi}\iint_{S_0} dS\,\frac{\partial \psi}{\partial n}\left(\frac{1}{r} - \frac{1}{r'}\right).$$

It may easily be shown that the first two terms of b_{jk} sum to zero using Green's theorem, which states

$$\iiint_V dV\left[\psi_1 \nabla^2 \psi_2 - \psi_1 \nabla^2 \psi_2\right] = \iint_S dS\,\left[\psi_1 \frac{\partial \psi_2}{\partial n} - \psi_2 \frac{\partial \psi_1}{\partial n}\right]. \tag{4.12}$$

Since ψ_1 and ψ_2 are harmonic in the fluid domain V, the left-hand side is $= 0$. S is given by $S_0 \cup S_\infty \cup S_f$. On S_f, $\psi_1 = \psi_2 = 0$, and on S_∞, $\partial\psi_1/\partial n = \partial\psi_2/\partial n = 0$. Thus, (4.12) may be rewritten as

$$\iint_{S_0} dS\,[\psi_1 m_j - \psi_2 n_j] = 0,$$

with $\partial\psi_1/\partial n$ and $\partial\psi_2/\partial n$ given by (4.11) above. Therefore, b_{jk} may be rewritten as simply

$$b_{jk} = -\rho \oint_\Gamma d\ell \psi_{1k} n_j (\underline{\ell} \times \underline{n}) \cdot \underline{W}.$$

The potential ψ_1 represents the infinite frequency limit of the radiation problem where no waves are produced. ψ_1 is zero on the free surface so that b_{jk} is zero for the vertical modes heave, pitch, and roll. For the other three modes the potential is singular at the free surface and body intersection. However, for all modes the damping must go to zero at infinite frequency, and thus b_{jk} must go to zero for the horizontal and vertical modes. The term b_{jk} will be dropped from further expressions for the force.

To relate the force due to a nonimpulsive motion to the general expression for the force (4.10), consider the motion $\varsigma_k(t)$ given by (4.8).

Equating (4.9) and (4.10) gives

$$-\mu_{jk}\ddot{\varsigma}_k(t) - c_{jk}\varsigma_k(t) - \int_{-\infty}^{t} K_{jk}(t-\tau)\dot{\varsigma}_k(\tau)\,d\tau = -\dot{g}_{jk}(t) - h_{jk}(t). \tag{4.13}$$

Taking the limit as $t \to \infty$ of this equation, assuming the limit as $t \to \infty$ of $K_{jk}(t) = 0$, gives

$$-c_{jk} = \lim_{t \to \infty} -\dot{g}_{jk}(t) - h_{jk}(t).$$

To determine c_{jk}, the large time limit of the radiation forces must be found.

4.5.2 The Large Time Limits of the Radiation Forces

To consider the limit as $t \to \infty$ of $\dot{g}_{jk}(t)$ and $h_{jk}(t)$, consider the potential $\phi_k(t)$. Since $\partial\phi_k/\partial n$ becomes independent of time for $t \to \infty$, ϕ_k must become independent of time for

$t \to \infty$. The limit for ϕ_k may be found from the integral equation (2.6) for the radiation problem

$$\begin{aligned}\phi_k(P,t) + \frac{1}{2\pi}\iint_{S_0} dS\,\phi_k(Q,t)\frac{\partial}{\partial n_Q}\left(\frac{1}{r}-\frac{1}{r'}\right) &= \frac{1}{2\pi}\iint_{S_0} dS\,\frac{\partial}{\partial n}\phi_k(Q,t)\left(\frac{1}{r}-\frac{1}{r'}\right)\\ -\frac{1}{2\pi}\int_{-\infty}^{t} d\tau \iint_{S_0} dS\left[\phi(Q,\tau)\frac{\partial}{\partial n}\tilde{G}(P,Q,t-\tau) - \tilde{G}(P,Q,t-\tau)\frac{\partial}{\partial n}\phi_k(Q,\tau)\right]&\\ +\frac{1}{2\pi g}\int_{-\infty}^{t} d\tau \oint_{\Gamma} d\eta\Big[U_0^2\big(\tilde{G}(P,Q,t-\tau)\phi_\xi(Q,\tau) - \phi(Q,\tau)\tilde{G}_\xi(P,Q,t-\tau)\big)&\\ + U_0\big(\phi(Q,\tau)\tilde{G}_\tau(P,Q,t-\tau) - \tilde{G}(P,Q,t-\tau)\phi_\tau(Q,\tau)\big)\Big]&\end{aligned} \tag{4.14}$$

where

$$\frac{\partial \phi_k}{\partial n} = n_k\dot{\varsigma}_k(t) + m_k\varsigma_k(t).$$

Using $\dot{\varsigma}_k(t)$ from (4.8), note that

$$\lim_{t\to\infty} \quad \frac{\partial \phi_k}{\partial n} = m_k.$$

It may be observed that for two functions, $f(t)$ and $g(t)$, the convolution may be rewritten as

$$\int_{-\infty}^{t} f(t)g(t-\tau)\,d\tau = \int_0^{\infty} f(t-\tau)g(\tau)\,d\tau.$$

If $f(t)$ and $g(t)$ have the properties that

$$\lim_{t\to\infty} \quad \begin{aligned} f(t) &= C\\ g(t) &= 0, \end{aligned} \tag{4.15}$$

then

$$\lim_{t\to\infty} \quad \int_0^{\infty} f(t-\tau)g(t)\,d\tau = C\int_0^{\infty} g(t)\,d\tau.$$

Noting that ϕ_k and $\partial\phi_k/\partial n$ meet the condition for $f(t)$ in (4.15) and $\tilde{G}(P,Q,t-\tau)$ meets the condition of $g(t)$, the limit $t\to\infty$ of (4.14) may be written

$$\begin{aligned}\phi_{k\infty}(P) + \frac{1}{2\pi}\iint_{S_0} dS\,\phi_{k\infty}\frac{\partial}{\partial n_Q}\left(\frac{1}{r}-\frac{1}{r'}\right) &= \frac{1}{2\pi}\iint_{S_0} dS\,m_k\left(\frac{1}{r}-\frac{1}{r'}\right)\\ -\frac{1}{2\pi}\iint_{S_0} dS\left[\phi_{k\infty}\int_0^{\infty}\frac{\partial \tilde{G}}{\partial n}\,dt - m_k\int_0^{\infty}\tilde{G}\,dt\right]&\\ +\frac{1}{2\pi g}\oint_{\Gamma} d\eta\,U_0^2\left[\phi_{k\infty\xi}\int_0^{\infty}\tilde{G}\,dt - \phi_{k\infty}\int_0^{\infty}\tilde{G}_\xi\,dt\right],&\end{aligned} \tag{4.16}$$

where use is made of the fact that

$$\frac{\partial}{\partial t}\phi_{k\infty} \to 0 \qquad \text{for} \qquad t\to\infty$$

$$\int_0^{\infty}\frac{\partial}{\partial t}\tilde{G}\,dt = \tilde{G}(\infty) - \tilde{G}(0) = 0.$$

Since in general,

$$\int_0^\infty \tilde{G}\, d\tau \neq 0 \quad \text{and} \quad \int_0^\infty \frac{\partial \tilde{G}}{\partial n}\, d\tau \neq 0,$$

$$\lim_{t \to \infty} \quad \phi_k(P,t) \to \phi_{k\infty}(P) \neq 0$$

$$\lim_{t \to \infty} \quad g_{jk}(t) = \rho \iint_{S_0} dS\, \phi_{k\infty} n_j$$

$$\lim_{t \to \infty} h_{jk}(t) = -\rho \iint_{S_0} dS\, \phi_{k\infty} m_j - \rho \oint_\Gamma d\ell \phi_{k\infty} n_j (\underline{\ell} \times \underline{n}) \cdot \underline{W}.$$

Since $\phi_{k\infty}$ is independent of time $\dot{g}_{jk}(\infty) = 0$, the force may be written as

$$F_{jk}(\infty) = \lim_{t \to \infty} - h_{jk}(t) = -c_{jk},$$

so that

$$c_{jk} = -\rho \iint_{S_0} dS\, \phi_{k\infty} m_j - \rho \oint_\Gamma d\ell \phi_{k\infty} n_j (\underline{\ell} \times \underline{n}) \cdot \underline{W}.$$

It may be shown that the term $K_{jk}(t)$ as defined in Liapis and Beck (1985) has the limit

$$\lim_{t \to \infty} K_{jk}(t) = c_{jk} - \tilde{c}_{jk} \neq 0$$

where

$$\tilde{c}_{jk} = -\rho \iint_{S_0} dS\, \psi_{2k} m_j - \rho \oint_\Gamma d\ell \psi_{2k} n_j (\underline{\ell} \times \underline{n}) \cdot \underline{W}.$$

The formulation of Liapis and Beck implies that $K_{jk} \to 0$ for $t \to \infty$ by taking the Fourier transform without regard to the large time limit. Ogilvie (1964) states in his Appendix B that, in fact, the term does go to zero. It may be shown that if their $K_{jk}(t) \to 0$ for large time, the free surface boundary condition is not met. The result is analagous to neglecting the terms involving $\int_0^\infty \tilde{G}\, d\tau$ and $\int_0^\infty \partial \tilde{G}/\partial n\, d\tau$ in (4.16). Their formulation may be corrected as follows by subtracting the large time limit and adding it to c_{jk}. Denote the terms $K_{jk}(t)$ and c_{jk}, which are given by equation 36 of Liapis and Beck, as $\tilde{K}_{jk}(t)$ and $\tilde{c}_{jk}$, respectively. The following substitutions,

$$K_{jk}(t) = \tilde{K}_{jk}(t) - \lim_{t \to \infty} \tilde{K}_{jk}(t)$$

$$c_{jk}(t) = \tilde{c}_{jk}(t) + \lim_{t \to \infty} \tilde{K}_{jk}(t),$$

may be employed in their equation 40 to produce the correct results for the added mass and damping.

4.5.3 The Fourier Transforms of the Radiation Forces

To determine the added mass and damping and impulse response functions for the radiation modes, (4.13) must be Fourier transformed as in Section 4.3 for the zero speed problem. Rearranging and Fourier transforming (4.13) gives

$$\mathcal{F}\{\dot{g}_{jk} + h_{jk} - \mu_{jk}\ddot{\varsigma}_k - c_{jk}\varsigma_k(t)\} = \mathcal{F}K_{jk}\mathcal{F}\dot{\varsigma}_k. \tag{4.17}$$

From the form of $\varsigma_k(t)$ and the previous discussion, it may be seen that the limits of the terms on the left-hand side are

$$\begin{aligned} \dot{g}_{jk} &= 0 \\ \mu_{jk}\ddot{\varsigma}_k(t) &= 0 \\ \lim_{t \to \infty} \quad c_{jk}\varsigma_k(t) &= c_{jk} \\ h_{jk}(t) &= c_{jk}, \end{aligned}$$

so that the term in braces goes to zero for $t \to \infty$.

The added mass and damping may be determined as in Section 4.3 for zero speed to be

$$\begin{aligned} A_{jk}(\omega) &= \mu_{jk} + \frac{1}{\omega}\,\mathrm{Im}\,\{\mathcal{F}K_{jk}\} \\ B_{jk}(\omega) &= \mathrm{Re}\,\{\mathcal{F}K_{jk}\}. \end{aligned} \tag{4.18}$$

Dividing (4.17) by $\mathcal{F}\dot{\varsigma}_k$ gives

$$\frac{\mathcal{F}\{\dot{g}_{jk} - \mu_{jk}\ddot{\varsigma}_k + h_{jk} - c_{jk}\varsigma_k\}}{\mathcal{F}\{\dot{\varsigma}_k\}} = \mathcal{F}\{K_{jk}\}. \tag{4.19}$$

Equation (4.19) may be used in conjunction with (4.18) to compute the added mass and damping from the nonimpulsive input case. It may be shown as was discussed for the zero speed case that the high frequency limit of the fraction in the left-hand side of (4.19) goes to zero.

4.6 A Nonimpulsive Input in the Diffraction Problem with Forward Speed

An incident wave with a nonimpulsive elevation was considered for the zero speed case in Section 4.4 and can be developed along similar lines for the forward speed case.

Consider an input $\varsigma_0(t)$ where the incident wave velocities are given by

$$\nabla\phi_0(P,t) = \int_{-\infty}^{\infty} \underline{K}(P, t-\tau)\varsigma_0(\tau)\,d\tau.$$

Fourier transforming with respect to ω_e produces

$$\begin{aligned} \mathcal{F}_e\nabla\phi_0 &= \mathcal{F}_e\underline{K}\mathcal{F}_e\varsigma_0 \\ &= \begin{bmatrix} \hat{\imath}\cos\beta \\ \hat{\jmath}\sin\beta \\ \hat{k}i \end{bmatrix} \omega e^{k(z-i\varpi)}\bar{\varsigma}_0(\omega_e) \end{aligned}$$

where $\mathcal{F}_e\underline{K}$ is given by (3.18). Let $\varsigma_0(t) = \sqrt{a/\pi}e^{-at^2}$; then $\bar{\varsigma}_0(\omega_e) = e^{-\omega_e^2/4a}$, and

$$\nabla\phi_0(P,t) = \frac{1}{\pi}\,\mathrm{Re}\left\{\begin{bmatrix}\hat{\imath}\cos\beta\\ \hat{\jmath}\sin\beta\\ \hat{k}i\end{bmatrix}\int_0^\infty \omega\, e^{k(z-i\varpi)}\, e^{-\omega_e^2/4a}\, e^{i\omega_e t}\, d\omega_e\right\}.$$

While it may not appear obvious from this formula, the integral is very difficult to evaluate because of the encounter frequency ω_e^2 in the exponential term.

A better choice of input is $\bar{\varsigma}_0(\omega_e) = e^{-\omega^2/4a}$ where $\omega_e = \omega - kU_0\cos\beta$. For this case,

$$\nabla\phi_0(P,t) = \frac{1}{\pi}\,\mathrm{Re}\left\{\begin{bmatrix}\hat{\imath}\cos\beta\\ \hat{\jmath}\sin\beta\\ \hat{k}i\end{bmatrix}\int_0^\infty \omega\, e^{k(z-i\varpi)}\, e^{-\omega^2/4a}\, e^{i\omega_e t}\, d\omega_e\right\}, \tag{4.20}$$

and

$$\varsigma_0(t) = \frac{1}{\pi}\,\mathrm{Re}\left\{\int_0^\infty e^{-\omega^2/4a}\, e^{i\omega_e t}\, d\omega_e\right\}.$$

The integral equation (2.6) may now be solved for ϕ_7 where

$$\frac{\partial\phi_7}{\partial n} = -n\cdot\nabla\phi_0(P,t)$$

from (4.20).

The force due to the diffracted wave is then given by (2.12) as

$$F_{j7}(t) = -\dot{g}_{j7}(t) - h_{j7}(t) \tag{4.21}$$

where

$$g_{j7}(t) = \rho\iint_{S_0} dS\,\phi_7 n_j$$

$$h_{j7}(t) = -\rho\iint_{S_0} dS\,\phi_7 m_j - \rho\oint_\Gamma d\ell\phi_7 n_j(\underline{\ell}\times\underline{n})\cdot\underline{W}.$$

Equating (4.21) with the expression for the force given by (3.33) yields

$$-\dot{g}_{jk}(t) - h_{jk}(t) = \int_{-\infty}^\infty K_{j7}(t-\tau)\varsigma_0(t)\,d\tau,$$

and Fourier transforming produces

$$-i\omega_e\mathcal{F}_e g_{jk} - \mathcal{F}_e h_{jk} = \mathcal{F}_e K_{j7}\mathcal{F}_e\varsigma_0.$$

Therefore,

$$\begin{aligned}\mathcal{F}_e K_{j7} &= \frac{-i\omega_e\mathcal{F}_e g_{jk} - \mathcal{F}_e h_{jk}}{\mathcal{F}_e\varsigma_0}\\ K_{j7} &= \mathcal{F}_e^{-1}\left\{\frac{-i\omega_e\mathcal{F}_e g_{jk} - \mathcal{F}_e h_{jk}}{\mathcal{F}_e\varsigma_0}\right\}.\end{aligned} \tag{4.22}$$

As was shown in Section 3.10, the exciting force in the frequency domain is given by

$$X_j(\omega_e) = \mathcal{F}_e K_{j0} + \mathcal{F}_e K_{j7}.$$

Therefore, it is possible to determine the frequency-domain representation or time-domain impulse response function for the diffraction forces at steady forward speed from a non-impulsive input. Equation (4.22) requires that the numerator goes to zero more quickly than $\mathcal{F}\varsigma_0$ does. Therefore, a must be sufficiently large so that the exciting force may be considered zero in the range that $e^{-\omega^2/4a}$ becomes small as discussed in Section 4.4 for the zero speed problem.

CHAPTER V

NUMERICAL METHODS

5.1 The Integral Equation

Equation (2.6) can be solved using a numerical scheme. The approach used here is very similar to that of Liapis and Beck (1985). The basic concept is to discretize the body surface S_0 into panels that approximate the surface and assume the potential ϕ constant on each panel. The boundary condition $\partial\phi/\partial n$ is known, and the function $\widetilde{G}(P, Q, t-\tau)$ is given in terms of an infinite integral. The evaluation of $\widetilde{G}$ and its derivatives follows the same basic approach as Liapis (1986); details are given in Appendix B. The integrals over the panels can then be performed partially numerically and partially analytically so that the equation reduces to a system of simultaneous algebraic equations, with the unknowns being the potential strength on each panel. The integral equation is a Volterra integral equation in time and is solved by a trapezoidal integration scheme. A consistent approach was used for zero and forward speed as well as for all modes of motion. The most general development is given here, with the zero speed case included by setting $U_0 = 0$ in the final result.

5.2 The Approximation of the Body by Discrete Panels

The approach given by Hess and Smith (1964) is used to discretize the body surface into plane panels. Points on the body surface are chosen as corners of the panels. In areas of compound curvature it has been noted that the panel cannot pass through the chosen corner points, so that the panel vertices approximate those of the input data in a least squares sense. Hess and Smith's development includes all the details of the determination of the pertinent geometric quantities for these panels. The direction of the unit normal chosen by Hess and Smith is opposite to that employed here and must be taken into account.

5.3 The Discretized Integral Equation

The integral equation (2.6) includes line integrals of a form that cannot be readily evaluated. The line integral terms are

$$-\frac{U_0^2}{2\pi g}\int_{-\infty}^{t} d\tau \oint_\Gamma d\eta \left[\phi_k \frac{\partial \tilde{G}}{\partial \xi} - \tilde{G}\frac{\partial \phi_k}{\partial \xi}\right] + \frac{U_0}{2\pi g}\int_{-\infty}^{t} d\tau \oint_\Gamma d\eta \left[\phi_k \frac{\partial \tilde{G}}{\partial \tau} - \tilde{G}\frac{\partial \phi_k}{\partial \tau}\right]. \tag{5.1}$$

The unknown terms are $\partial\phi_k/\partial\xi$ and $\partial\phi_k/\partial\tau$. Liapis has shown that for a wall-sided body the term

$$-\oint_\Gamma d\eta \tilde{G}\frac{\partial \phi_k}{\partial \xi} \cong -\oint_\Gamma d\eta \tilde{G}\frac{\partial \phi_k}{\partial n}(\underline{n}\cdot\hat{\imath}) + \oint_\Gamma d\eta \phi_k \frac{\partial \tilde{G}}{\partial \ell}(\underline{\ell}\cdot\hat{\imath}) + \oint_\Gamma d\ell \phi_k \tilde{G}\frac{\partial}{\partial \ell}[(\underline{\ell}\cdot\hat{\imath})(\underline{\ell}\cdot\hat{\jmath})], \tag{5.2}$$

which does not include derivatives of the unknown potential and is more easily determined numerically. It is assumed that most bodies of interest are wall-sided or nearly so at the waterline.

The line integral contribution results from the application of Stokes theorem on the free surface. The line integral is properly evaluated on the free surface. However, the potential is not known on the free surface. The value at $z = 0$ is approximated here by a linear interpolation of the constant potentials on the panel that meets the free surface and the next panel directly below it. Because the intersection of the body and free surface represents a singular line, the implications of this approximation are not altogether obvious.

The second term of (5.1) was integrated by parts by Liapis to give

$$\frac{U_0}{\pi g}\int_{-\infty}^{t} d\tau \oint_\Gamma d\eta \phi_k \frac{\partial \tilde{G}}{\partial \tau}. \tag{5.3}$$

Alternatively, this term may be integrated by parts as

$$\begin{aligned}\frac{U_0}{2\pi g}\int_{-\infty}^{t} d\tau \oint_\Gamma d\eta \left[\phi_k \frac{\partial \tilde{G}}{\partial \tau} - \tilde{G}\frac{\partial \phi_k}{\partial \tau}\right] &= -\frac{U_0}{\pi g}\int_{-\infty}^{t} d\tau \oint_\Gamma d\eta \tilde{G}\frac{\partial \phi_k}{\partial \tau} \\ &+\frac{U_0}{\pi g}\oint_\Gamma d\eta \left[\phi_k(P,t)\tilde{G}(P,Q,0) - \phi_k(P,-\infty)\tilde{G}(P,Q,\infty)\right]\end{aligned}$$

where the second term on the right-hand side goes to zero because of the initial conditions on ϕ_k and the characteristics of $\tilde{G}$. The final result is

$$-\frac{U_0}{\pi g}\int_{-\infty}^{t} d\tau \oint_\Gamma d\eta \tilde{G}\frac{\partial \phi_k}{\partial \tau}. \tag{5.4}$$

Either of these forms may be used, but (5.4) requires numerical differentiation of ϕ_k with respect to time. However, it has been found that better results are produced when the form (5.4) is used rather than (5.3), because ϕ_k is a slowly varying function. Although $\partial\tilde{G}/\partial\tau$ is known analytically, it becomes large near $t = 0$ and amplifies errors in ϕ_k.

The line integral (5.4) is computed as follows:

$$\frac{U_0}{\pi g}\int_{-\infty}^{t} d\tau \oint_{\Gamma} d\eta \tilde{G}\frac{\partial \phi_k}{\partial \tau} = \frac{U_0}{\pi g}\sum_{i=1}^{M'}\oint_{\Gamma_i} d\eta \int_{-\infty}^{t} d\tau \tilde{G}\frac{\partial \phi_k}{\partial \tau}$$

where M' denotes the number of panels on the free surface.

Approximating the derivative of ϕ_k as

$$\frac{\partial \phi_k}{\partial \tau} \cong \frac{\phi_k(t_{n+1}) - \phi_k(t_{n-1})}{2\Delta t}$$

and integrating using a trapezoidal rule gives

$$\int_{-\infty}^{t} d\tau \tilde{G}\frac{\partial \phi_k}{\partial \tau} \cong \Delta t \sum_{n=1}^{N-1} \tilde{G}(t_N - t_n)\frac{\phi_k(t_{n+1}) - \phi_k(t_{n-1})}{2\Delta t}. \tag{5.5}$$

The end weights of the integration are not included because the end terms are 0.

It was found that this trapezoidal integration scheme was not accurate enough for $\tilde{G}$ with $t-\tau$ small, because of the magnitude and oscillatory nature of $\tilde{G}$ near the free surface. The line integral may be approximated more closely by dividing it into two parts as

$$\int_{-\infty}^{t} d\tau \tilde{G}\frac{\partial \phi_k}{\partial \tau} = \int_{-\infty}^{t_{N^*}} d\tau \tilde{G}\frac{\partial \phi_k}{\partial \tau} + \int_{t_{N^*}}^{t} d\tau \tilde{G}\frac{\partial \phi_k}{\partial \tau}.$$

Using the approximation given in (5.5) for the first part,

$$\int_{-\infty}^{t_{N^*}} d\tau \tilde{G}\frac{\partial \phi_k}{\partial \tau} \cong \Delta t \sum_{n=1}^{N^*-1} \tilde{G}(t_N - t_n)\frac{\phi_k(t_{n+1}) - \phi_k(t_{n-1})}{2\Delta t} + \frac{1}{2}\Delta t \tilde{G}(t_N - t_{N^*})\frac{\phi_k(t_{N^*+1}) - \phi_k(t_{N^*-1})}{2\Delta t}.$$

The sum may be rewritten as

$$\begin{aligned}
&\frac{1}{2}\sum_{n=1}^{N^*-1} \tilde{G}(t_N - t_n)\phi_k(t_{n+1}) - \frac{1}{2}\sum_{n=1}^{N^*-1} \tilde{G}(t_N - t_n)\phi_k(t_{n-1}) \\
&\qquad = \frac{1}{2}\sum_{n=2}^{N^*} \tilde{G}(t_N - t_{n-1})\phi_k(t_n) - \frac{1}{2}\sum_{n=1}^{N^*-2} \tilde{G}(t_N - t_{n+1})\phi_k(t_n) \\
&\qquad = \frac{1}{2}\sum_{n=2}^{N^*-2} \phi_k(t_n)\left[\tilde{G}(t_N - t_{n-1}) - \tilde{G}(t_N - t_{n+1})\right] + \frac{1}{2}\tilde{G}(t_N - t_{N^*-1})\phi_k(t_{N^*}) \\
&\qquad\qquad + \frac{1}{2}\tilde{G}(t_N - t_{N^*-2})\phi_k(t_{N^*-1}) - \frac{1}{2}\tilde{G}(t_N - t_2)\phi_k(t_1).
\end{aligned}$$

Noting that from the initial conditions $\phi_k(t_1) = 0$, assuming ϕ_k constant across a panel, and combining terms gives

$$\begin{aligned}
\oint_{\Gamma_i} d\eta \int_{-\infty}^{t_{N^*}} d\tau \tilde{G}\frac{\partial \phi_k}{\partial \tau} &\cong \frac{1}{2}\sum_{n=2}^{N^*-2} \phi_k(t_n)\left[\oint_{\Gamma_i} d\eta \tilde{G}(t_N - t_{n-1}) - \oint_{\Gamma_i} d\eta \tilde{G}(t_N - t_{n+1})\right] \\
&\quad + \frac{1}{2}\oint_{\Gamma_i} d\eta \tilde{G}(t_N - t_{N^*-2})\phi_k(t_{N^*-1}) + \frac{1}{2}\oint_{\Gamma_i} d\eta \tilde{G}(t_N - t_{N^*-1})\phi_k(t_{N^*}) \\
&\quad + \frac{1}{4}\oint_{\Gamma_i} d\eta \tilde{G}(t_N - t_{N^*})\left[\phi_k(t_{N^*+1}) - \phi_k(t_{N^*-1})\right].
\end{aligned}$$

The integral from t_{N^*} to t may be evaluated more accurately as follows. Let $\partial\phi_k/\partial\tau$ be assumed constant over the interval Δt and given as

$$\frac{\partial\phi_k}{\partial\tau} = \frac{\phi_k(t_{n+1}) - \phi_k(t_n)}{\Delta t};$$

substituting gives

$$\int_{t_{N^*}}^{t_N} d\tau\, \tilde{G}\frac{\partial\phi_k}{\partial\tau} \cong \sum_{n=N^*}^{N-1} \frac{\phi_k(t_{n+1}) - \phi_k(t_n)}{\Delta t} \int_{t_n}^{t_{n+1}} d\tau\, \tilde{G}(P, Q, t_N - \tau).$$

To compute the line integral, ϕ_k is assumed constant along the panel, and Gaussian quadrature is used to evaluate the integral in time. The result is

$$\oint_{\Gamma_i} d\eta \int_{t_{N^*}}^{t_N} d\tau\, \tilde{G}\frac{\partial\phi_k}{\partial\tau} \cong \frac{1}{\Delta t}\sum_{n=N^*}^{N-1} \left[\phi_k(t_{n+1}) - \phi_k(t_n)\right] \oint_{\Gamma_i} d\eta \int_{t_n}^{t_{n+1}} d\tau\, \tilde{G}(P, Q, t_N - \tau).$$

Using this development for (5.4) and the line integral terms given in (5.2), the integral equation (2.6) in discretized form is

$$\sum_{i=1}^{M} A_{mi}\left[\phi_k(t_N)\right]_i = B_m(t_N) \qquad m = 1, 2, \ldots, M \tag{5.6}$$

where

$M =$ number of quadrilateral panels

$N =$ current time step

$\left[\phi_k(t_N)\right]_i =$ value of the potential $\phi_k(P,t)$ on the ith panel at t_N

$$A_{mi} = 1 - \frac{1}{2\pi}\iint_{S_i} dS\, \underline{n}\cdot\nabla\left(\frac{1}{r'}\right) + \frac{U_0}{2\pi g\Delta t}\oint_{\Gamma_i} d\eta \int_{t_{N-\Delta t}}^{t_N} d\tau\, \tilde{G}(t_N - \tau) \quad i = m$$

$$= \frac{1}{2\pi}\iint_{S_i} dS\, \underline{n}\cdot\nabla\left(\frac{1}{r} - \frac{1}{r'}\right) + \frac{U_0}{2\pi g\Delta t}\oint_{\Gamma_i} d\eta \int_{t_{N-\Delta t}}^{t_N} d\tau\, \tilde{G}(t_N - \tau) \quad i \neq m$$

$$B_m = B_m^{(1)} + B_m^{(2)}$$

$$B_m^{(1)} = \sum_{i=1}^{M}\left\{\frac{1}{2\pi}\iint_{S_i} dS\left(\frac{1}{r} - \frac{1}{r'}\right)\frac{\partial}{\partial n}\phi_k(Q, t_N)\right.$$

$$\left. + \frac{\Delta t}{2\pi}\sum_{n=1}^{N-1}\iint_{S_i} dS\, \tilde{G}(P, Q, t_N - t_n)\frac{\partial}{\partial n}\phi_k(Q, t_n)\right\}$$

$$+ \sum_{i=1}^{M'}\left\{\frac{\Delta t U_0^2}{2\pi g}\sum_{n=1}^{N-1}\oint_{\Gamma_i} d\eta\, \tilde{G}(P, Q, t_N - t_n)\frac{\partial}{\partial n}\phi_k(Q, t_n)\right\}$$

$$B_m^{(2)} = -\sum_{i=2}^{M}\left\{\frac{\Delta t}{2\pi}\sum_{n=1}^{N-1}\iint_{S_i} dS\,\phi_k(Q,t_n)\frac{\partial}{\partial n_Q}\tilde{G}(P,Q,t_N-t_n)\right\}$$
$$-\sum_{i=1}^{M'}\frac{\Delta t U_0^2}{2\pi g}\sum_{n=1}^{N-1}\phi_k(Q,t_n)\left[\oint_{\Gamma_i} d\eta\left((\underline{\ell}\cdot\hat{\imath})\frac{\partial\tilde{G}}{\partial\ell}+\frac{\partial\tilde{G}}{\partial\xi}\right)\right.$$
$$\left.+\oint_{\Gamma_i} d\ell\tilde{G}\frac{\partial}{\partial\ell}((\underline{\ell}\cdot\hat{\imath})(\underline{\ell}\cdot\hat{\jmath}))\right]$$
$$-\frac{U_0}{\pi g}\sum_{i=1}^{M'}\left\{\frac{1}{2}\sum_{n=2}^{N^*-1}\phi_k(Q,t_n)\oint_{\Gamma_i} d\eta\left[\tilde{G}(t_N-t_n+\Delta t)-\tilde{G}(t_N-t_n-\Delta t)\right]\right.$$
$$+\sum_{n=N^*}^{N-2}\frac{\left[\phi_k(t_{n+1})-\phi_k(t_n)\right]}{\Delta t}\oint_{\Gamma_i} d\eta\int_{t_n}^{t_{n+1}} d\tau\,\tilde{G}(P,Q,t_N-\tau)$$
$$+\frac{1}{4}\left[(\phi_k(t_{N^*-1})+\phi_k(t_{N^*+1})\right]\oint_{\Gamma_i} d\eta\,\tilde{G}(t_N-t_{N^*})+\frac{1}{2}\phi_k(t_{N^*})\oint d\eta\,\tilde{G}(t_N-t_{N^*-1})$$
$$\left.-\frac{\phi_k(t_{N-1})}{\Delta t}\oint_{\Gamma_i} d\eta\int_{t_{N-1}}^{t_N} d\tau\,\tilde{G}(P,Q,t_N-\tau)\right\}$$

$M' =$ number of panels that intersect the free surface.

The initial conditions on the potential and on the Green's function are $\phi_k(P,t_1)=0$ and $G(P,Q,t_N-t_N)=0$, so that the endpoints of the trapezoidal integration $(n=1, n=N)$ are zero and the half weights are not included. The contribution to $B_m^{(2)}$ due to the term involving $\partial\phi_k/\partial\tau$ has been manipulated into a form that is simpler to calculate numerically.

The term $B_m^{(2)}$ includes the unknown potential ϕ_k, while the term $B_m^{(1)}$ includes known functions only. The term $B_m^{(1)}$ may therefore be computed more efficiently by a fast Fourier transform convolution than by the direct convolution as shown. Because $\phi_k(t_N)$ is unknown, all terms involving it have been moved to the left-hand side of (5.6). It may also be noted that the left-hand side matrix is independent of time and needs to be inverted only once.

5.4 The Green's Function Integration over Panels

The assumption of a constant potential over a panel leaves surface integrals of the following forms to be evaluated:

$$I_1 = \iint_{S_i} dS\,\frac{\partial\phi}{\partial n}\left(\frac{1}{r}-\frac{1}{r'}\right)$$
$$I_2 = \iint_{S_i} dS\,\frac{\partial}{\partial n_Q}\left(\frac{1}{r}-\frac{1}{r'}\right)$$
$$I_3 = \iint_{S_i} dS\,\frac{\partial\phi}{\partial n}\tilde{G}(P,Q,t-\tau)$$
$$I_4 = \iint_{S_i} dS\,\frac{\partial}{\partial n_Q}\tilde{G}(P,Q,t-\tau).$$

The integral I_2 has been evaluated analytically by Hess and Smith, who give a very complete development of its evaluation with a multipole and simple source approach given for large r. The integral I_1 may also be calculated analytically for the radiation case where $\partial\phi/\partial n$ is constant across the panel. For the diffraction problems this is not the case, and a bilinear mapping and Gaussian quadrature method as employed by Liapis (1986) and discussed in Appendix B is used. It was found that when r is small it is important to determine the terms involving $(1/r - 1/r')$ accurately. $\partial\phi/\partial n$ is assumed constant when r is small, so I_1 may be evaluated analytically. The integrals I_3 and I_4 are both computed by the coordinate mapping and Gaussian quadrature method. For the diffraction problem, $\partial\phi/\partial n$ is not constant across a panel and must be included in the integration. For the radiation problems, $\partial\phi/\partial n$ is constant and may be taken outside the integrals I_1, I_3, and I_4.

5.5 The Numerical Determination of Forces

The forces on the ship due to the potential ϕ_k may be computed by (2.7):

$$F_{jk}(t) = -\frac{\partial}{\partial t} g_{jk}(t) - h_{jk}(t)$$

$$g_{jk} = \rho \iint_{S_0} dS\, \phi_k n_j$$

$$h_{jk} = -\rho \iint_{S_0} dS\, \phi_k m_j - \rho \oint_{\Gamma} d\ell \phi_k n_j (\underline{\ell} \times \underline{n}) \cdot \underline{W}.$$

Using the discretized body shape and potentials, these may be rewritten as

$$g_{jk}(t_n) = \rho \sum_{i=1}^{M} \left[\phi_k(t_n)\right]_i [n_j]_i A_i$$

$$h_{jk}(t_n) = -\rho \sum_{i=1}^{M} \left[\phi_k(t_n)\right]_i A_i [m_j]_i$$

$$- \rho \sum_{i=1}^{M'} \left[\phi_k(t_n)\right]_i \ell_i [n_j]_i \left[(\underline{\ell} \times \underline{n}) \cdot \underline{W}\right]_i$$

where

$A_i =$ area of ith panel

$[n_j]_i = n_j$ on ith panel

$[m_j]_i = m_j$ on ith panel

$\ell_i =$ waterline length of ith panel

$\left[(\underline{\ell} \times \underline{n}) \cdot \underline{W}\right]_i = (\underline{\ell} \times \underline{n}) \cdot \underline{W}$ on the ith panel.

The derivative of $g_{jk}(t)$ with respect to time may then be taken numerically to obtain the force $F_{jk}(t)$.

CHAPTER VI

NUMERICAL RESULTS

6.1 The Results of Zero Speed Calculations

Calculations on a Sphere

The theory as developed was first tested on a half-submerged sphere. The sphere was approximated by 65 panels on a quarter of the submerged body, exploiting the sphere's two planes of symmetry. The use of symmetry planes for the diffraction problem requires that the diffraction boundary condition be divided into appropriate symmetric and anti-symmetric parts; the resulting potentials are summed. Four potentials must be solved for two planes of symmetry. However, this approach is much more efficient than multiplying the number of panels by four without the use of symmetry planes. Figure 6.1 shows the nondimensional diffraction impulse response functions for both heave and sway. These results can be compared with frequency-domain results by Fourier transform as in (3.37). The diffraction force is computed from the Fourier transform of K_{j7}, as well as by the Haskind relation, using the results of Liapis (1986). These are compared with the results of Cohen (1986), who used a multipole expansion, which, in the limit of infinite terms, is exact for the special case of the sphere. The resulting amplitude and phase are shown in Figures 6.2 and 6.3 for heave and Figures 6.4 and 6.5 for sway. Good agreement is shown throughout the frequency range. It is believed that the slight variation is due primarily to the panel definition of the sphere. The panels tend to be very narrow near the bottom of the sphere due to the simple paneling scheme used. Thus, as the number of panels increases, the body shape is more closely modeled, but the numerical accuracy becomes worse.

To verify the approach of using impulse response functions to determine forces due to an arbitrary wave, a direct convolution of a sum of sine waves was performed. The frequency domain gives

$$F_j(t) = \mathrm{Im}\left\{\sum_{n=1}^{N} X_j(\omega_n) e^{i\omega_n t}\right\}$$

where ω_n represents an arbitrary frequency. The force from the time-domain approach is given by (3.12) as

$$F_j(t) = \int_{-\infty}^{\infty} d\tau \Big[K_{j7}(t-\tau) + K_{j0}(t-\tau)\Big]\varsigma_0(\tau)$$

where

$$\varsigma_0(t) = \text{Im}\left\{\sum_{n=1}^{N} e^{i\omega_n t}\right\}.$$

The chosen wave is plotted in Figure 6.6. For the time-domain formulation, the wave begins and ends as in the figure. For the frequency domain, the wave system is assumed to have always existed. Thus, the time-domain approach is expected to have a beginning and ending transient. The results are in Figure 6.7 and show excellent agreement. The sine waves are of unit amplitude, and the forces are scaled accordingly. The relationship with the frequency-domain method has thus been verified. The time-domain approach also demonstrates the capacity to deal with transients.

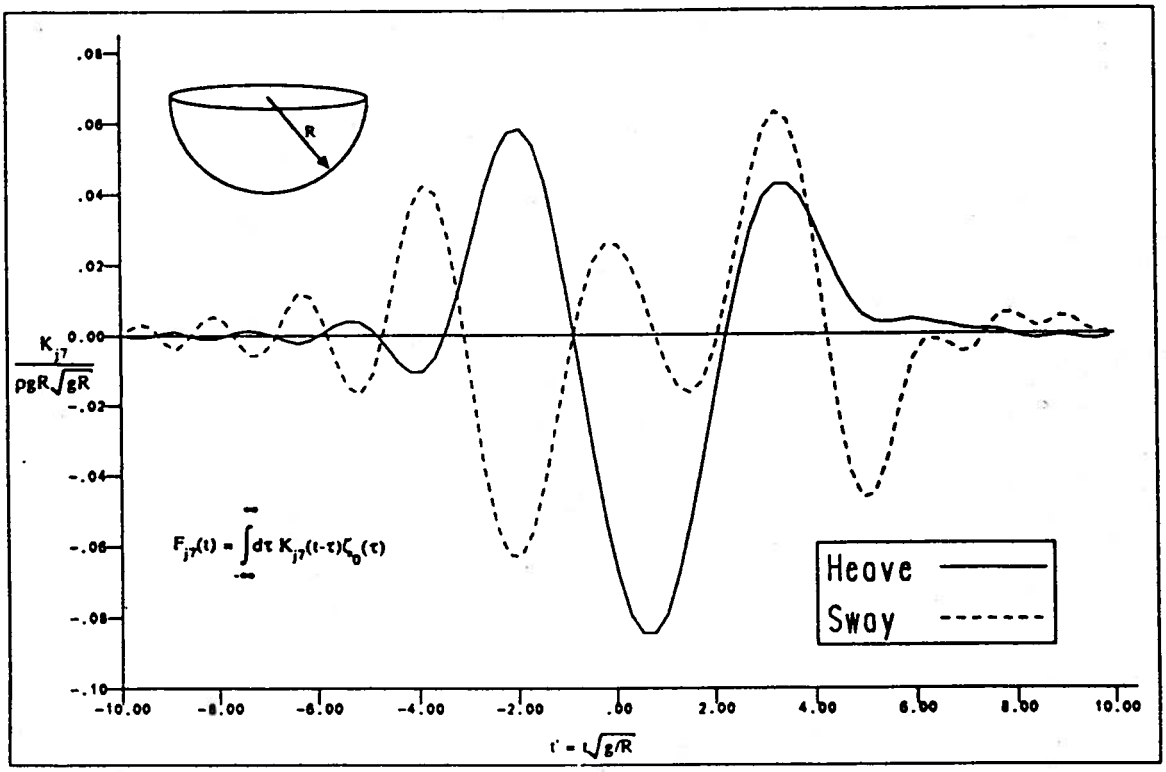

Figure 6.1 — Nondimensional Diffraction Force Impulse Response Functions for a Sphere

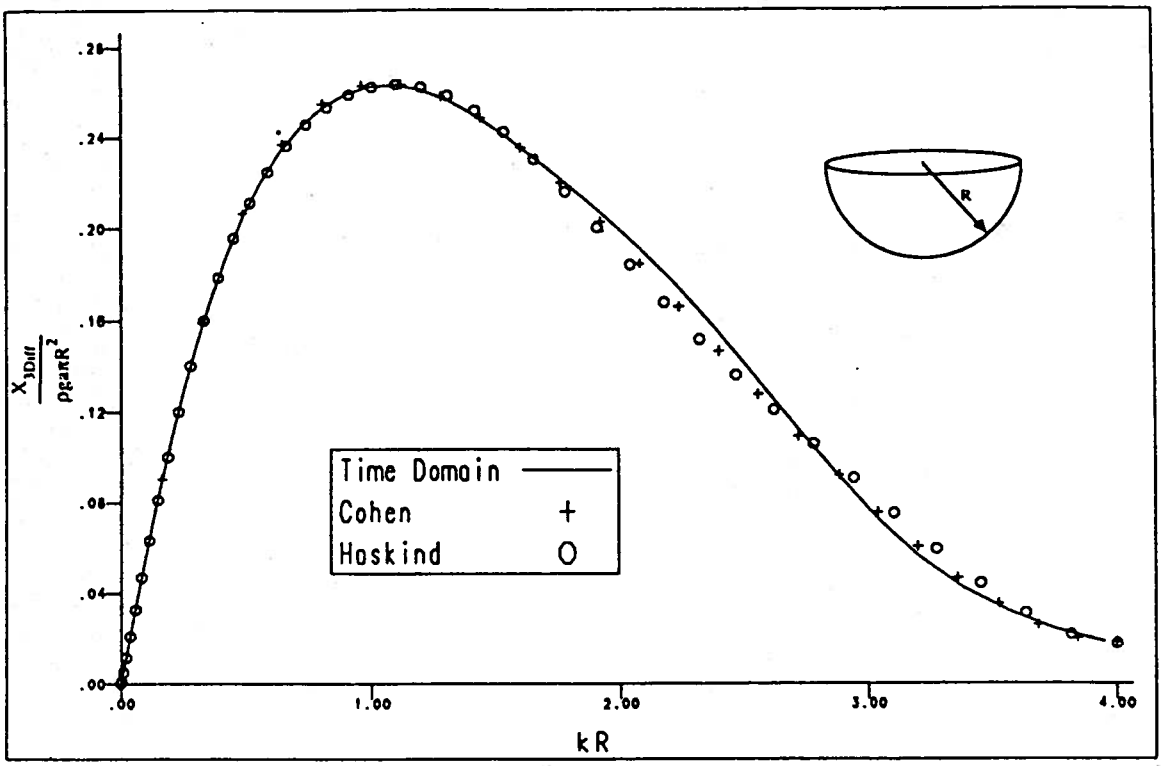

Figure 6.2 — Nondimensional Heave Diffraction Force for a Sphere

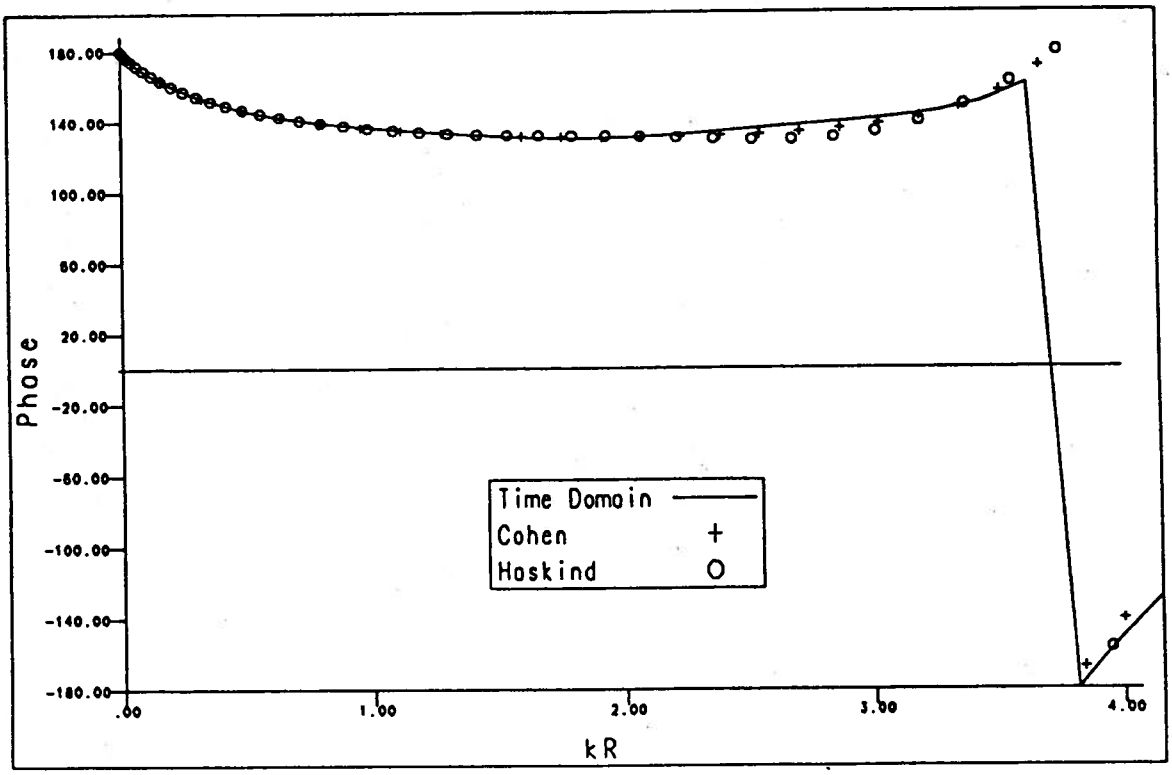

Figure 6.3 — Phase of Heave Diffraction Force for a Sphere

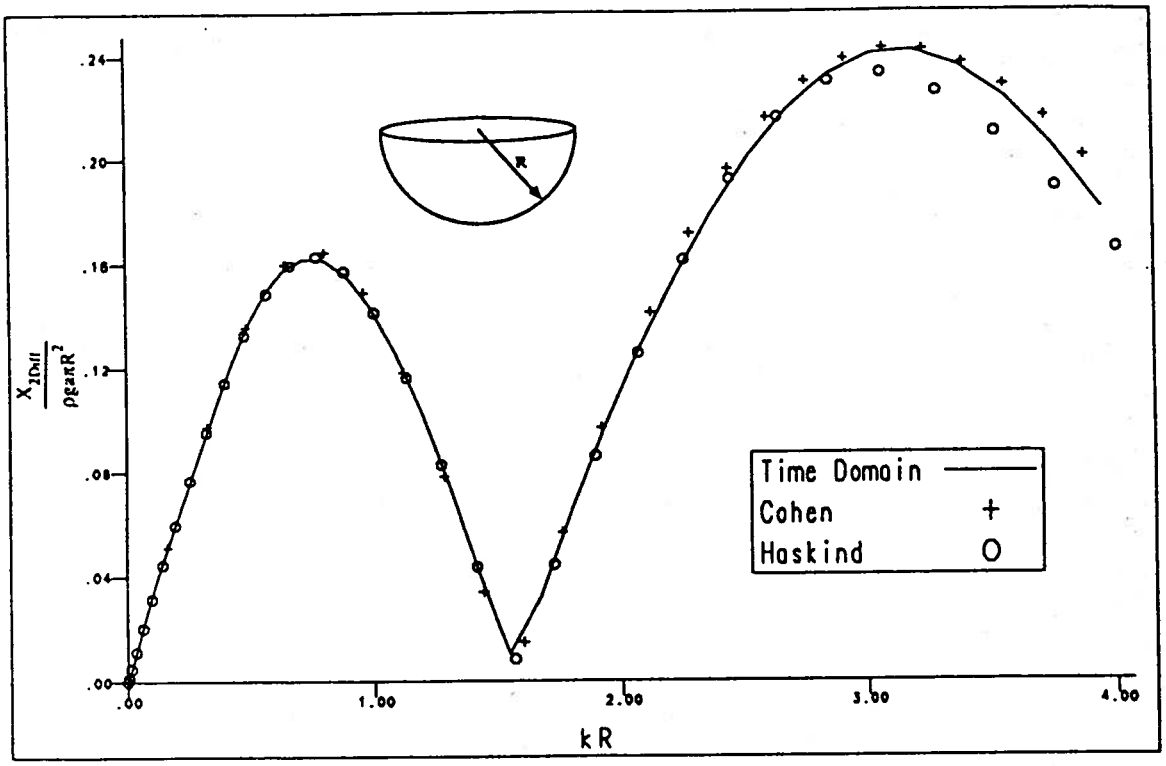

Figure 6.4 — Nondimensional Sway Diffraction Force for a Sphere

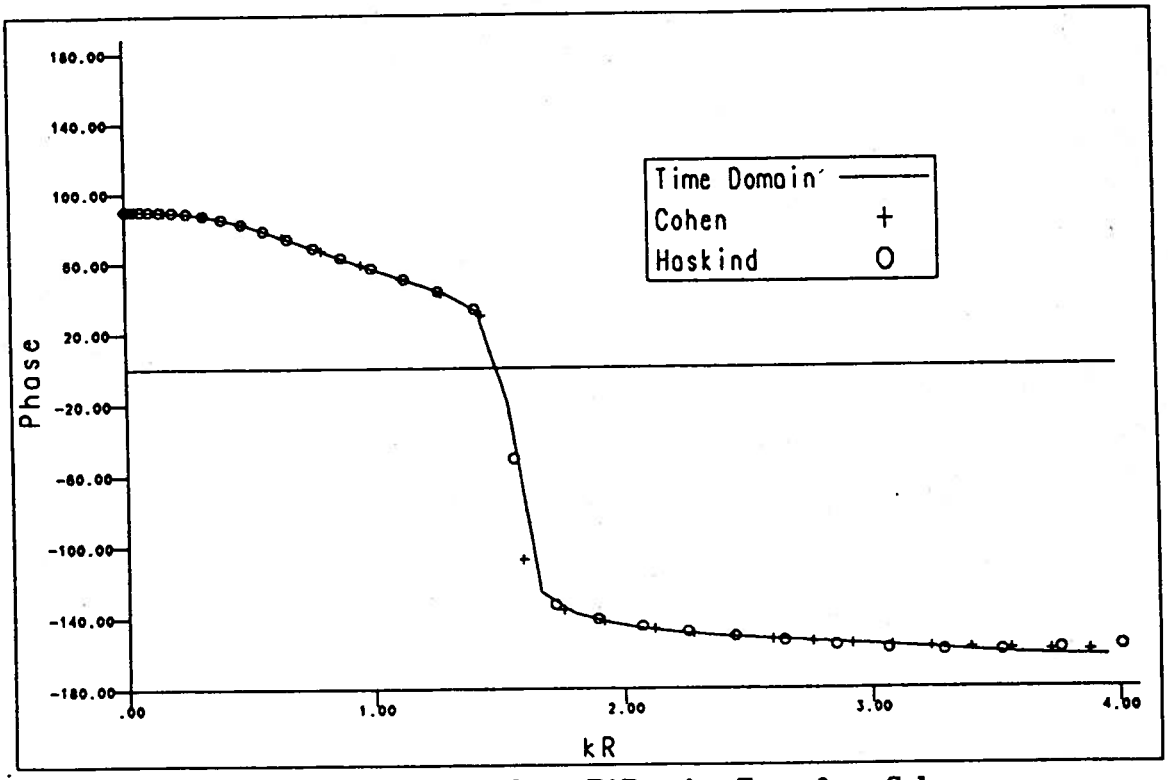

Figure 6.5 — Phase of Sway Diffraction Force for a Sphere

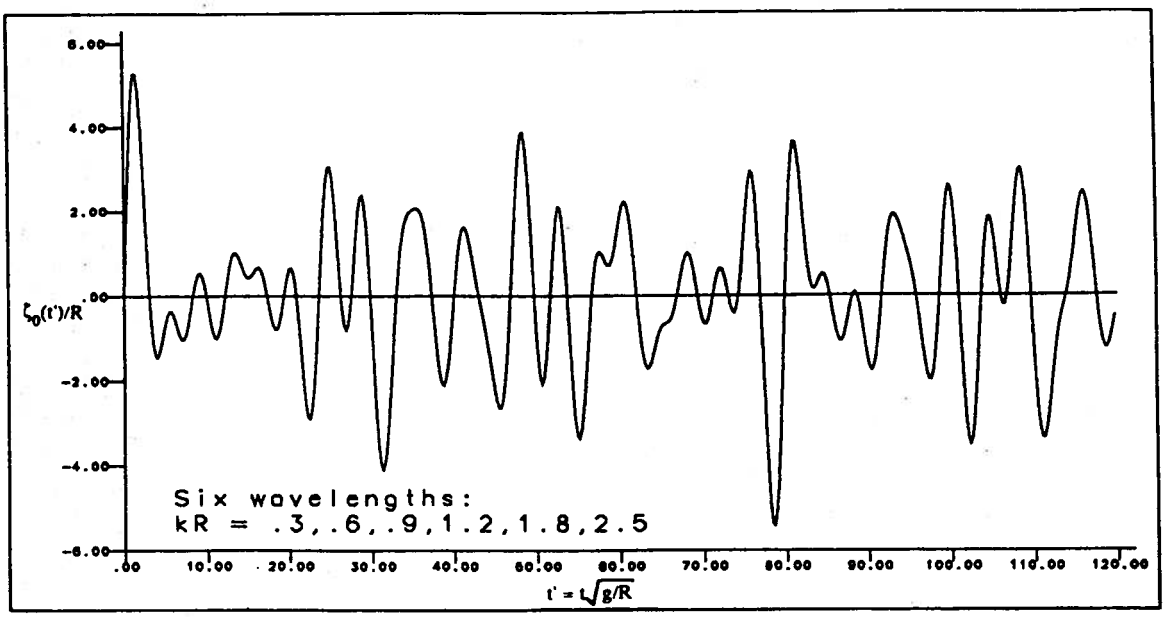

Figure 6.6 — Incident Wave Given by the Sum of Sine Waves

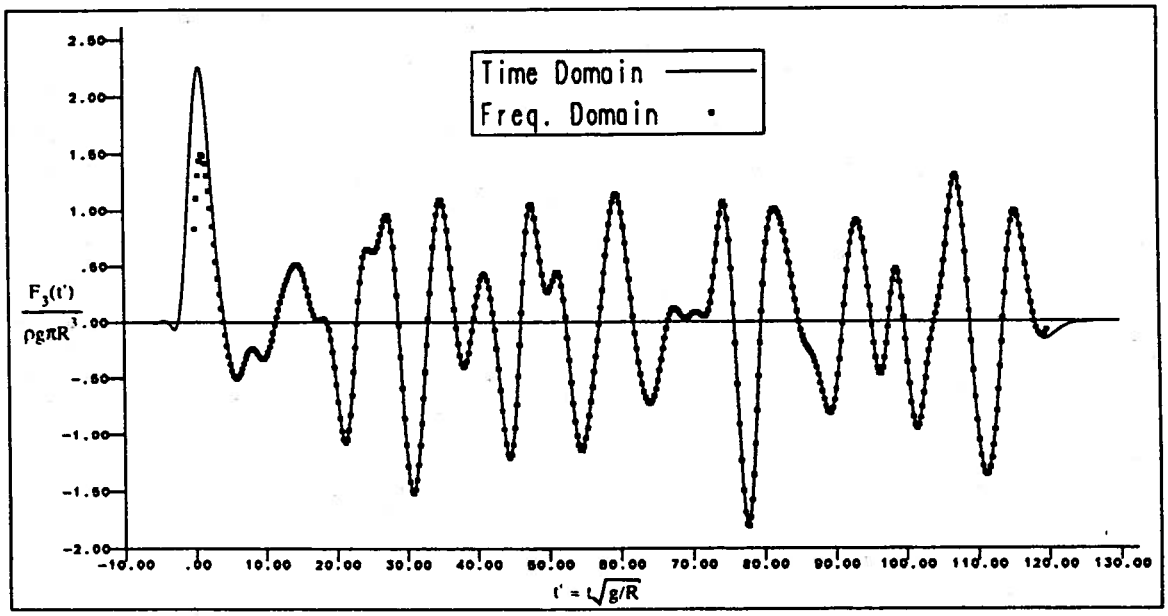

Figure 6.7 — Heave Exciting Force Due to the Sum of Sine Waves

Calculations on a Wigley Hull Form

The exciting forces were also determined at zero forward speed for a Wigley mathematical hull with the hull shape given by the formula

$$\frac{y}{B} = \left(1 - \left(\frac{z}{T}\right)^2\right)\left(1 - \left(\frac{2x}{L}\right)^2\right)\left(1 + 0.2\left(\frac{2x}{L}\right)^2\right) + \left(\frac{z}{T}\right)^2\left(1 - \left(\frac{z}{T}\right)^8\right)\left(1 - \left(\frac{2x}{L}\right)^2\right)^4.$$

The hull was approximated by 120 panels on half of the body. The heave and pitch impulse response functions for the Froude-Krylov and diffraction forces are plotted to show the character of the curves. Since the body is fore-aft symmetric, the heave and pitch Froude-Krylov force impulse response functions are symmetric and antisymmetric, respectively. The diffraction impulse response functions show no such symmetry. These impulse response functions are Fourier transformed as in (3.37) to give the frequency-domain exciting force. The results are compared with the strip theory of Salvesen, Tuck, and Faltinsen (1970). As may be seen from the impulse response functions, the exciting force is dominated by the Froude-Krylov force, and there is good agreement between the two approaches. Since the body is symmetric, the Froude-Krylov force is either in phase or 90 degrees out of phase, so that the phase is determined from the ratio of the diffraction force to Froude-Krylov force. The phase shows good agreement also.

6.2 The Results of Forward Speed Calculations

For the forward speed calculations two approximations have been made. The first is to neglect the steady perturbation velocities due to steady translation. The body boundary condition term $\underline{m}$ for the radiation problem becomes simply $\underline{m} = (0,0,0,0, U_0 n_3, -U_0 n_2)$. This approximation does not simplify the calculation of the unsteady problems but was made because a reliable method of determining the steady perturbation potential was unavailable. A parallel approximation is made in the evaluation of the pressure from Bernoulli's equation for force calculations. The steady velocity vector $\underline{W}$ is approximated by $\underline{W} = (-U_0, 0, 0)$.

Diffraction Calculations

The diffraction force calculations were performed for the Wigley hull as in the previous section. For the forward speed results, recent experimental results by Gerritsma were used for comparison. These results were made available through private correspondence. Calculations were performed at Froude numbers 0.2 and 0.3 for head seas. Some calculations were performed for non-head seas, but no experimental results are available for comparison.

The results from strip theory calculations are also included. Good agreement is seen for the slower case, with the results appearing a bit worse for the higher speed. In general the results appear better than the strip theory calculations. The current pitch phase results appear to be mirrored about -90 degrees compared to Gerritsma's experiments. Results

from other ship shapes indicate that the phase of the pitch exciting force increases from -90 degrees rather than decreasing, as given by Gerritsma. Private communications with Gerritsma indicated that he could find no errors in his preliminary results. It may be noted that strip theories tend to give results that go from -90 degrees at infinite wavelength to a larger negative phase angle for shorter waves, opposite to what most experiments indicate. The current method follows the trend of increasing phase angles with shorter wavelengths.

Radiation Calculations

Radiation calculations were performed at both zero and forward speed to determine the effect of using a nonimpulsive input as was discussed in Chapter 4. For comparison with the zero speed impulsive results of Liapis, the same Series 60 $C_B = 0.7$ discretization used by Liapis and Beck (1985) was employed, with 108 panels on the half body. The heave memory function $K_{33}(t)$ is plotted in nondimensional form for both a nonimpulsive input where $\varsigma_3(t) = \sqrt{a/\pi}e^{-at^2}$ and an impulsive input where $\varsigma_3(t) = \delta(t)$. The impulsive results are taken from Liapis and Beck, with the nondimensional time-step size given as $\Delta t' = \Delta t\sqrt{g/L} = .06263$. For the nonimpulsive input, $\Delta t' = .1565$ and $a(L/g) = 10.204$. It may be noted that the nonimpulsive method gives a smoother curve with a larger time-step size. The added mass and damping as determined by the two methods are comparable with the nonimpulsive approach, giving a slightly smoother curve.

To perform the Fourier transforms of the radiation forces computed directly in the time domain at forward speed, it was shown in Chapter 4 that the value of the large time force, c_{jk}, must be determined. For the simple choice of $\underline{m}$ used in this work, only the pitch and yaw modes have a nonzero value of m_j and thus a nonzero value of $\phi_{k\infty}$. The function $h_{jk}(t)$ defined in (4.9) was shown to go to c_{jk} at the limit of infinite time. However, the numerical solution shows oscillatory behavior, and this limit is difficult to determine. Because of the simple choice of $\underline{m}$, the limit may be obtained in an alternate fashion as follows. Integrating (4.14) with respect to t gives

$$\int_{-\infty}^{\infty} dt\,\phi_k(P,t) + \frac{1}{2\pi}\int_{-\infty}^{\infty} dt \iint_{S_0} dS\,\phi_k(Q,t)\frac{\partial}{\partial n_Q}\left(\frac{1}{r}-\frac{1}{r'}\right)$$
$$= \frac{1}{2\pi}\int_{-\infty}^{\infty} dt \iint_{S_0} dS\,\frac{\partial \phi_k}{\partial n}(Q,t)\left(\frac{1}{r}-\frac{1}{r'}\right)$$
$$-\frac{1}{2\pi}\int_{-\infty}^{\infty} dt\int_{-\infty}^{t} d\tau \iint_{S_0} dS\left[\phi(Q,\tau)\frac{\partial \tilde{G}}{\partial n}(P,Q,t-\tau) - \tilde{G}(P,Q,t-\tau)\frac{\partial \phi_k}{\partial n}(Q,\tau)\right]$$
$$+\frac{1}{2\pi g}\int_{-\infty}^{\infty} dt\int_{-\infty}^{t} d\tau \oint_{\Gamma} d\eta\Big[U_0^2\big(\tilde{G}(P,Q,t-\tau)\phi_\xi(Q,\tau) - \phi(Q,\tau)\tilde{G}_\xi(P,Q,t-\tau)\big)$$
$$+U_0\big(\phi(Q,\tau)\tilde{G}_\tau(P,Q,t-\tau) - \tilde{G}(P,Q,t-\tau)\phi_\tau(Q,\tau)\big)\Big].$$

Exchanging orders of integration and making the substitution

$$\hat{\phi}_k(P) = \int_{-\infty}^{\infty} dt\,\phi_k(P,t)$$

yields

$$\widehat{\phi}_k(P) + \frac{1}{2\pi}\iint_{S_0} dS\,\widehat{\phi}_k \frac{\partial}{\partial n_Q}\left(\frac{1}{r}-\frac{1}{r'}\right) = \frac{1}{2\pi}\iint_{S_0} dS\,\frac{\partial \widehat{\phi}_k}{\partial n}\left(\frac{1}{r}-\frac{1}{r'}\right)$$
$$-\frac{1}{2\pi}\iint_{S_0} dS\left[\widehat{\phi}_k\int_0^\infty \frac{\partial \widetilde{G}}{\partial n}\,dt - \frac{\partial \widehat{\phi}_k}{\partial n}\int_0^\infty \widetilde{G}\,dt\right]$$
$$+\frac{1}{2\pi g}\oint_\Gamma d\eta\, U_0^2\left[\widehat{\phi}_{k\xi}\int_0^\infty \widetilde{G}\,dt - \widehat{\phi}_k\int_0^\infty \widetilde{G}_\xi\,dt\right],$$

which is the same integral equation as that for $\phi_{k\infty}$ given by (4.16) with m_j replaced by $\partial\widehat{\phi}_k/\partial n$. For the simple choice of $\underline{m}$ given, it may be noted that

$$\frac{\partial \widehat{\phi}_2}{\partial n} = \int_{-\infty}^{\infty} dt\,\frac{\partial \phi_2}{\partial n} = \int_{-\infty}^{\infty} dt\, n_2 \dot{\zeta}_2 = n_2$$
$$= -\frac{m_6}{U_0}$$

and

$$\frac{\partial \widehat{\phi}_3}{\partial n} = \int_{-\infty}^{\infty} dt\,\frac{\partial \phi_3}{\partial n} = n_3$$
$$= \frac{m_5}{U_0}.$$

Thus it may be shown that

$$c_{26} = -U_0\int_{-\infty}^{\infty} dt\, h_{22}(t)$$
$$c_{66} = -U_0\int_{-\infty}^{\infty} dt\, h_{62}(t)$$
$$c_{35} = U_0\int_{-\infty}^{\infty} dt\, h_{33}(t)$$
$$c_{55} = U_0\int_{-\infty}^{\infty} dt\, h_{53}(t).$$

The constants c_{jk} were found to be more accurately determined by this method than an attempt to determine a large time average value directly from $h_{jk}(t)$.

Forward speed calculations were performed for the Series 60 ship at Froude number = 0.2, with 176 panels on half the hull. Results are plotted for heave and pitch added mass and damping. While the curves plotted here are somewhat smoother than those of Liapis and Beck, there is not significant improvement over their results. Fairly close agreement is shown with Inglis and Price's results (1981), which were determined by a frequency-domain approach analagous to that employed here in the time domain. The results plotted here are those referred to by Inglis and Price as method IP2.

Some experimental results for the horizontal modes are available in Vugts (1971). Results are presented from Inglis, as well as strip theory results, for comparison. While the agreement with Vugts's experiments is not particularly good, the agreement with Inglis and Price's computational method is good for most of the frequency range. This fact lends

credence to the argument that the mathematical model may neglect some fundamental physical effect, such as viscosity or the nonlinearity of the free surface boundary condition.

Finally, results for the heave, heave-pitch cross coupling, and pitch added mass and damping are presented for the Wigley mathematical hull used for the exciting forces. Experimental results were made available by Gerritsma. The results are plotted for Froude numbers 0.2 and 0.3. The agreement with the experiments is generally good, with improvements over the strip theory results in almost all cases. The pitch results are the worst, with the higher Froude number giving particularly poor agreement for the pitch added mass. The pitch curves show an unexpected lack of smoothness. Changes in time-step size and panel number seemed to have little effect on these results. The explanation for this is not altogether clear. Several possibilities exist. The first is that the line integral terms cannot be determined as accurately as desired because of the difficulty of determining the potential or its derivatives at the free surface. A second possibility is that the approximation of the steady perturbation velocity by the free stream causes the errors. Inglis and Price found that if the steady perturbation velocities were included, they would have to be determined quite accurately or worse results might occur.

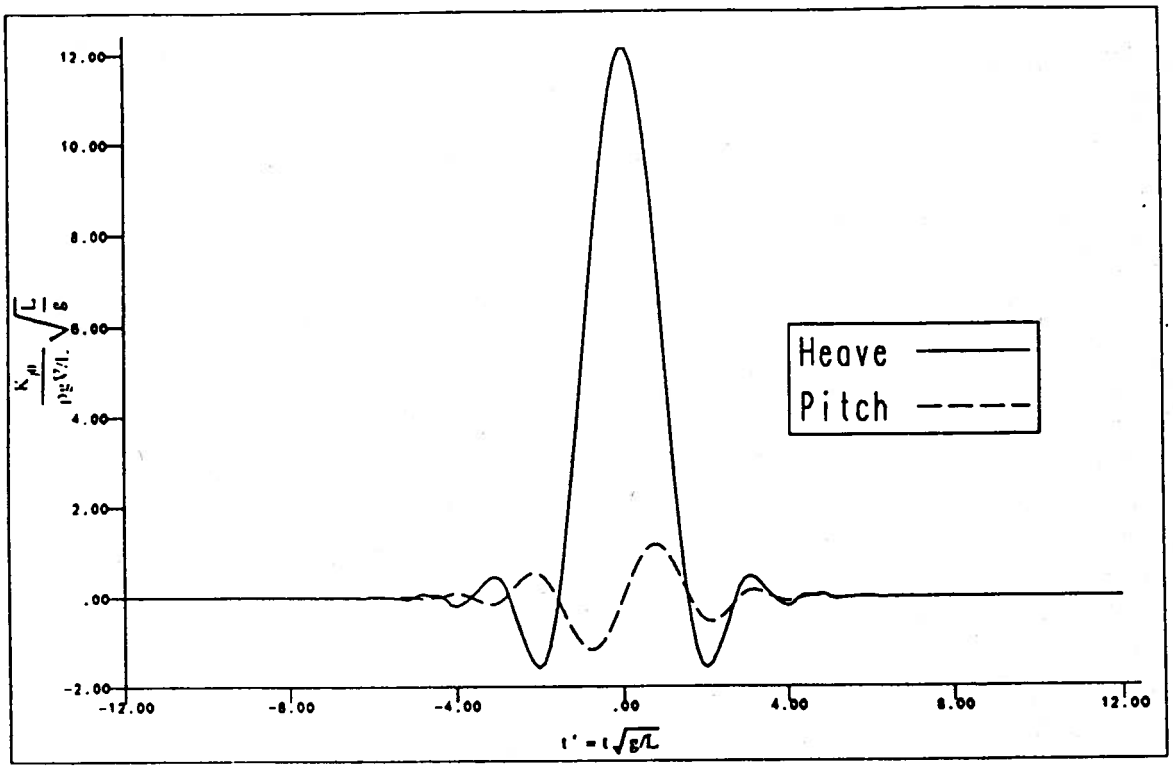

Figure 6.8 — Nondimensional Froude-Krylov Impulse Response Function for a Wigley Hull (Fn = 0)

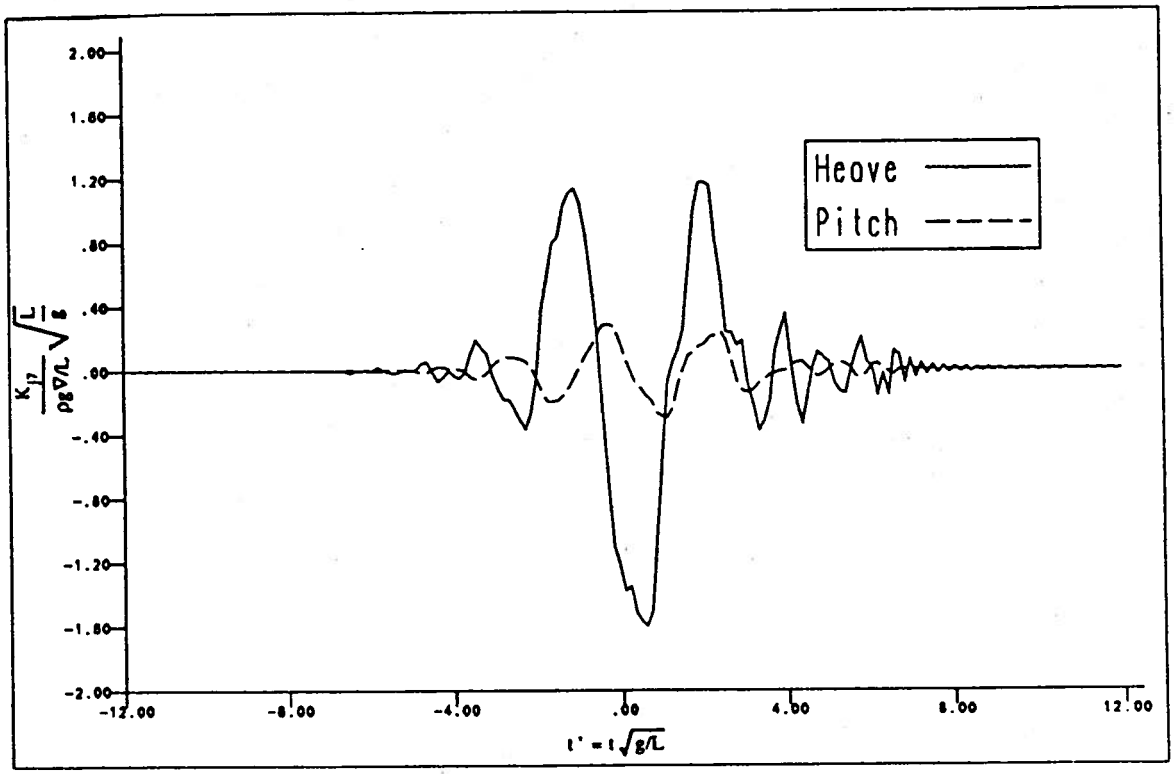

Figure 6.9 — Nondimensional Diffraction Force Impulse Response Function for a Wigley Hull (Fn = 0)

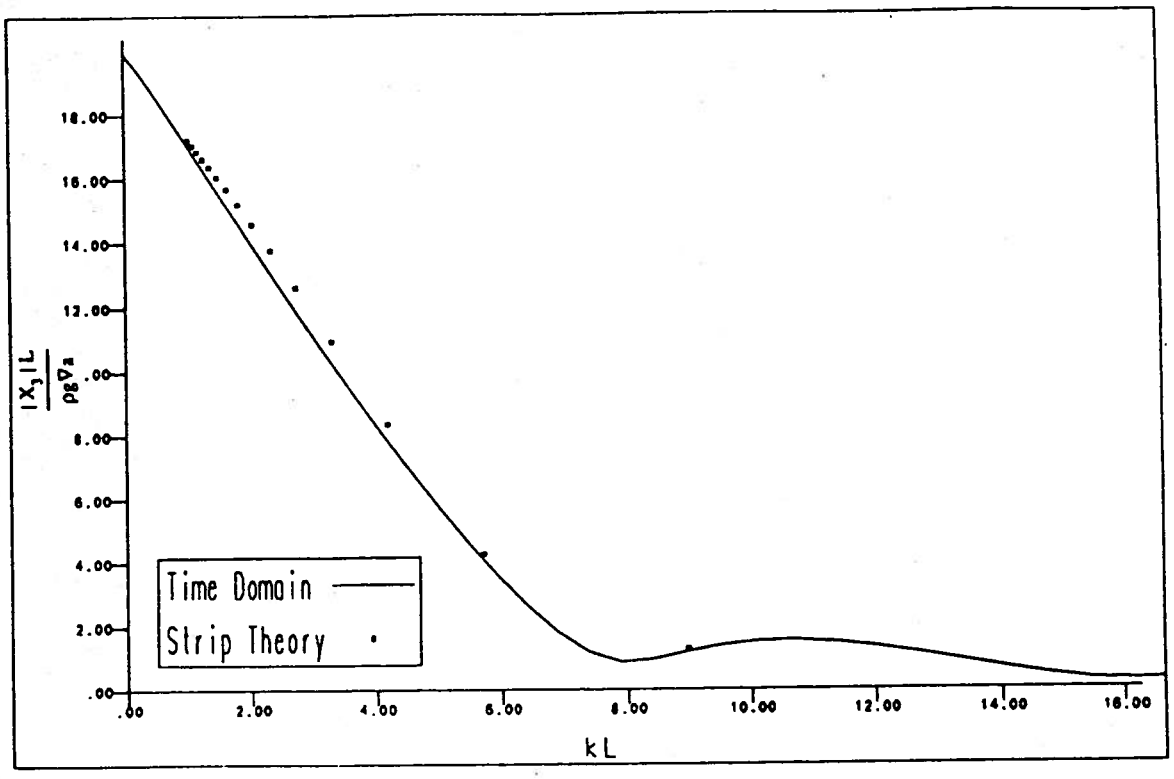

Figure 6.10 — Heave Exciting Force Amplitude for a Wigley Hull (Fn = 0)

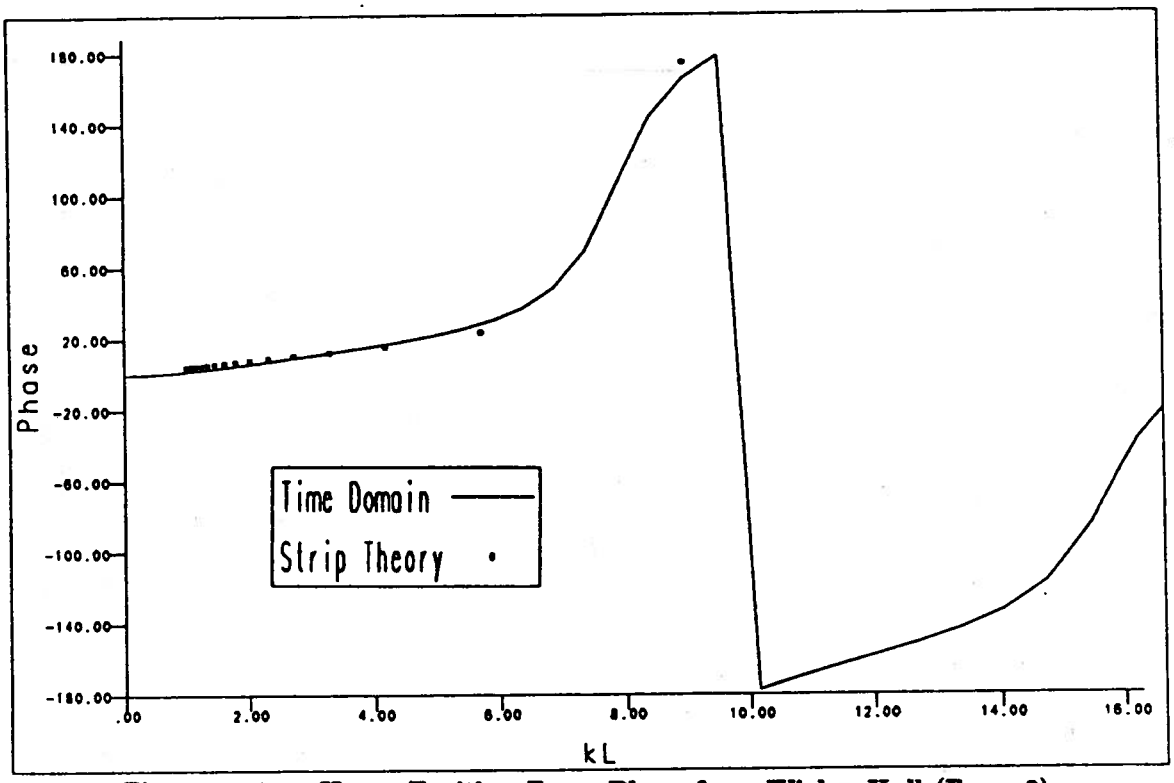

Figure 6.11 — Heave Exciting Force Phase for a Wigley Hull (Fn = 0)

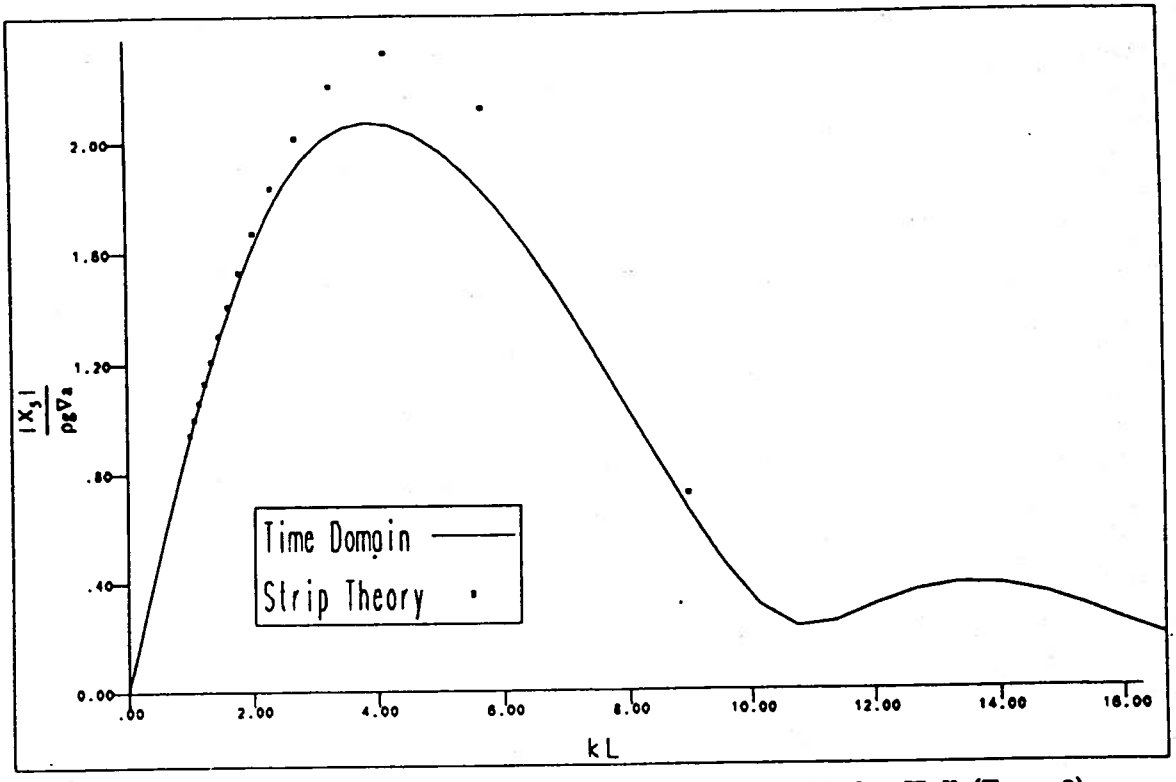

Figure 6.12 — Pitch Exciting Force Amplitude for a Wigley Hull (Fn = 0)

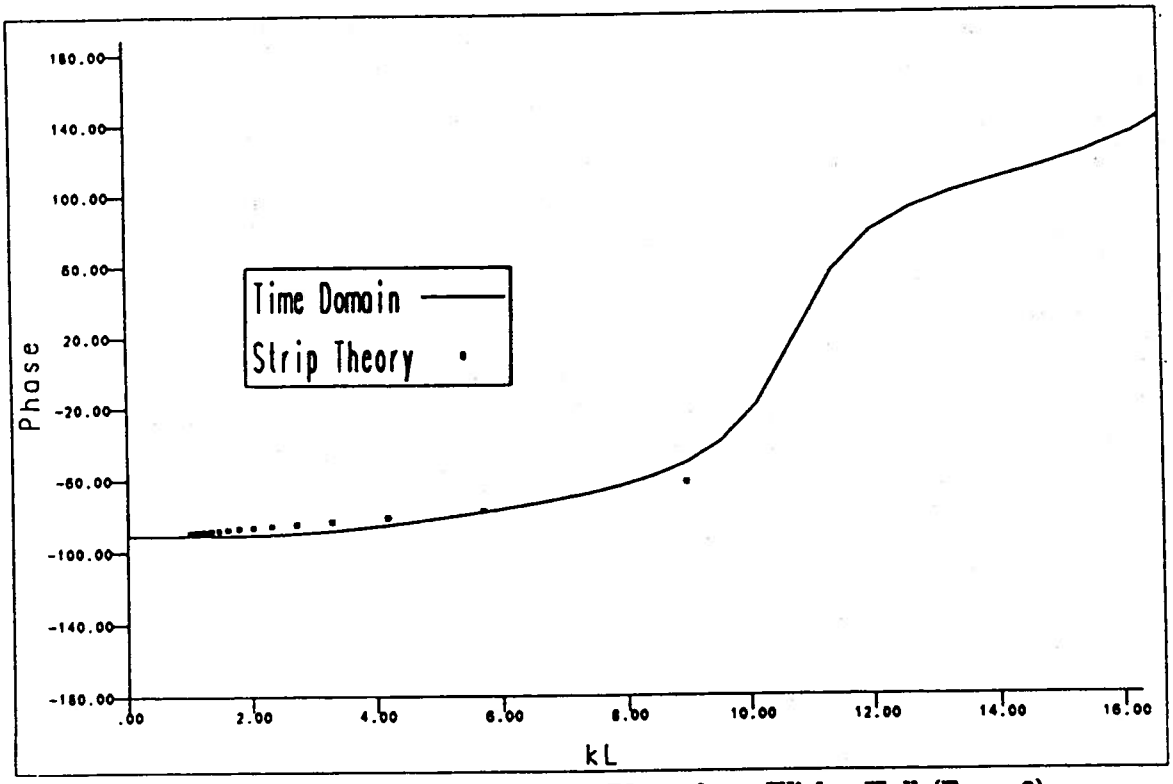

Figure 6.13 — Pitch Exciting Force Phase for a Wigley Hull (Fn = 0)

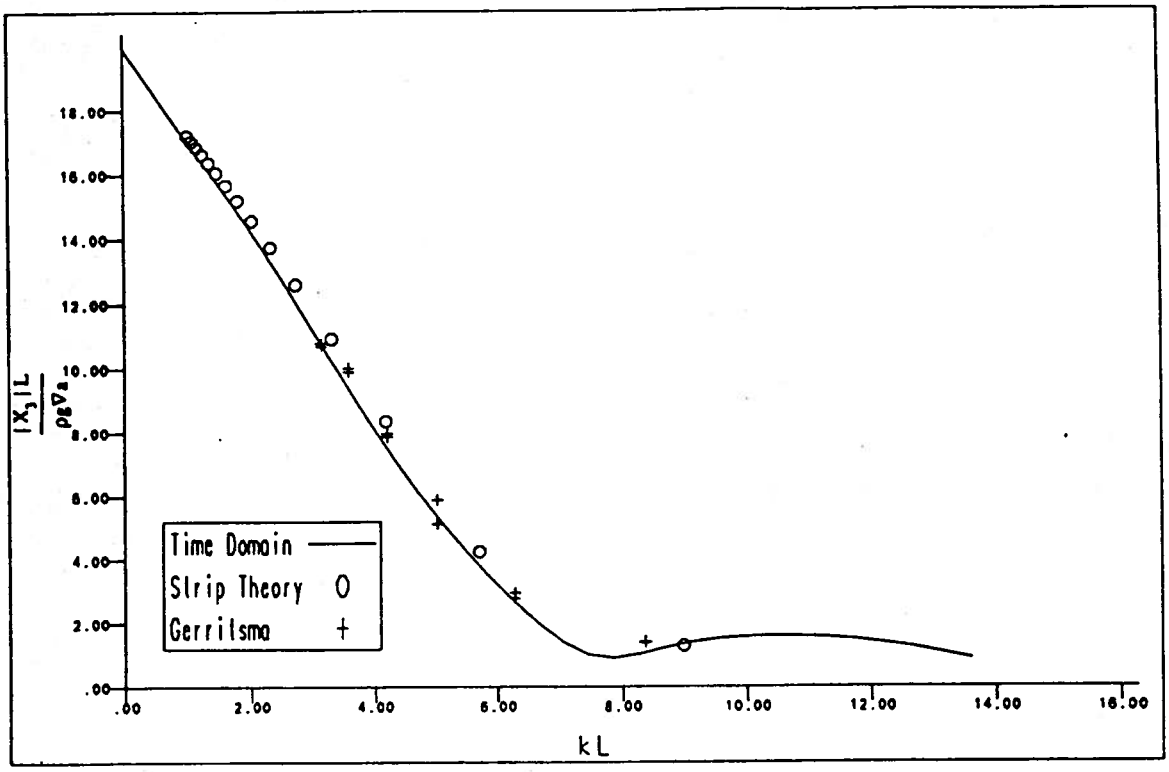

Figure 6.14 — Heave Exciting Force Amplitude for a Wigley Hull (Fn = .2)

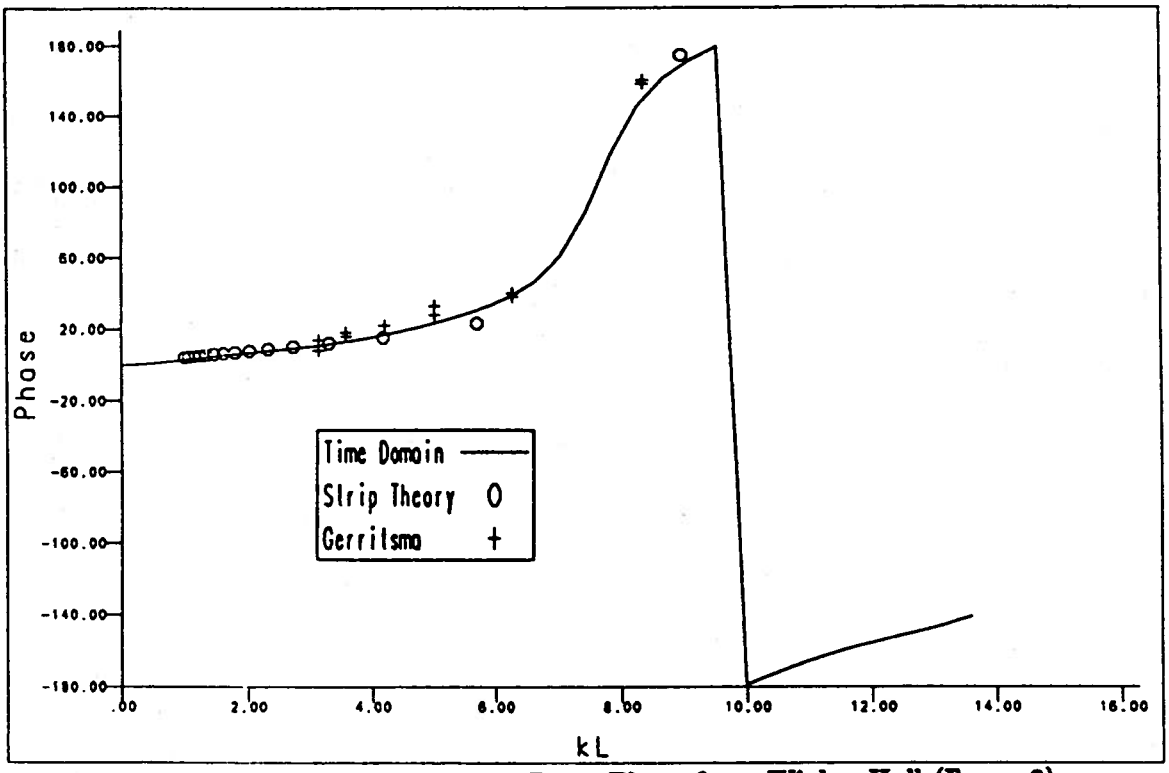

Figure 6.15 — Heave Exciting Force Phase for a Wigley Hull (Fn = .2)

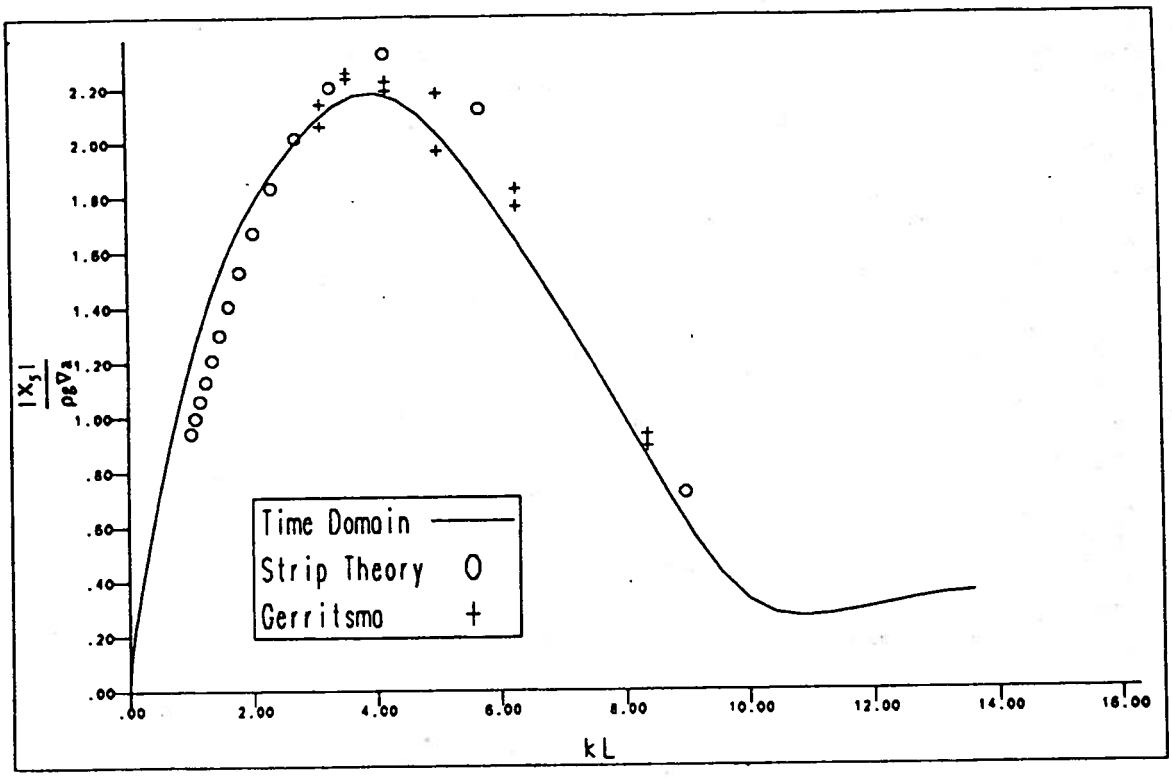

Figure 6.16 — Pitch Exciting Force Amplitude for a Wigley Hull (Fn = .2)

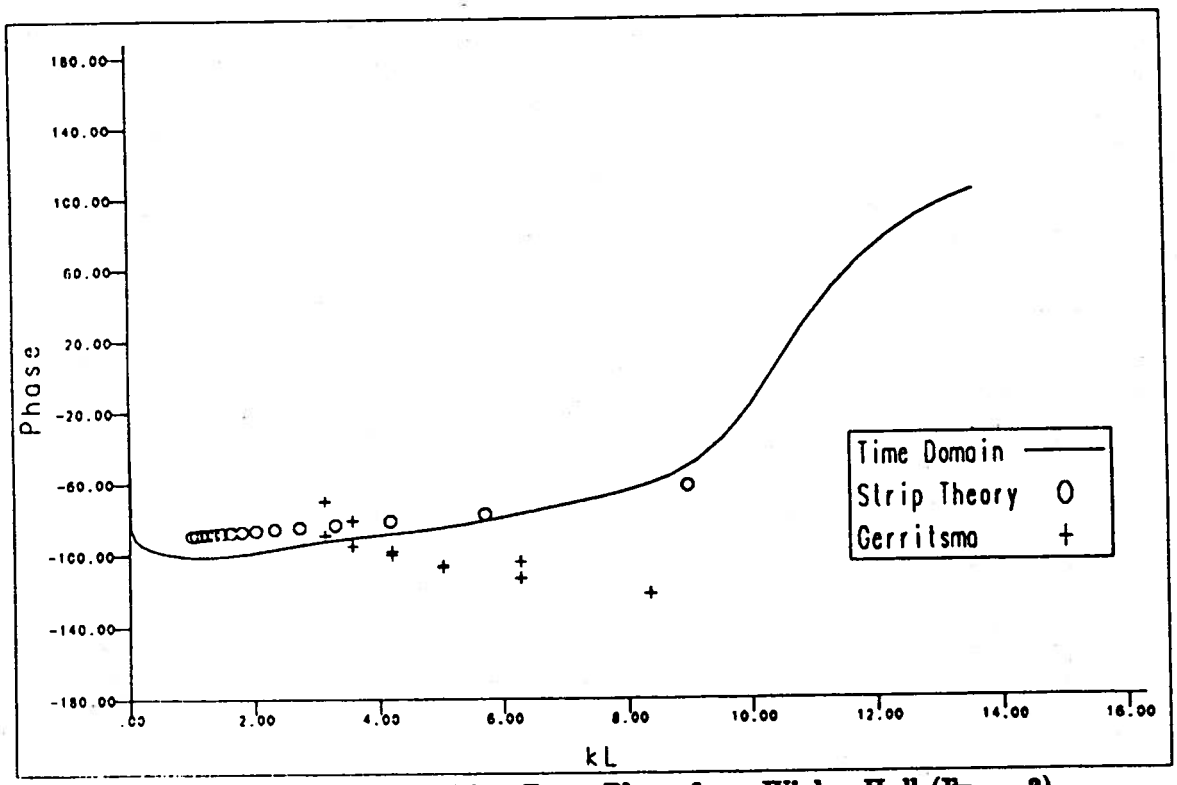

Figure 6.17 — Pitch Exciting Force Phase for a Wigley Hull (Fn = .2)

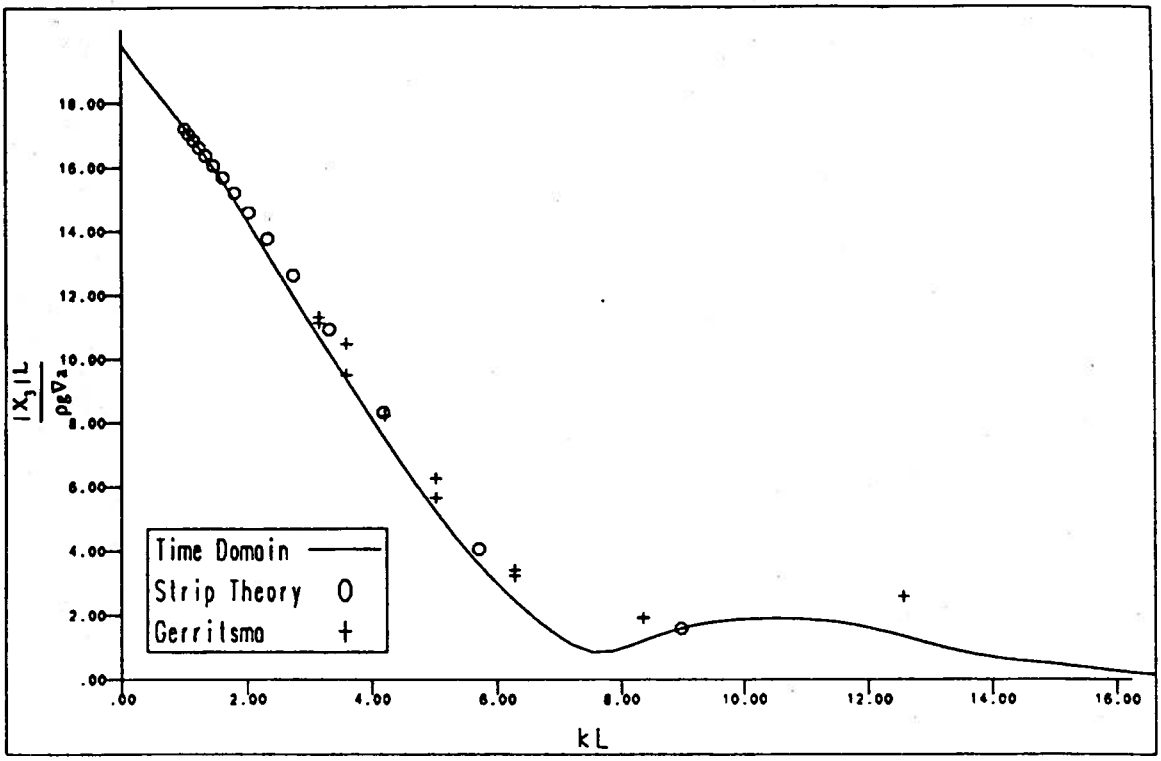

Figure 6.18 — Heave Exciting Force Amplitude for a Wigley Hull (Fn = .3)

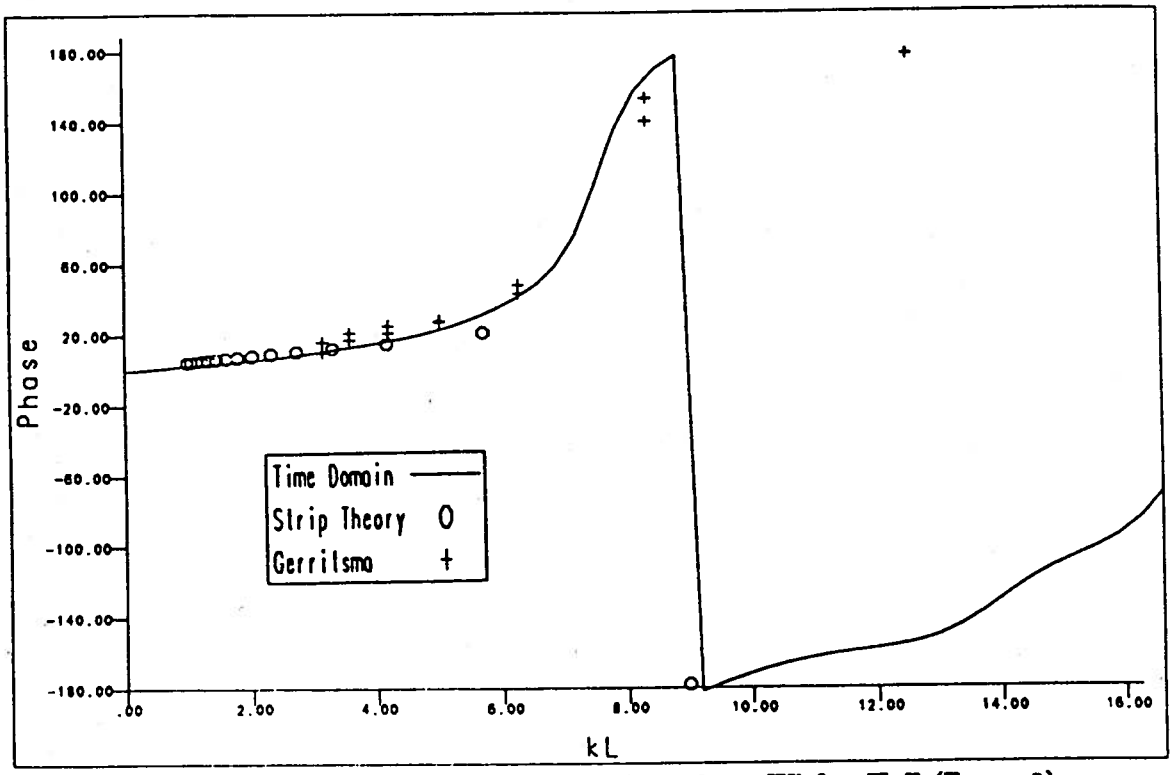

Figure 6.19 — Heave Exciting Force Phase for a Wigley Hull (Fn = .3)

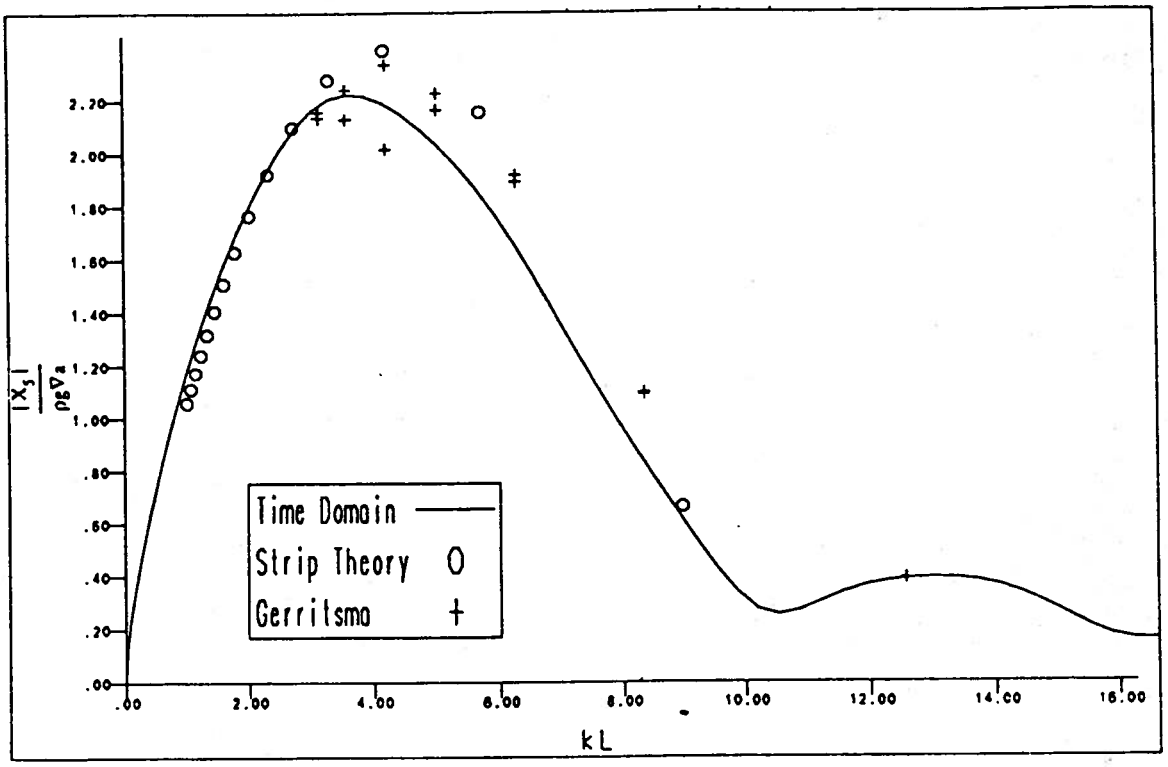

Figure 6.20 — Pitch Exciting Force Amplitude for a Wigley Hull (Fn = .3)

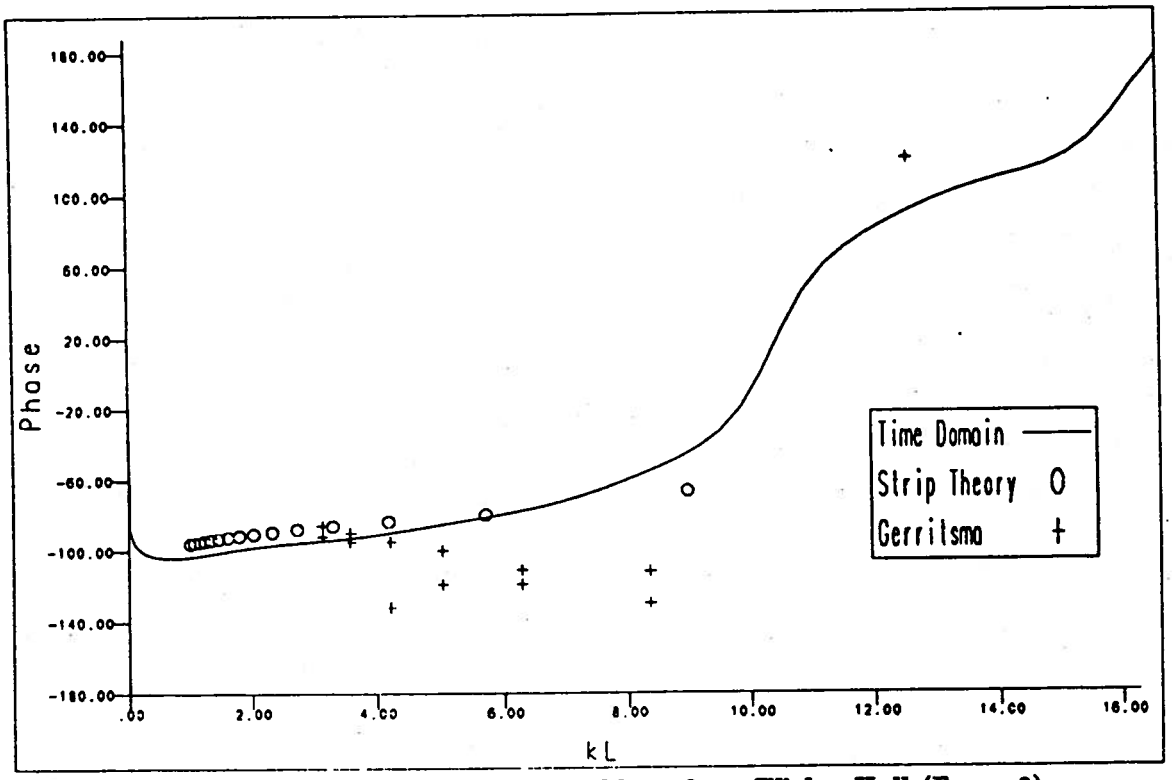

Figure 6.21 — Pitch Exciting Force Phase for a Wigley Hull (Fn = .3)

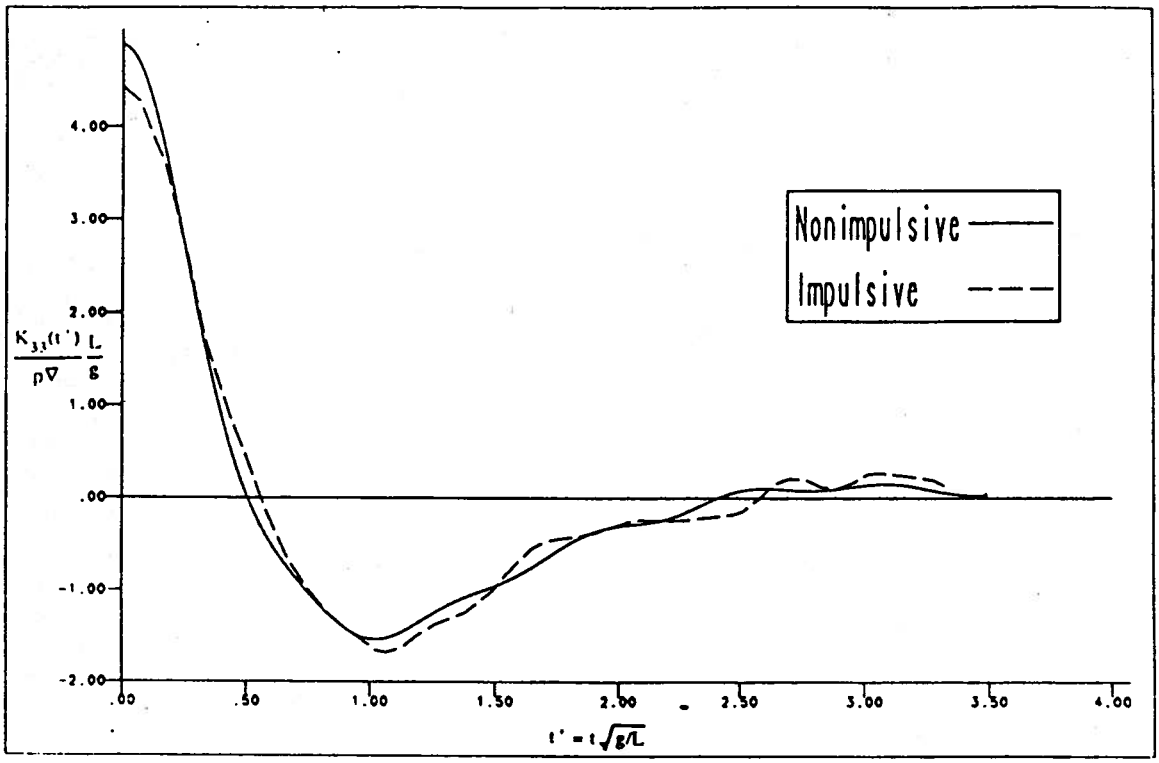

Figure 6.22 — Heave Memory Function for a Series 60 $C_B = .70$ Hull (Fn = 0)

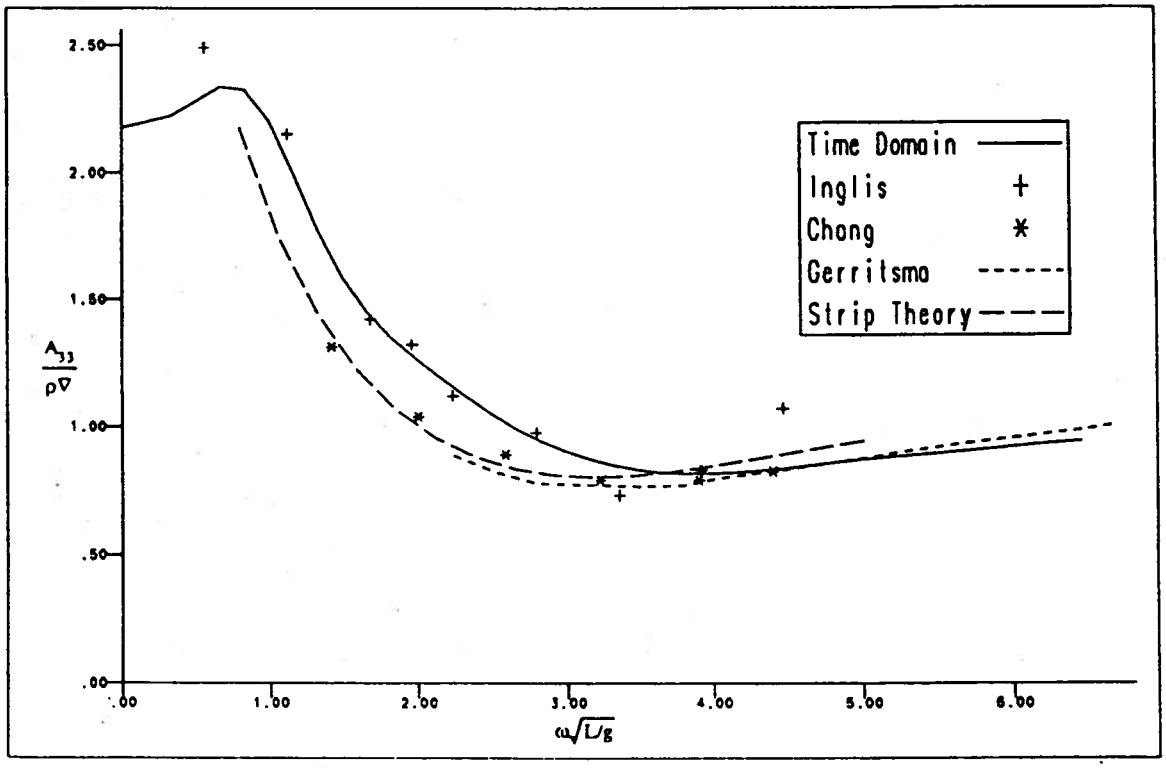

Figure 6.23 — Heave Added Mass Coefficient for a Series 60 $C_B = .70$ Hull (Fn = .2)

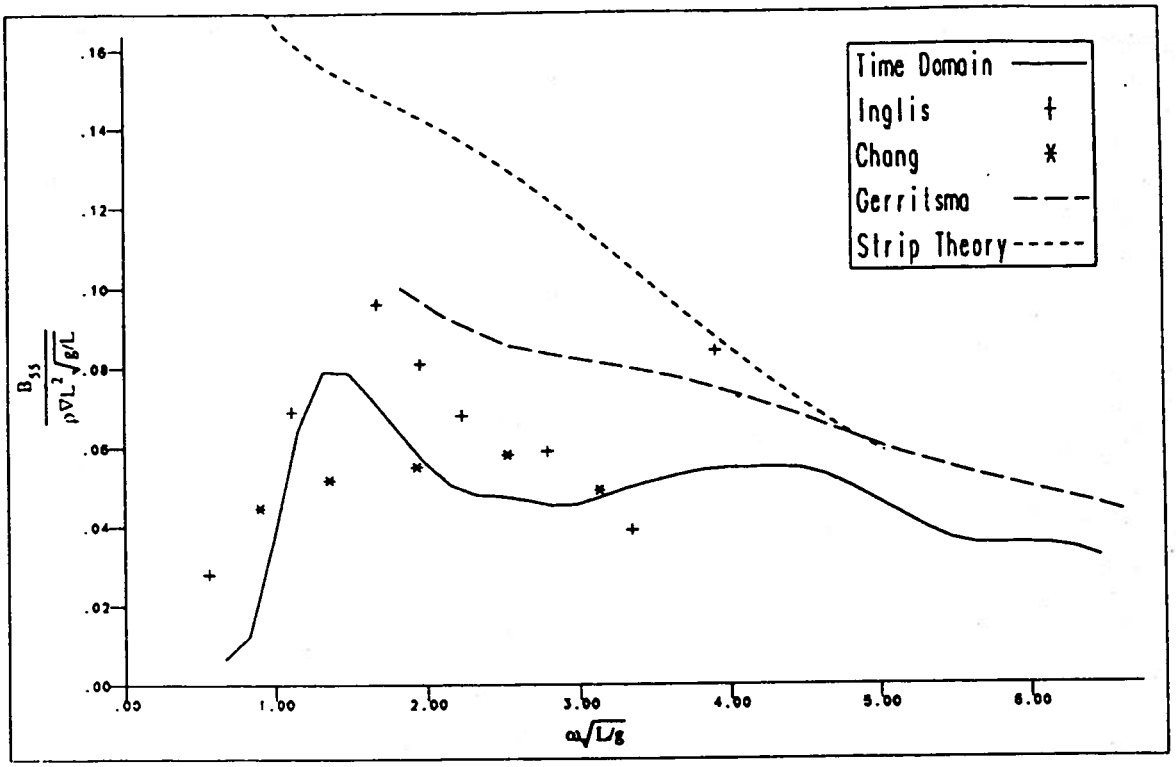

Figure 6.26 — Pitch Damping Coefficient for a Series 60 $C_B = .70$ Hull (Fn = .2)

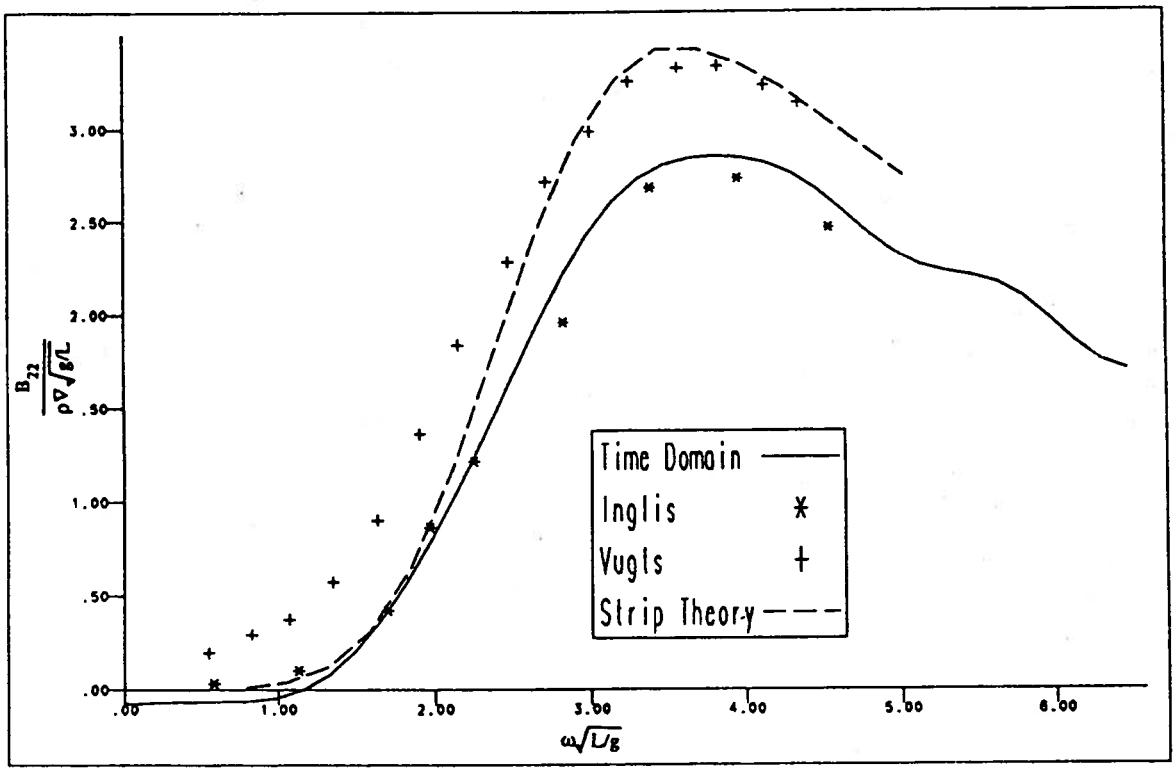

Figure 6.27 — Sway Damping Coefficient for a Series 60 $C_B = .70$ Hull (Fn = .2)

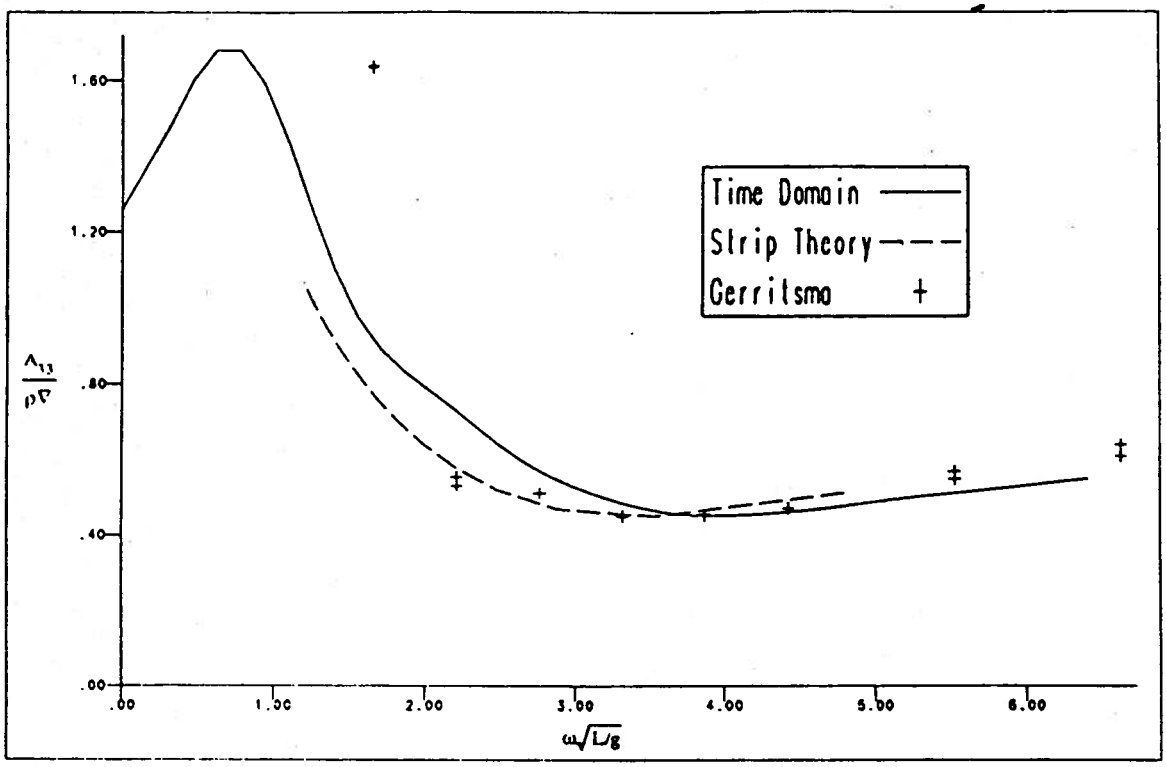

Figure 6.30 — Heave Added Mass Coefficient for a Wigley Hull (Fn = .2)

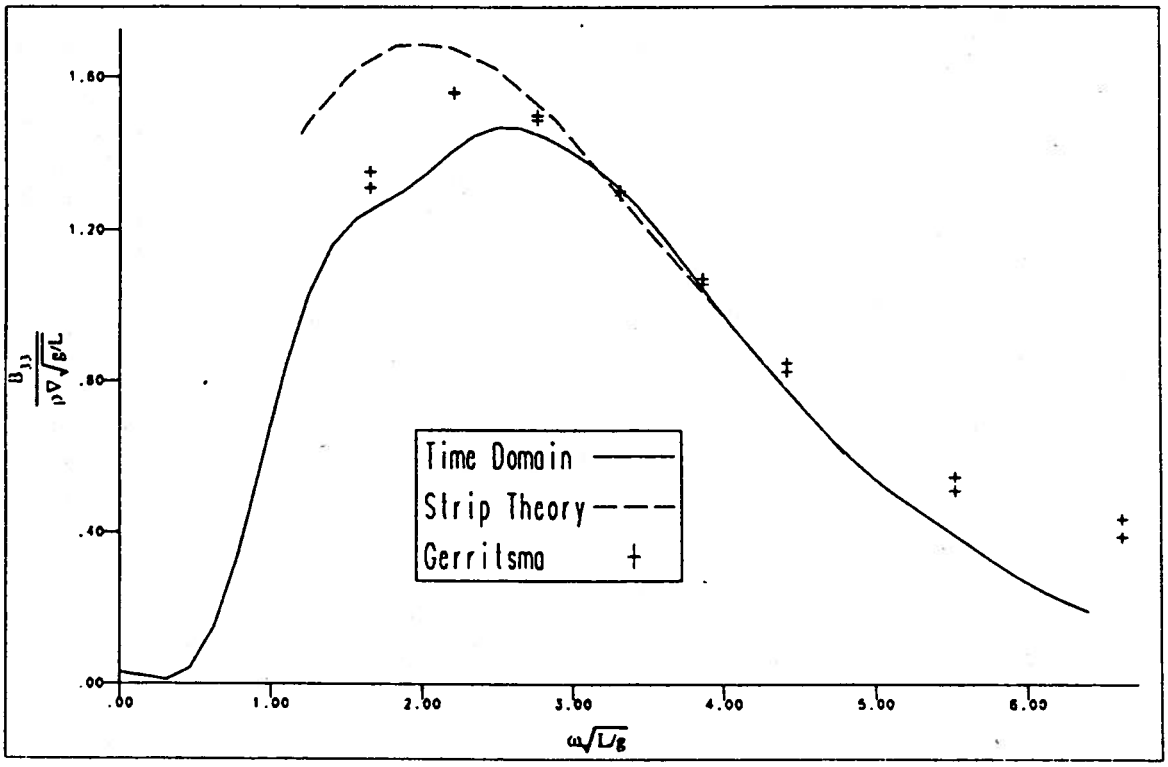

Figure 6.31 — Heave Damping Coefficient for a Wigley Hull (Fn = .2)

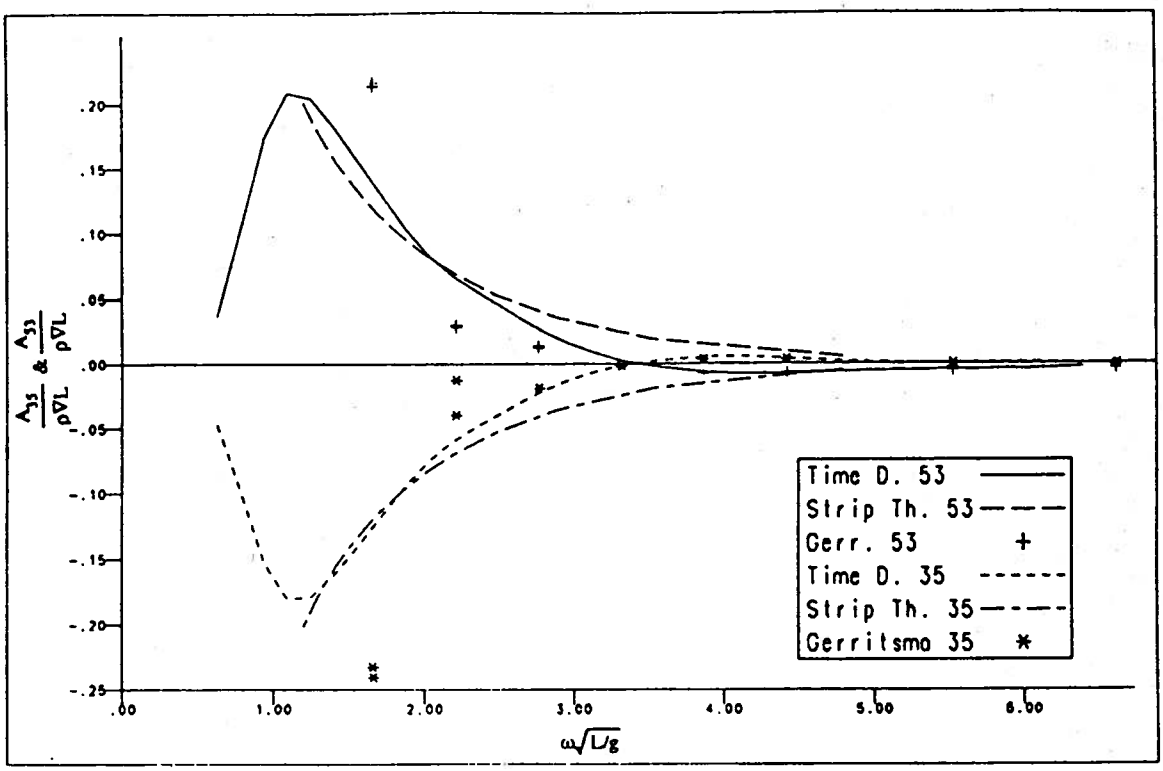

Figure 6.32 — Heave-Pitch Added Mass Cross Coupling Coefficients for a Wigley Hull (Fn = .2)

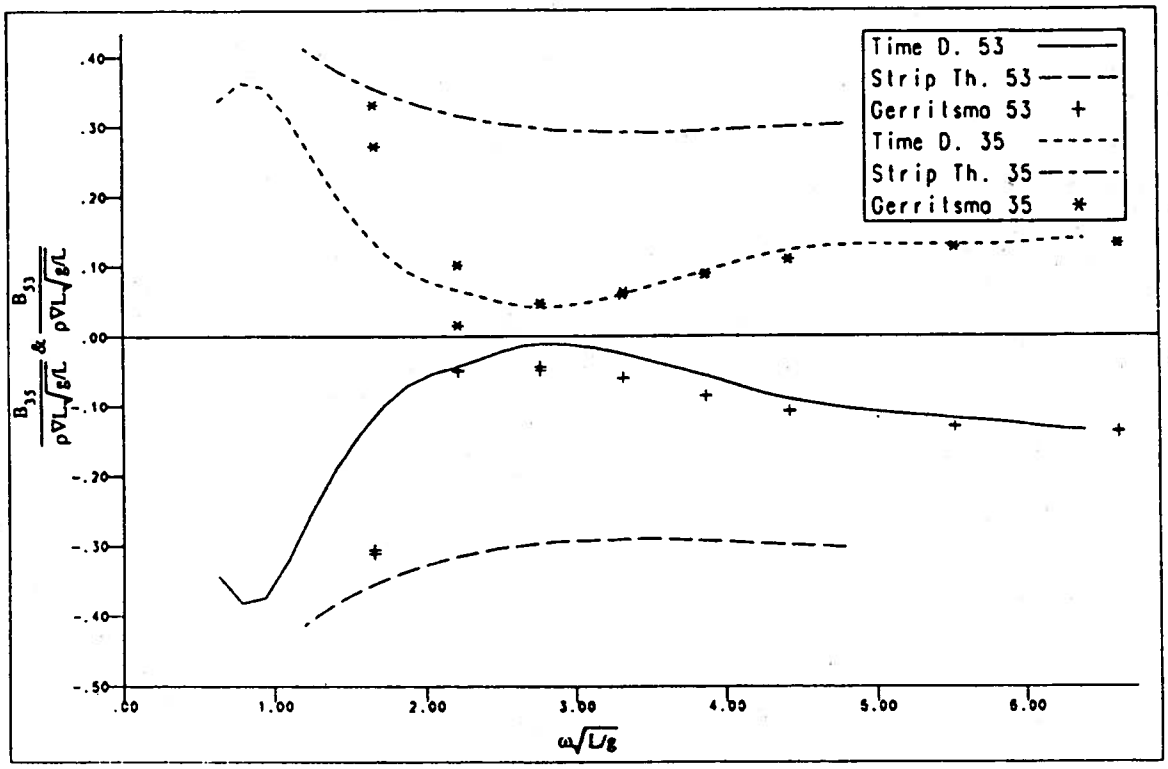

Figure 6.33 — Heave-Pitch Damping Cross Coupling Coefficients for a Wigley Hull (Fn = .2)

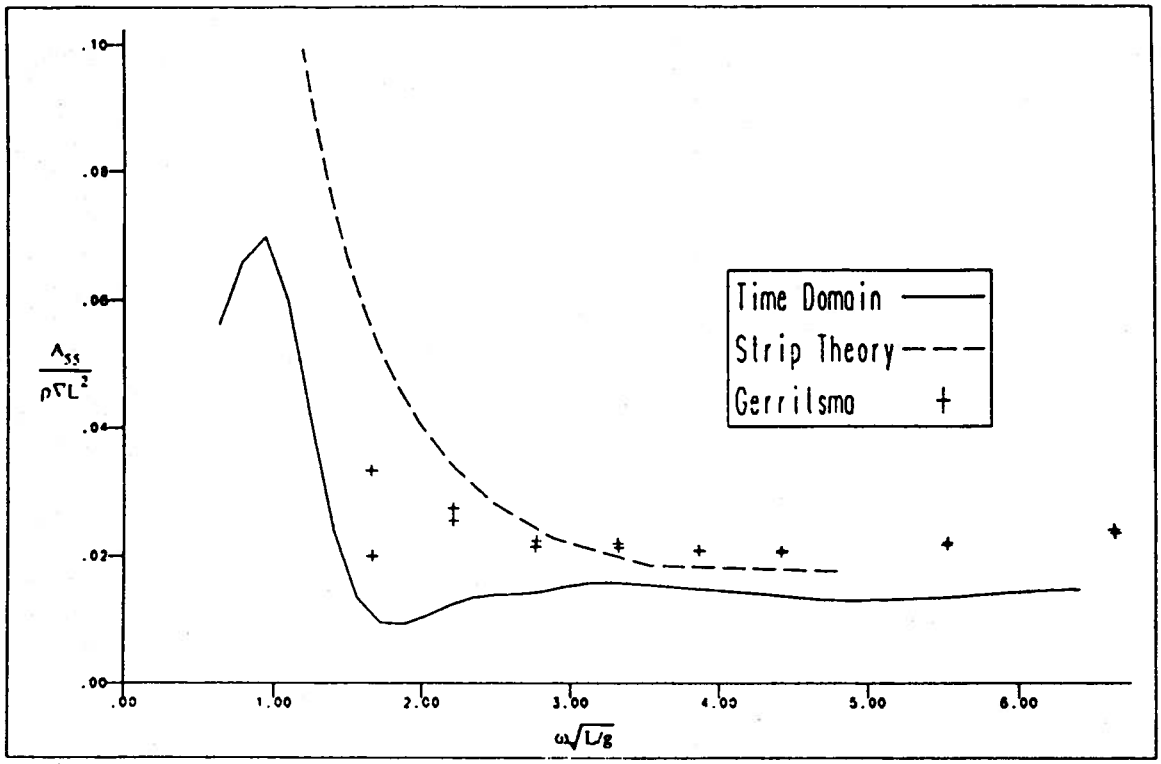

Figure 6.34 — Pitch Added Mass Coefficient for a Wigley Hull (Fn = .2)

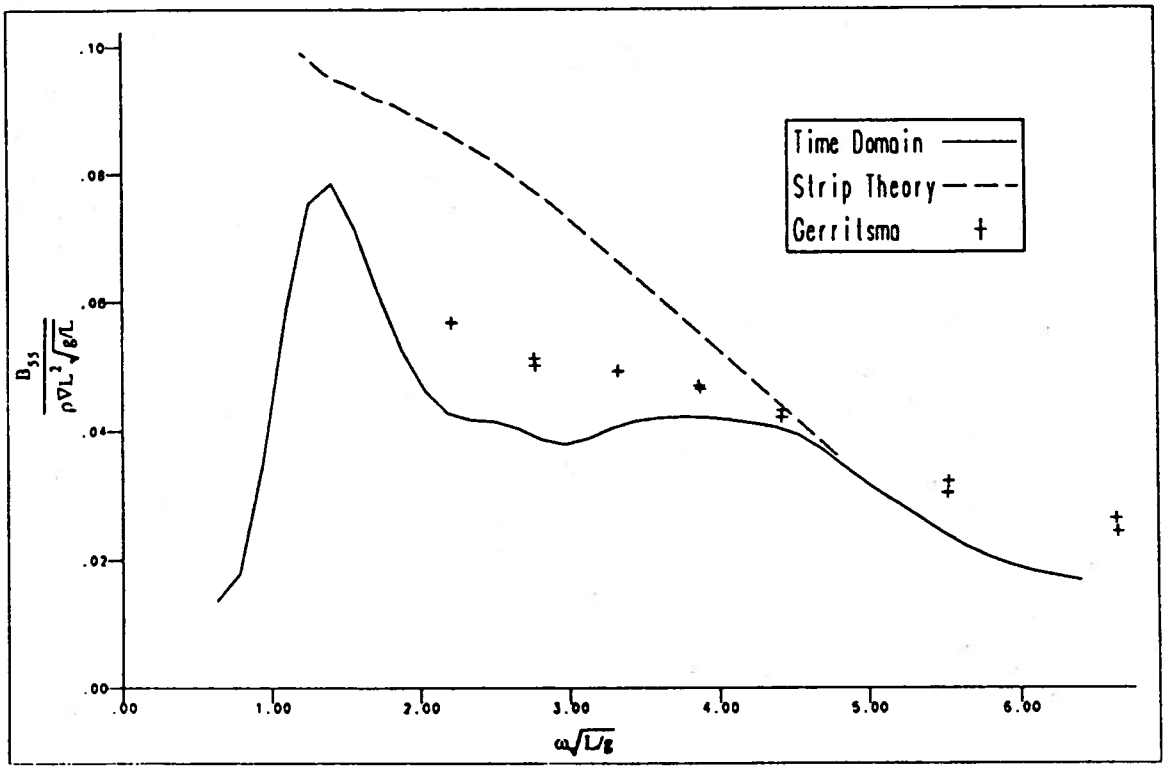

Figure 6.35 — Pitch Damping Coefficient for a Wigley Hull (Fn = .2)

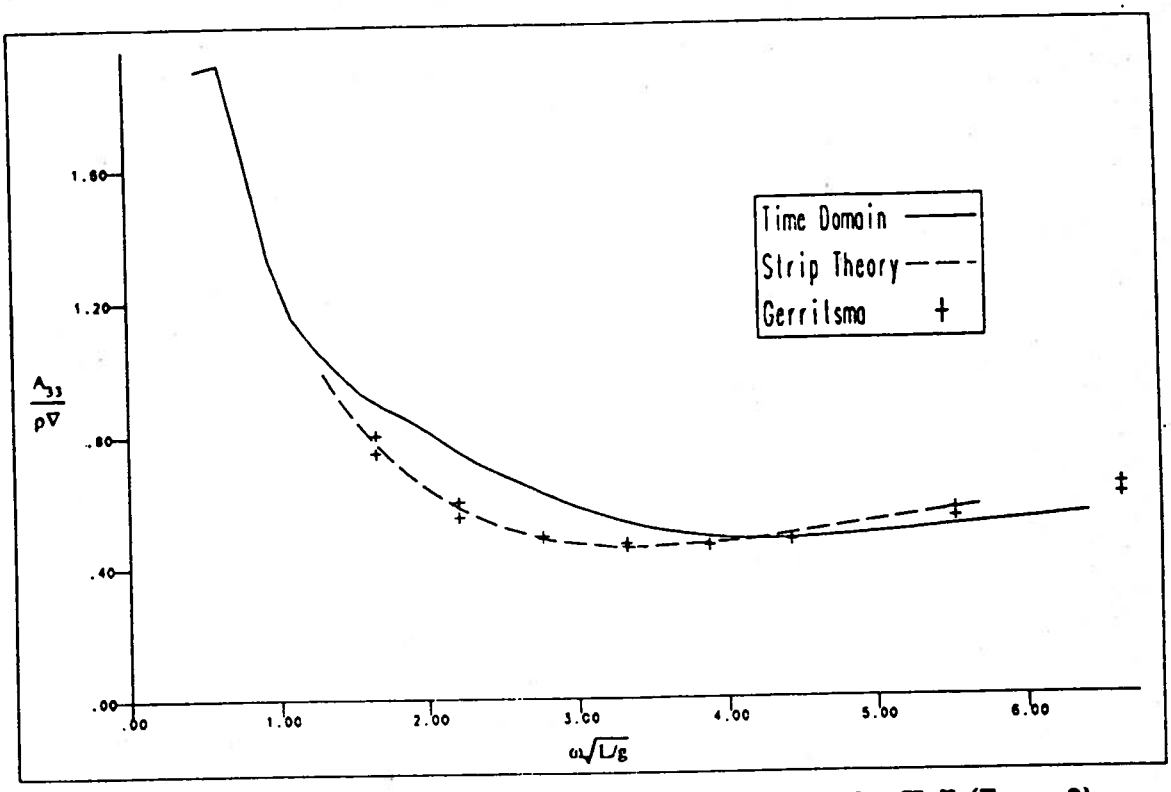

Figure 6.36 — Heave Added Mass Coefficient for a Wigley Hull (Fn = .3)

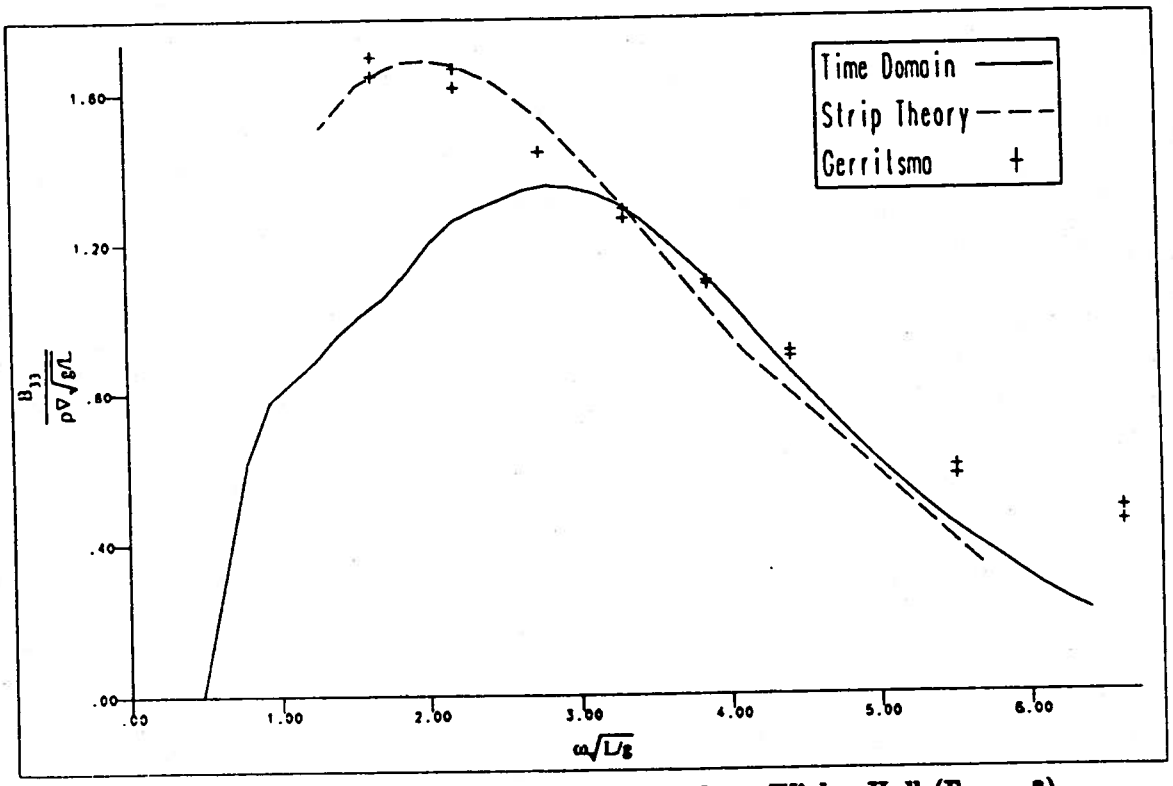

Figure 6.37 — Heave Damping Coefficient for a Wigley Hull (Fn = .3)

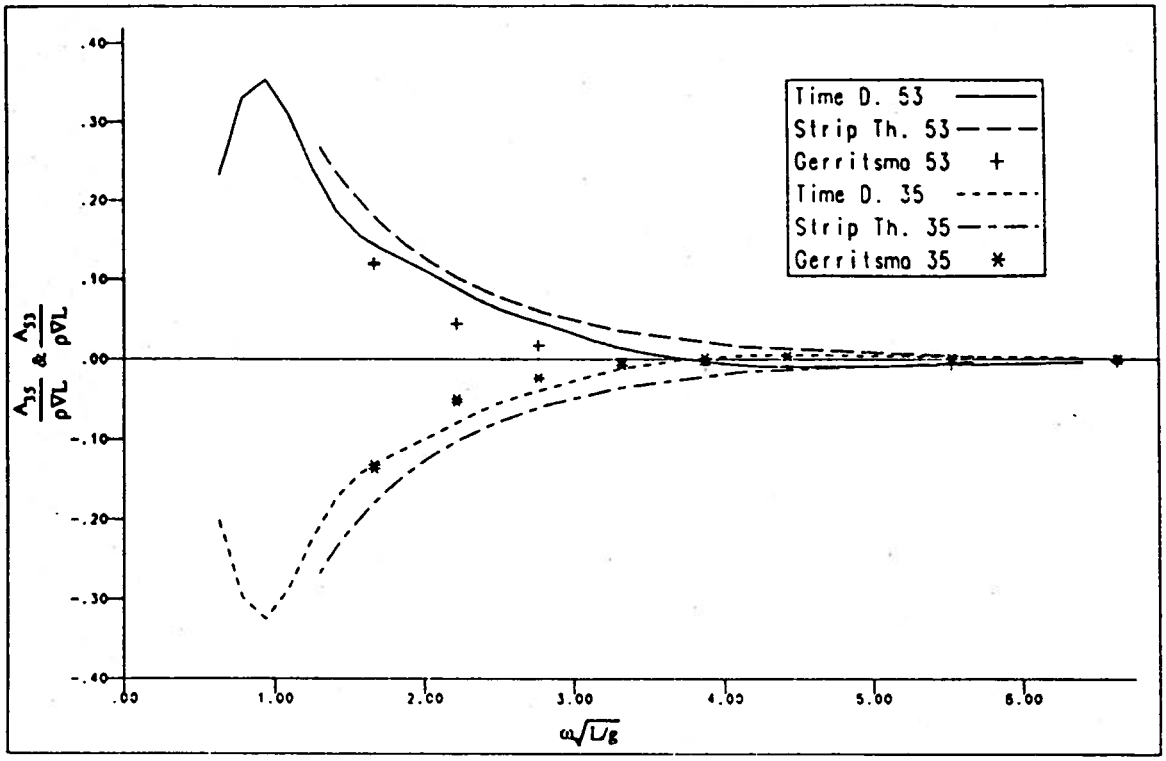

Figure 6.38 — Heave-Pitch Added Mass Cross Coupling Coefficients for a Wigley Hull (Fn = .3)

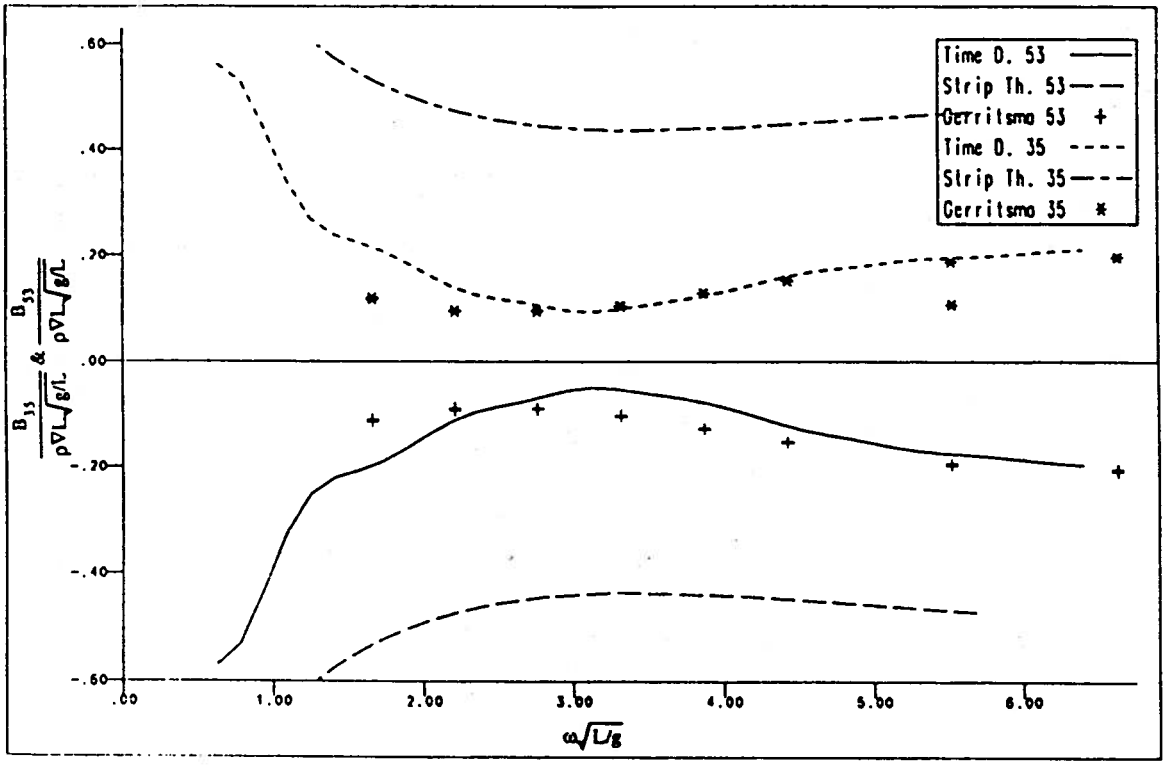

Figure 6.39 — Heave-Pitch Damping Cross Coupling Coefficients for a Wigley Hull (Fn = .3)

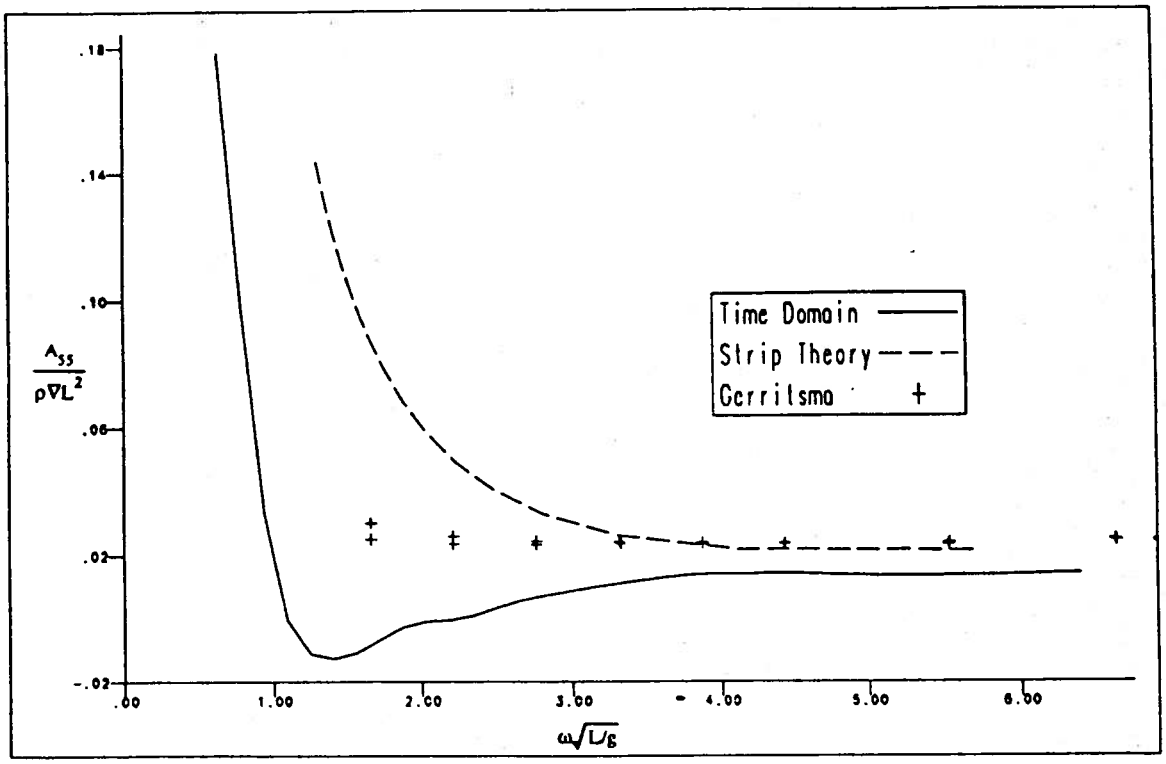

Figure 6.40 — Pitch Added Mass Coefficient for a Wigley Hull (Fn = .3)

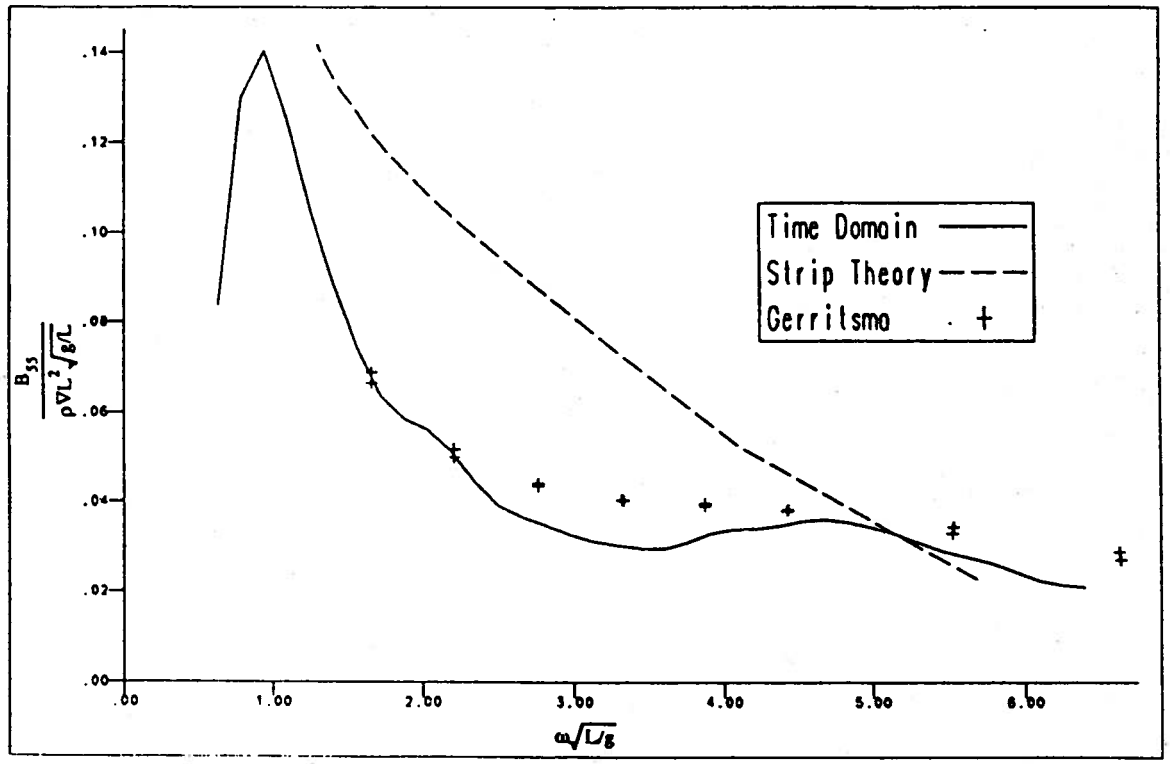

Figure 6.41 — Pitch Damping Coefficient for a Wigley Hull (Fn = .3)

CHAPTER VII

CONCLUSION

The initial objective to solve the problem of the diffraction of waves due to a ship at zero speed and steady forward speed directly in the time domain has been achieved. The results allow the forces due to an arbitrary wave on a ship to be calculated in a deterministic sense. By the use of Fourier transforms, the technique employed here has been shown to be consistent with more traditional frequency-domain methods. It has also been shown that nonimpulsive motions for radiation problems may be employed to determine responses to impulsive motions. Because of this, a consistent method may be used to solve the radiation and diffraction problems for any of the six modes of motion.

While the time-domain approach employed here may be considered more general than the three-dimensional frequency approach, it is important to note that the basic physical assumptions are much the same. The fluid was considered as inviscid and irrotational, and the problem was linearized with respect to the free surface boundary condition, the body boundary conditions, and the pressure evaluations employing Bernoulli's equation.

The work completed here may be considered as a generalization of previous work and includes the computation of the diffracted wave potential at forward speed due to an arbitrary wave. No other work is known that develops a fully three-dimensional solution to the diffraction problem. The results obtained appear reasonable and agree most closely with those of Inglis and Price (1981), who employed the same basic assumptions but in a frequency-domain formulation.

Much of the time gained by the use of the simpler Green's function available in the time-domain approach is lost in the computation of convolution integrals. The convolution integrals as developed here are simply numerous multiplications and additions that should be very amenable to calculation by modern vector and parallel processing computers. The computation of the necessary Green's function remains the greatest difficulty with the frequency-domain approach. On the other hand, the time-domain Green's function is much simpler and could be made less time consuming to compute by more sophisticated methods or polynomial approximations.

An additional advantage of the time-domain approach is the ability to consider unsteady forward speed or a ship maneuver. In these cases, the frequency-domain approach cannot be applied. The time-domain solutions discussed here demonstrate the validity of this approach for an arbitrary motion about the equilibrium position at steady forward speed. The extension to unsteady forward velocity is not unrealistic and was discussed in detail by Liapis (1986).

The theory as developed thus far allows for the determination of all hydrodynamic forces necessary to compute the linear ship motions. The motions may easily be computed by Fourier transform as in Chapter 6 or by direct numerical solution of the differential equations of motion. By that approach it would be possible to include other linear or nonlinear effects into the analysis, such as a nonlinear mooring line force.

An important area needing further research is the asymptotic behavior of the radiation impulse response functions. If valid expressions could be developed for large time in the various modes of motion, numerical computations could be truncated when the asymptotic range was reached, which would save computer time and storage and improve accuracy.

The computational scheme could certainly be improved, and possibly the area worthy of most consideration is that of improving accuracy without decreasing time-step size. One possible solution might be to return to the integration of the Green's function over Δt intervals. This was done analytically by Beck and Liapis (1986) for the zero speed case but could be done numerically for the forward speed case.

A topic needing further research not only in this problem but also many related ones is the evaluation of the line integrals produced by the application of Stokes theorem. The singular line at the intersection of the body and the free surface is not well understood. Common practice has been to evaluate the potential on the free surface as if it were on the body just below the free surface. Because of the proximity to the singular line, this approximation is not expected to produce accurate results. In addition, the physical significance of the line integral contribution is not clear; hence, the effect of neglecting or improperly evaluating the line integrals is not at all obvious.

The inclusion of the actual steady wave due to the translating ship instead of the free stream as was discussed in Chapter 6 is an area needing further research. The difficulty does not really lie in the steady wave being included in the current formulation but in the actual calculation of the steady wave potential and, possibly more important, the velocities due to the wave and wake system combined.

There is value in pursuing linear theories that attempt to reduce further the required assumptions, as was done here. The knowledge gained from doing so includes understanding the effects that a linear theory, no matter how complete, cannot model. The need to understand nonlinear influences, especially those that make significant contributions, is great, and it remains a challenge for further research.

APPENDICES

APPENDIX A

THE EVALUATION OF IMPULSIVE PRESSURE AND VELOCITY FOURIER TRANSFORMS

In Chapters 3 and 4, the pressure and velocity due to impulsive and nearly impulsive waves were derived in terms of certain Fourier transforms. These Fourier transforms will be evaluated here. The integrals have the following forms:

$$\hat{p}(P,t) = \frac{\rho g}{\pi} \operatorname{Re}\left\{ \int_0^\infty d\omega\, e^{k(z-i\varpi)}\, e^{i\omega t} \right\} \tag{A.1}$$

$$\underline{K}(P,t) = \frac{1}{\pi} \operatorname{Re}\left\{ \begin{bmatrix} \hat{\imath}\cos\beta \\ \hat{\jmath}\sin\beta \\ \hat{k}i \end{bmatrix} \int_0^\infty d\omega\omega\, e^{k(z-i\varpi)}\, e^{i\omega t} \right\} \tag{A.2}$$

and, with forward speed,

$$\hat{p}(P,t) = \frac{\rho g}{\pi} \operatorname{Re}\left\{ \int_0^\infty d\omega_e e^{k(z-i\varpi)}\, e^{i\omega_e t} \right\} \tag{A.3}$$

$$\underline{K}(P,t) = \frac{1}{\pi} \operatorname{Re}\left\{ \begin{bmatrix} \hat{\imath}\cos\beta \\ \hat{\jmath}\sin\beta \\ \hat{k}i \end{bmatrix} \int_0^\infty d\omega_e \omega\, e^{k(z-i\varpi)}\, e^{i\omega_e t} \right\}. \tag{A.4}$$

The evaluation of the forward speed integrals (A.3) and (A.4) is more easily performed by a change of variables. Since

$$\omega_e = \omega - kU_0\cos\beta$$

$$d\omega_e = \left(1 - \frac{2\omega}{g} U_0\cos\beta\right) d\omega,$$

substituting gives

$$\hat{p}(P,t) = \frac{\rho g}{\pi} \operatorname{Re}\left\{ \int_0^\infty d\omega \left(1 - \frac{2\omega}{g} U_0\cos\beta\right) e^{k[z-i(\varpi+U_0 t\cos\beta)]}\, e^{i\omega t} \right\} \tag{A.5}$$

$$\underline{K}(P,t) = \frac{1}{\pi} \operatorname{Re}\left\{ \begin{bmatrix} \hat{\imath}\cos\beta \\ \hat{\jmath}\sin\beta \\ \hat{k}i \end{bmatrix} \int_0^\infty d\omega \left(1 - \frac{2\omega}{g} U_0\cos\beta\right) \omega\, e^{k[z-i(\varpi+U_0 t\cos\beta)]}\, e^{i\omega t} \right\}. \tag{A.6}$$

It may be noted that all of the required integrals then have the following form:

$$I_n(\alpha, b) = \int_0^\infty x^n e^{-(\alpha x^2 + 2bx)}\, dx \tag{A.7}$$

where

$$\alpha = -\frac{z}{g} + \frac{i}{g}(\varpi + U_0 t\cos\beta)$$

$$b = -\frac{it}{2}.$$

Abramowitz and Stegun (1964) give the following integral (7.4.32), which may be used to evaluate I_n:

$$\int e^{-(\alpha x^2+2bx+c)}\,dx = \frac{1}{2}\sqrt{\frac{\pi}{\alpha}}e^{\frac{b^2-\alpha c}{\alpha}}\,\mathrm{erf}\left(\sqrt{\alpha}x+\frac{b}{\sqrt{\alpha}}\right) + \text{ constant}$$

with the restriction that $\alpha \neq 0$. Letting $c = 0$ and taking derivatives,

$$\frac{\partial}{\partial b}\int e^{-(\alpha x^2+2bx)}\,dx = -2\int xe^{-(\alpha x^2+2bx)}\,dx$$

$$\int xe^{-(\alpha x^2+2bx)}\,dx = \frac{-b}{2\alpha}\sqrt{\frac{\pi}{\alpha}}e^{b^2/\alpha}\,\mathrm{erf}\left(\sqrt{\alpha}x+\frac{b}{\sqrt{\alpha}}\right) - \frac{1}{2\alpha}e^{b^2/\alpha}e^{-(\alpha x^2+2bx+b^2/\alpha)}$$

$$\frac{\partial}{\partial \alpha}\int e^{-(\alpha x^2+2bx)}\,dx = -\int x^2 e^{-(\alpha x^2+2bx)}\,dx$$

$$\int x^2 e^{-(\alpha x^2+2bx)}\,dx = \frac{1}{4\alpha}\sqrt{\frac{\pi}{\alpha}}e^{b^2/\alpha}\,\mathrm{erf}\left(\sqrt{\alpha}x+\frac{b}{\sqrt{\alpha}}\right) + \frac{b^2}{2\alpha^2}\sqrt{\frac{\pi}{\alpha}}e^{b^2/\alpha}\,\mathrm{erf}\left(\sqrt{\alpha}x+\frac{b}{\sqrt{\alpha}}\right) + \frac{1}{2}\left(\frac{x}{\alpha}-\frac{b}{\alpha^2}\right)e^{b^2/\alpha}e^{-(\alpha x^2+2bx+b^2/\alpha)}.$$

Now the integrals must be evaluated on the interval $[0;\infty]$. Consider the function $\mathrm{erf}(z)$ for large arguments. Abramowitz and Stegun state (7.1.16)

$$\lim_{z\to\infty}\mathrm{erf}(z) = 1 \text{ for } \left|\arg(z)\right| < \frac{\pi}{4}. \tag{A.8}$$

Here $z = \sqrt{\alpha}x + b/\sqrt{\alpha}$. For $x \to \infty$, consider only $\arg\sqrt{\alpha}x$

$$\alpha = \frac{z}{g} - \frac{i}{g}(\varpi + U_0 t\cos\beta).$$

Since $z \leq 0$, α is in the right half of the complex plane so that

$$\lim_{x\to\infty}\arg\sqrt{\alpha}x + \frac{b}{\sqrt{\alpha}} \leq \frac{\pi}{4}.$$

Using the limit (A.8) for $\mathrm{erf}(z)$, the three definite integrals become

$$\int_0^\infty e^{-(\alpha x^2+2bx)}\,dx = \frac{1}{2}\sqrt{\frac{\pi}{\alpha}}e^{b^2/\alpha} - \frac{1}{2}\sqrt{\frac{\pi}{\alpha}}e^{b^2/\alpha}\,\mathrm{erf}\left(\frac{b}{\sqrt{\alpha}}\right)$$

$$\int_0^\infty xe^{-(\alpha x^2+2bx)}\,dx = -\frac{b}{2\alpha}\sqrt{\frac{\pi}{\alpha}}e^{b^2/\alpha} + \frac{b}{2\alpha}\sqrt{\frac{\pi}{\alpha}}e^{b^2/\alpha}\,\mathrm{erf} + \frac{1}{2\alpha} \tag{A.9}$$

$$\int_0^\infty x^2 e^{-(\alpha x^2+2bx)}\,dx = \sqrt{\frac{\pi}{\alpha}}\left(\frac{1}{4\alpha}+\frac{b^2}{2\alpha^2}\right)\left(e^{b^2/\alpha} - e^{\frac{b^2}{\alpha}}\,\mathrm{erf}\left(\frac{b}{\sqrt{\alpha}}\right)\right) - \frac{b}{2\alpha^2}.$$

The three integrals can then be written recursively as

$$I_0 = \frac{1}{2}\sqrt{\frac{\pi}{\alpha}}e^{b^2/\alpha}\operatorname{erfc}\left(\frac{b}{\sqrt{\alpha}}\right)$$

$$I_1 = -\frac{b}{\alpha}I_0 + \frac{1}{2}\alpha$$

$$I_2 = -\frac{b}{\alpha}I_1 + \frac{1}{2}\alpha I_0.$$

The error function may be related to the function $w(z)$ by (7.1.3) of Abramowitz and Stegun,

$$w(z) = e^{-z^2}\operatorname{erfc}(-iz),$$

so that I_0 may be rewritten as

$$I_0(\alpha, b) = \frac{1}{2}\sqrt{\frac{\pi}{\alpha}}w\left(\frac{ib}{\sqrt{\alpha}}\right).$$

Thus, (A.1), (A.2), (A.5), and (A.6) may be rewritten as

$$\hat{p}(P,t) = \frac{\rho g}{\pi}\operatorname{Re}\left\{I_0(\alpha, b) - \frac{2U_0\cos\beta}{g}I_1(\alpha, b)\right\}$$

$$\underline{K}(P,t) = \frac{1}{\pi}\operatorname{Re}\left\{\begin{bmatrix}\hat{\imath}\cos\beta\\ \hat{\jmath}\sin\beta\\ \hat{k}i\end{bmatrix}\left(I_1(\alpha, b) - \frac{2U_0\cos\beta}{g}I_2(\alpha, b)\right)\right\} \qquad U_0 \geq 0$$

where

$$\alpha = -\frac{z}{g} + \frac{i}{g}(\varpi + U_0 t\cos\beta)$$

$$b = -\frac{it}{2}.$$

For the nonimpulsive wave case,

$$\varsigma_0(t) = \sqrt{\frac{\pi}{a}}e^{-at^2}$$

at zero forward speed and

$$\varsigma_0(t) = \frac{1}{\pi}\operatorname{Re}\left\{\int_0^\infty e^{-\omega^2/4a}e^{i\omega_e t}\,d\omega_e\right\}$$

at steady forward speed.

The velocity may be computed easily by the substitution

$$\alpha' = \alpha + \frac{1}{4a}.$$

Then (4.7) and (4.23) become

$$\nabla\phi_0(P,t) = \frac{1}{\pi}\operatorname{Re}\left\{\begin{bmatrix}\hat{\imath}\cos\beta\\ \hat{\jmath}\sin\beta\\ \hat{k}i\end{bmatrix}\left(I_1(\alpha', b) - \frac{2U_0\cos\beta}{g}I_2(\alpha', b)\right)\right\} \qquad U_0 \geq 0.$$

The function $w(z)$ may be calculated numerically in a straightforward manner. The algorithm employed in the numerical analysis was developed by Gautschi (1969).

APPENDIX B

THE NUMERICAL EVALUATION OF $\widetilde{G}$

The oscillatory part of the Green's function $\widetilde{G}(P, Q, t-\tau)$ given by (2.4) is unavailable in closed form and must be calculated numerically. Because its computation represents a significant portion of the computational effort, the approach used here must be considered carefully. The method employed here closely follows that developed by Liapis (1986).

The Green's function as written is a function of the two spatial points P and Q and time $t-\tau$. By appropriate substitutions it may be reduced to a function of two nondimensional parameters for evaluation.

From (2.4) $\widetilde{G}$ is given as

$$\widetilde{G}(P, Q, t-\tau) = 2\int_0^\infty dk\sqrt{kg}\sin\left(\sqrt{kg}(t-\tau)\right)e^{k(z+\varsigma)}J_0(kR).$$

The substitutions

$$\lambda = kr'$$

$$\beta = \sqrt{\frac{g}{r'}}(t-\tau)$$

$$\mu = -\left(\frac{z+\varsigma}{r'}\right) = 1/\sqrt{1+R^2/(z+\varsigma)^2}$$

$$r' = \sqrt{\left(x-\xi+U_0(t-\tau)\right)^2+(y-\eta)^2+(z+\varsigma)^2}$$

yield

$$\widetilde{G} = 2\sqrt{\frac{g}{r'^3}}\int_0^\infty d\lambda\sqrt{\lambda}\sin\left(\beta\sqrt{\lambda}\right)e^{-\lambda\mu}J_0\left(\lambda\sqrt{1-\mu^2}\right).$$

To obtain the derivations of $\widetilde{G}$, the chain rule may be applied to this parametrized form as follows. Let

$$\widetilde{G}(P, Q, t-\tau) = \sqrt{\frac{g}{r'^3}}\widehat{G}(\mu, \beta)$$

so that

$$\widehat{G}(\mu, \beta) = 2\int_0^\infty d\lambda\sqrt{\lambda}\sin\left(\beta\sqrt{\lambda}\right)e^{-\lambda\mu}J_0\left(\lambda\sqrt{1-\mu^2}\right). \qquad (B.1)$$

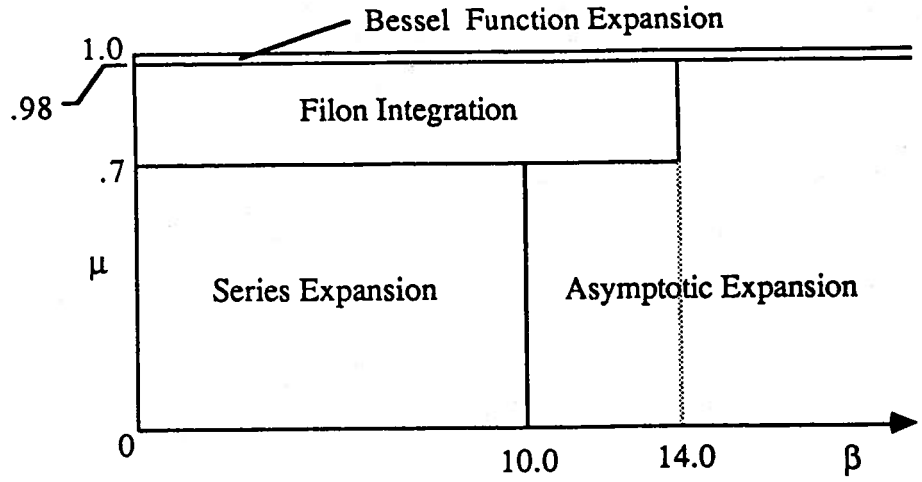

Figure B.1 — Regions for Green's Function Evaluations

The derivatives are

$$\frac{\partial \tilde{G}}{\partial x} = \sqrt{\frac{g}{r'^3}}\left(\frac{\partial \hat{G}}{\partial \mu}\frac{\partial \mu}{\partial x} + \frac{\partial \hat{G}}{\partial \beta}\frac{\partial \beta}{\partial x}\right) + \hat{G}\frac{\partial}{\partial x}\sqrt{\frac{g}{r'^3}}$$

$$\frac{\partial \tilde{G}}{\partial y} = \sqrt{\frac{g}{r'^3}}\left(\frac{\partial \hat{G}}{\partial \mu}\frac{\partial \mu}{\partial y} + \frac{\partial \hat{G}}{\partial \beta}\frac{\partial \beta}{\partial y}\right) + \hat{G}\frac{\partial}{\partial y}\sqrt{\frac{g}{r'^3}}$$

$$\frac{\partial \tilde{G}}{\partial z} = \sqrt{\frac{g}{r'^3}}\left(\frac{\partial \hat{G}}{\partial \mu}\frac{\partial \mu}{\partial z} + \frac{\partial \hat{G}}{\partial \beta}\frac{\partial \beta}{\partial z}\right) + \hat{G}\frac{\partial}{\partial z}\sqrt{\frac{g}{r'^3}}$$

$$\frac{\partial \tilde{G}}{\partial t} = U_0\frac{\partial \tilde{G}}{\partial x} + \frac{g}{r'^2}\frac{\partial \hat{G}}{\partial \beta}.$$

The determination of $\hat{G}(\mu,\beta)$ may be computed by various methods depending on the values of μ and β. Figure B.1 shows the regions for the different evaluations.

Series Expansion

For small β, $\sin\left(\beta\sqrt{\lambda}\right)$ may be expanded in an infinite series and the terms integrated individually to give Legendre polynomials. The result is

$$\hat{G}(\mu,\beta) = 2\beta\left[P_1(\mu) - \frac{2!}{3!}P_2(\mu)\beta^2 + \frac{3!}{5!}P_3(\mu)\beta^4 - \frac{4!}{7!}P_4(\mu)\beta^6 + \ldots\right] \qquad (B.2)$$

and is convergent for β in the range shown, if double precision and a sufficient number of terms are used.

Asymptotic Expansion

For large values of β, an asymptotic form may be employed. The details of the derivation are given in Liapis. The final result is

$$\begin{aligned}\widehat{G}(\mu,\beta) = 2\Bigg[&-\frac{4}{\beta^3} - \frac{48\mu}{\beta^5} - \frac{360}{\beta^7}(3\mu^2-1) + \dots \\ &+ \frac{e^{-\beta^2\mu/4}}{\sqrt{2}}\Bigg(\frac{\beta}{(1-\mu^2)^{1/4}}\sin\Big(\frac{\beta^2\sqrt{1-\mu^2}}{4} + \frac{3\theta}{2}\Big) \\ &+ \frac{1}{2\beta(1-\mu^2)^{3/4}}\cos\Big(\frac{\beta^2\sqrt{1-\mu^2}}{4} - \frac{\theta}{2}\Big) \\ &+ \frac{1}{\beta^3(1-\mu^2)^{3/4}}\sin\Big(\frac{\beta^2\sqrt{1-\mu^2}}{4} - \frac{3\theta}{2}\Big) \\ &- \frac{9}{8\beta^3(1-\mu^2)^{5/4}}\sin\Big(\frac{\beta^2\sqrt{1-\mu^2}}{4} - \frac{5\theta}{2}\Big) \\ &- \frac{9}{\beta^5(1-\mu^2)^{3/4}}\cos\Big(\frac{\beta^2\sqrt{1-\mu^2}}{4} - \frac{7\theta}{2}\Big) \\ &+ \frac{24}{\beta^5(1-\mu^2)^{3/4}}\cos\Big(\frac{\beta^2\sqrt{1-\mu^2}}{4} - \frac{5\theta}{2}\Big)\Bigg)\Bigg] + O(\beta^{-7})\end{aligned}$$

where

$$\theta = \sin^{-1}(\mu).$$

Filon Quadrature

For $\mu > .7$, the exponential factor in $\widehat{G}(\mu,\beta)$ decays rapidly enough that a numerical integration scheme is applicable. $\widehat{G}$ may be rewritten as

$$\begin{aligned}\widehat{G}(\mu,\beta) = 2\int_0^\infty d\lambda \sin(\beta\sqrt{\lambda})e^{-\lambda\mu}\Bigg[&\sqrt{\lambda}J_0(\lambda\sqrt{1-\mu^2}) \\ &- \sqrt{\frac{2}{\pi}}(1-\mu^2)^{-1/4}\cos\Big(\lambda\sqrt{1-\mu^2} - \frac{\pi}{4}\Big)\Bigg] \\ &+ \frac{2\beta}{(1-\mu^2)^{1/4}}e^{-\beta^2\mu/4}\sin\Big(\frac{\beta^2\sqrt{1-\mu^2}}{4} + \frac{3\theta}{2}\Big)\end{aligned}$$

where $\theta = \sin^{-1}(\mu)$. The first term of the asymptotic expansion for J_0 has been added, subtracted, and integrated analytically to improve the accuracy of the integration. The substitutions

$$k^2 = \lambda\sqrt{1-\mu^2}$$

$$\gamma = \frac{\beta}{(1-\mu^2)^{1/4}}$$

give

$$\widehat{G} = \frac{4}{(1-\mu^2)^{3/4}} \int_0^\infty dk\, k \sin(\gamma k) e^{-k^2\mu/\sqrt{1-\mu^2}} \left[kJ_0(k^2) - \sqrt{\frac{2}{\pi}} \cos\left(k^2 - \frac{\pi}{4}\right) \right]$$
$$+ \frac{2\beta}{(1-\mu^2)^{1/4}} e^{-\beta^2\mu/4} \sin\left(\frac{\beta^2\sqrt{1-\mu^2}}{4} + \frac{3\theta}{2} \right).$$

To compute the integral, the factor in brackets is computed in advance at equal intervals and stored as $f(k)$. The integration is performed from 0 to $k = \kappa$ where

$$\kappa f(\kappa) e^{-\kappa^2\mu/\sqrt{1-\mu^2}} < 10^{-7}.$$

By setting the term

$$ke^{-k^2\mu/\sqrt{1-\mu^2}} \left[kJ_0(k^2) - \sqrt{\frac{2}{\pi}} \cos\left(k^2 - \frac{\pi}{4}\right) \right] = ke^{-k^2\mu/\sqrt{1-\mu^2}} f(k) = g(k),$$

the integral may be rewritten as

$$\int_0^\kappa dk g(k) \sin \gamma k.$$

Approximating $g(k)$ by parabolas over the intervals $\Delta k = h$, Abramowitz and Stegun give the Filon integration rule as

$$\int_0^\kappa g(k) \sin \gamma k dk = h[\alpha(\gamma h) S_{2n} + \beta(\gamma h) S_{2n-1}]$$
$$\alpha(\gamma h) = 2\left(\frac{1 + \cos^2 \gamma h}{(\gamma h)^2} - \frac{\sin 2\gamma h}{(\gamma h)^3} \right)$$
$$\beta(\gamma h) = 4\left(\frac{\sin \gamma h}{(\gamma h)^3} - \frac{\cos \gamma h}{(\gamma h)^2} \right),$$

or for small γh

$$\alpha = \frac{2}{3} + \frac{2(\gamma h)^2}{15} - \frac{4(\gamma h)^4}{105} + \frac{2(\gamma h)^6}{367} - \dots$$
$$\beta = \frac{4}{3} - \frac{2(\gamma h)^2}{15} + \frac{(\gamma h)^4}{210} - \frac{(\gamma h)^6}{11,340} + \dots$$
$$S_{2n} = \sum_{i=1}^{n} g(k_{2i}) \sin(\gamma k_{2i})$$
$$S_{2n-1} = \sum_{i=1}^{n} g(k_{2i-1}) \sin(\gamma k_{2i-1})$$

where $k_i = hi$.

The terms due to the endpoints have been left off for the sake of simplicity, since those at the endpoint $k = 0$ are zero and κ is chosen so that no significant contribution is made by that endpoint.

All of these forms are not valid in the region where $\mu \cong 1$. The asymptotic expansion is singular, as well as the recursion relation for the Legendre polynomials $P_n(\mu)$. The filon quadrature is no longer accurate because the exponential decay is too rapid. In this region a different form is needed. In general, expanding the J_0 Bessel function as a power series is unacceptable because the resulting integrals are divergent. However, in the case of μ near 1, a valid expansion may be developed.

Substituting $k^2 = \lambda$ into (B.1) gives

$$\widehat{G}(\mu,\beta) = 4\int_0^\infty dk\, k^2 \sin(\beta k) e^{-k^2/\mu} J_0\left(k^2\sqrt{1-\mu^2}\right). \qquad (B.3)$$

The Bessel function has an accurate polynomial approximation in the range $0 \le x \le 3$, given by Abramowitz and Stegun (9.4.1) as

$$J_0(x) = \sum_{n=0}^{5} a_n \left(\frac{x}{3}\right)^{2n}$$

where

$$a_0 = 1 \qquad a_1 = -2.2499997$$
$$a_2 = 1.2656208 \qquad a_3 = -.3163866$$
$$a_4 = .0444479 \qquad a_5 = .0002100.$$

To employ this, consider the argument of the Bessel function

$$k^2\sqrt{1-\mu^2} \le 3.$$

The integral (B.3) may be rewritten as

$$\widehat{G}(\mu,\beta) = 4\int_0^\kappa dk\, k^2 \sin(\beta k) e^{-k^2\mu} J_0\left(k^2\sqrt{1-\mu^2}\right) + 4\int_\kappa^\infty dk\, k^2 \sin(\beta k) e^{-k^2\mu} J_0\left(k^2\sqrt{1-\mu^2}\right)$$

where the largest possible value for κ, employing the expression above, is

$$\kappa = \sqrt{\frac{3}{\sqrt{1-\mu^2}}}.$$

For $k^2\sqrt{1-\mu^2} \ge 3$,

$$\left| \sin(\beta k) J_0\left(k^2\sqrt{1-\mu^2}\right) \right| \le \frac{1}{2},$$

so that the second integral may be bounded by

$$\left| \int_\kappa^\infty dk\, k^2 \sin(\beta k) e^{-k^2\mu} J_0\left(k^2\sqrt{1-\mu^2}\right) \right| \le \frac{1}{2}\int_\kappa^\infty dk\, k^2 e^{-k^2\mu}.$$

This integral may be bounded by

$$\int_\kappa^\infty dk\, k^2 e^{-k^2\mu} \le \int_\kappa^\infty dk\, k^2 e^{-k\kappa\mu} = e^{-\kappa^2\mu}\left(\frac{\kappa}{\mu} + \frac{2}{\kappa\mu^2} + \frac{2}{(\kappa\mu)^3}\right),$$

so that

$$\left| \int_\kappa^\infty dk\, k^2 \sin(\beta k) e^{-k^2\mu} J_0\left(k^2\sqrt{1-\mu^2}\right) \right| \le \frac{1}{2} e^{-\kappa^2\mu}\left(\frac{\kappa}{\mu} + \frac{2}{\kappa\mu^2} + \frac{2}{(\kappa\mu)^3}\right). \qquad (B.4)$$

The first term is the largest and, assuming μ constant, has a maximum at $\kappa = 1$. For $\mu > .98$ and $\kappa > 3.8827$, the error for truncating the integral (B.3) at κ is given by (B.4) as

$$\frac{\kappa}{2\mu} e^{-\mu\kappa^2} < 8 \times 10^{-7}.$$

Substituting the polynomial approximation for the Bessel function into (B.3) gives

$$\widehat{G}(\mu,\beta) = 4\sum_{n=0}^{5} a_n \left(\frac{\sqrt{1-\mu^2}}{3}\right)^{2n} \int_0^\kappa dk\, k^{2+4n} \sin\beta k e^{-k^2\mu}. \qquad (B.5)$$

The integrals may be evaluated by use of the form given in Appendix A.

Defining the integral I_n as in (A.7) as

$$I_n(\alpha, b) = \int_0^\kappa x^n e^{-(\alpha x^2 + 2bx)}\, dx,$$

a recursive relation may be developed by integration by parts:

$$I_n = \int_0^\kappa x^n e^{-(\alpha x^2+2bx)}\, dx = \frac{\kappa^{n-1}}{-2\alpha} e^{-\kappa^2\mu} e^{-2b\kappa} + \frac{1}{2\alpha}\int_0^\kappa dx\left[(n-1)x^{n-2}e^{-2bx} - 2bx^{n-1}e^{-2bx}\right]e^{-\alpha x^2}$$

$$I_n = \frac{\kappa^{n-1}}{-2\alpha} e^{\kappa^2\mu} e^{-2b\kappa} - \frac{2b}{2\alpha} I_{n-1} + \frac{(n-1)}{2\alpha} I_{n-2}.$$

Letting

$$\alpha = \mu$$

$$2b = -i\beta,$$

$$\int_0^\kappa dk\, k^n \sin\beta k e^{-k^2\mu} = \mathrm{Im}\left\{-\frac{\kappa^{n-1}}{2\mu} e^{-\kappa^2\mu} e^{i\beta\kappa} + \frac{i\beta}{2\mu} I_{n-1} + \frac{(n-1)}{2\mu} I_{n-2}\right\}.$$

It may be noted that the first term when multiplied by the coefficient in front of the integral (B.5) may be ignored, that is,

$$\left(\frac{\sqrt{1-\mu^2}}{3}\right)^{2n} \mathrm{Im}\left\{-\frac{\kappa^{2n+1}}{2\mu} e^{-\kappa^2\mu} e^{i\beta\kappa}\right\}$$

$$= \left(\frac{\sqrt{1-\mu^2}\kappa^2}{3}\right)^{2n} \frac{\kappa}{2\mu} e^{-\kappa^2\mu}\, \mathrm{Im}\left\{e^{i\beta\kappa}\right\}.$$

By the choice of κ, $(\sqrt{1-\mu^2}/3)\kappa^2 = 1$, so that

$$\left| \left(\frac{\sqrt{1-\mu^2}\kappa^2}{3} \right)^{2n} \frac{\kappa}{2\mu} e^{-\kappa^2\mu} \operatorname{Im}\{e^{-\beta\kappa}\} \right| \leq \frac{\kappa}{2\mu} e^{-\kappa^2\mu} < 8 \times 10^{-7}.$$

Thus,

$$\widehat{G}(\mu,\beta) \cong 4 \sum_{n=0}^{5} a_n \left(\frac{\sqrt{1-\mu^2}}{3} \right)^{2n} \operatorname{Im}\{I_{4n+2}\} \tag{B.6}$$

where

$$I_n(\alpha, b) = \frac{i\beta}{2\mu} I_{n-1} + \frac{(n-1)}{2\mu} I_{n-2} \tag{B.7}$$

and $\alpha = \mu$, $b = -i\beta/2$.

The integrals I_0 and I_1 for the limit of integration κ may be shown to be equal to the integral with infinite limit as in Appendix A, within the accuracy of the rest of the expansion. Thus, they may be written as

$$I_0(\alpha, b) = \frac{1}{2}\sqrt{\frac{\pi}{\alpha}} w\left(\frac{ib}{\sqrt{\alpha}} \right)$$

$$I_1(\alpha, b) = \frac{i\beta}{2\mu} I_0(\alpha, b) + \frac{1}{2\mu}.$$

The recursion relation (B.7) breaks down numerically for large β. In that range, an expression may be found using the asymptotic form of the error function. The final result is

$$\widehat{G}(\mu,\beta) = -4 \sum_{i=0}^{2} a_n \left(\frac{\sqrt{1-\mu^2}}{3} \right)^{2n} S_{4n+2}(\mu,\beta)$$

$$\begin{aligned} S_{4n+2}(\mu,\beta) &= \frac{2}{\beta^3} + \frac{12(2\mu)}{\beta^5} + \frac{90(2\mu)^2}{\beta^7} + \frac{840(2\mu)^3}{\beta^7} \\ &\quad + \frac{9,450(2\mu)^4}{\beta^{11}} + \frac{124,740(2\mu)^5}{\beta^{13}} + \ldots \quad n = 0 \\ &= \frac{720}{\beta^7} + \frac{20,160(2\mu)}{\beta^9} + \frac{453,600(2\mu)^2}{\beta^{11}} \\ &\quad + \frac{9,979,200(2\mu)^3}{\beta^{13}} + \frac{2.270268 \times 10^8 (2\mu)^4}{\beta^{15}} \\ &\quad + \frac{5.6942636 \times 10^9 (2\mu)^5}{\beta^{17}} + \ldots \quad n = 1 \\ &= \frac{3,628,800}{\beta^{11}} + \frac{2.395008 \times 10^8 (2\mu)}{\beta^{13}} + \frac{1.0897286 \times 10^{10}(2\mu)^2}{\beta^{15}} + \ldots \quad n = 2. \end{aligned} \tag{B.8}$$

The expression is valid for $\beta > 10$. It may be noted that in the limit as $\mu \to 1$, only the first term in the sum remains in (B.6) and (B.8). Thus, the proper limit is obtained,

which is

$$\lim_{\mu \to 1} \quad \widehat{G}(\mu, \beta) = 4 \int_0^\infty dk\, k^2 e^{-k^2} \sin(\beta k)$$
$$= 4\, \mathrm{Im} \left\{ I_2(\alpha, b) \right\}$$

where

$$\alpha = 1$$

$$b = \frac{-i\beta}{2}.$$

APPENDIX C

LINE AND PANEL INTEGRATIONS

The integral equation solution requires the numerical integration of various functions along lines and over surfaces. The evaluations are performed by mapping the integrations onto standard regions and using a Gaussian quadrature scheme over the standard region.

Line Integrations

The line integration is performed by linear mapping onto the line segment -1 to 1. The typical integral is of the form

$$\oint_a^b d\eta F(\eta, \xi).$$

To perform the integration, let $\eta = (1 - x)a + (1 + x)b$ and $\xi = (d\xi/d\eta)\eta$ where $d\xi/d\eta$ is constant on the interval a to b. Letting $\overline{F}(x) = F\big(\eta(x), \xi(\eta)\big)$,

$$\oint_b^a d\eta F(\eta, \xi) = \frac{b-a}{2} \int_{-1}^{1} dx \overline{F}(x)$$

where $(b - a)/2$ represents the Jacobian of the linear mapping.

A Gaussian quadrature scheme

$$\int_{-1}^{1} dx \overline{F}(x) \cong \sum_{i=1}^{M} w_i \overline{F}(x_i)$$

is employed where

w_i = Gaussian weights

x_i = Gaussian points

M = number of integration points used.

The Gaussian weights and points are taken from Abramowitz and Stegun (1964). Because of the oscillatory nature of the Green's function being integrated, 12 to 16 Gauss points were typically taken along one panel.

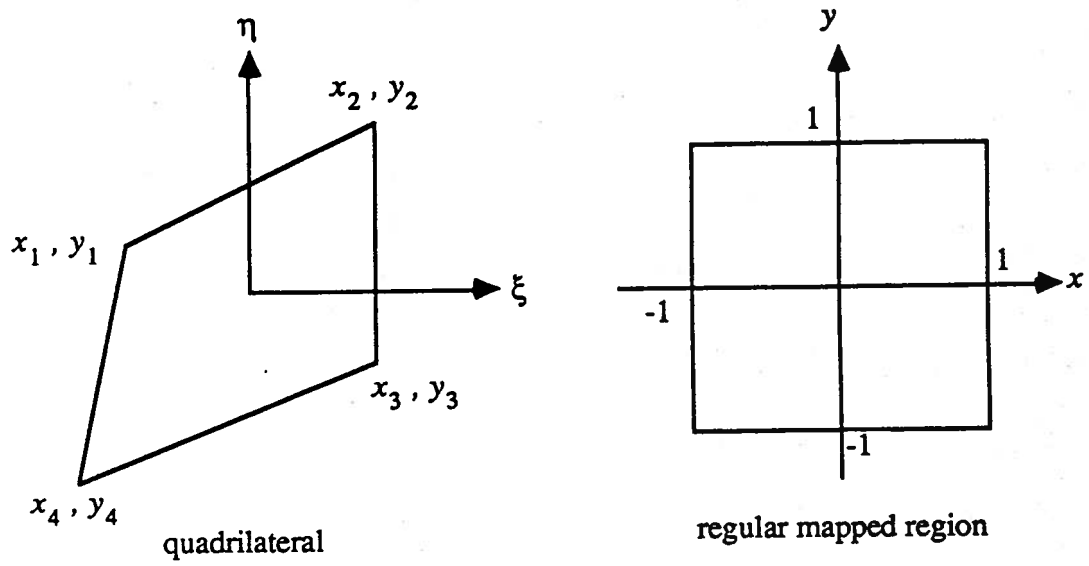

Figure C.1— Panel and Mapped Region Coordinate Systems

Surface Integrations

The integration over a panel is done in a way similar to that along a line and follows the same approach as Liapis. The panel discretization scheme of Hess and Smith, which is employed here, uses plane panels with a local coordinate system as in Figure C.1. The quadrilateral is mapped on a 2×2 square as in the figure. Typical integrals are of the form

$$\iint_{S_{\text{panel}}} dS\, F(\xi, \eta)$$

where ξ, η are mapped onto the square region by

$$\xi = N_1 x_1 + N_2 x_2 + N_3 x_3 + N_4 x_4$$

$$\eta = N_1 y_1 + N_2 y_2 + N_3 y_3 + N_4 y_4$$

$$N_1 = \frac{1}{4}(1 - x)(1 - y)$$

$$N_2 = \frac{1}{4}(1 - x)(1 + y)$$

$$N_3 = \frac{1}{4}(1 + x)(1 + y)$$

$$N_4 = \frac{1}{4}(1 + x)(1 - y).$$

Writing $\overline{F}(x,y) = F\big(\xi(x,y),\eta(x,y)\big)$, the integral over the panel may be written

$$\iint_{S_{\text{panel}}} dS F(\xi,\eta) = \int_{-1}^{1}\int_{-1}^{1} dx dy \overline{F}(x,y)\frac{\partial(\xi,\eta)}{\partial(x,y)}$$

where $\partial(\xi,\eta)/\partial(x,y)$ is the Jacobian of the transformation. Employing a Gaussian integration rule in two directions, the integral may be performed numerically as

$$\int_{-1}^{1}\int_{-1}^{1} dx dy\, \overline{F}(x,y)\frac{\partial(\xi,\eta)}{\partial(x,y)} \cong \sum_{i=1}^{Mx}\sum_{j=1}^{My} w_i\, w_j\, \overline{F}(x_i,y_i)\frac{\partial(\xi,\eta)}{\partial(x,y)}$$

where

w_i are the Gaussian weights

x_i, y_j are the Gaussian points

M_x = number of points in x direction

M_y = number of points in y direction

as in the previous section on line integrations.

It was found that for both line and surface integrals it was better to use fewer integration points with more panels, rather than many integration points on large panels. The reason for this is that greater numbers of panels allow the potential to vary more smoothly over the body surface. For the analysis done here, a 2×2 quadrature was employed.

BIBLIOGRAPHY

BIBLIOGRAPHY

Abramowitz, M., and I. A. Stegun. 1964. *Handbook of mathematical functions.* Washington, DC: National Bureau of Standards.

Adachi, H., and S. Ohmatsu. 1979. On the influence of irregular frequencies in the integral equation solutions of the time-dependent free surface problems. *Journal of Engineering Mathematics* 16(2):97–119.

Adachi, H., and S. Ohmatsu. 1980. On the time dependent potential and its application to wave problems. In *Proceedings of the thirteenth symposium on naval hydrodynamics,* 281–302. Washington, DC: Office of Naval Research.

Beck, R. F., and S. J. Liapis. 1986. Transient motions of floating bodies at zero forward speed. To be published in the *Journal of Ship Research.*

Breslin, J. P., D. Savitsky, and S. Tsakonos. 1964. Deterministic evaluation of motions of marine craft in irregular seas. In *Proceedings of the fifth symposium on naval hydrodynamics,* 461–505. Washington, DC: Office of Naval Research.

Chang, M.-S. 1977. Computation of three-dimensional ship motions with forward speed. In *Proceedings of the second international conference on numerical ship hydrodynamics,* 124–35. Berkeley, CA: University of California.

Cohen, S. B. 1986. A time domain approach to three-dimensional free surface hydrodynamic interactions in narrow basins. Ph.D. Diss., The University of Michigan.

Comstock, J. P., ed. 1967. *Principles of naval architecture.* New York: The Society of Naval Architects and Marine Engineers.

Cummins, W. E. 1962. The impulse response function and ship motions. *Schiffstechnik* 9:101–9.

Davis, M. C., and E. E. Zarnick. 1964. Testing ship models in transient waves. In *Proceedings of the fifth symposium on naval hydrodynamics,* 507–43. Washington, DC: Office of Naval Research.

Faltinsen, O. 1971. Wave forces on a restrained ship in head-sea waves. Ph.D. Diss., The University of Michigan.

Froude, W. 1861. On the rolling of ships. *Transactions of the Institute of Naval Architecture* 2:180–229.

Gautschi, W. 1969. The complex error function. In *Collected algorithms from communications of the association for computing machinery,* 363-P 1-R1.

Haskind, M. D. 1946. The hydrodynamic theory of ship oscillations in rolling and pitching. *Prikl. Mat. Mekh.* 10:33–66. (English translation, Technical research bulletin No. 1-12, 3–43. New York: The Society of Naval Architects and Marine Engineers, 1953.)

Hess, J. L., and A. M. O. Smith. 1964. Calculation of nonlifting potential flow about arbitrary three-dimensional bodies. *Journal of Ship Research* 8(2):22–44.

Inglis, R. B., and W. G. Price. 1981. A three-dimensional ship motion theory—Comparison between theoretical prediction and experimental data of the hydrodynamic coefficients with forward speed. *Transactions of the Royal Institution of Naval Architects* 124:141–57.

Kriloff, A. 1896. A new theory of the pitching motion of ships on waves, and of the stresses produced by this motion. *Transactions of the Institute of Naval Architecture* 37:326–68.

Lamb, H. 1932. *Hydrodynamics.* Cambridge: Cambridge University Press.

Liapis, S. J. 1986. Time-domain analysis of ship motions. Ph.D. Diss., The University of Michigan.

Liapis, S. J., and R. F. Beck. 1985. Seakeeping computations using time-domain analysis. In *Proceedings of the fourth international symposium on numerical hydrodynamics,* 34–54. Washington, DC: National Academy of Sciences.

Maruo, H., and N. Sasaki. 1974. On the wave pressure acting on the surface of an elongated body fixed in head seas. *Journal of the Society of Naval Architecture in Japan* 136:34–42.

Newman, J. N. 1964. A slender-body theory for ship oscillations in waves. *Journal of Fluid Mechanics* 18:602–18.

Newman, J. N. 1965. The exciting forces on a moving body in waves. *Journal of Ship Research* 9:190–99.

Newman, J. N. 1977. *Marine hydrodynamics.* Cambridge, MA: MIT Press.

Newman, J. N. 1985. Transient axisymmetric motion of a floating cylinder. *Journal of Fluid Mechanics* 157:17–33.

Ogilvie, T. F. 1964. Recent progress toward the understanding and prediction of ship motions. In *Proceedings of the fifth symposium on naval hydrodynamics,* 3–128. Washington, DC: Office of Naval Research.

Ogilvie, T. F. 1977. Singular-perturbation problems in ship hydrodynamics. *Advances in Applied Mechanics* 17:91-188.

Ogilvie, T. F., and E. O. Tuck. 1969. A rational strip theory for ship motions, Part 1. The University of Michigan, Department of Naval Architecture and Marine Engineering Report No. 013.

Price, W. G., and R. E. D. Bishop. 1974. *Probabilistic theory of ship dynamics.* London: Chapman and Hall.

Salvesen, N., E. O. Tuck, and O. Faltinsen. 1970. Ship motions and sea loads. *Transactions of the Society of Naval Architects and Marine Engineers* 78:250–87.

Sclavounos, P. D. 1984. The diffraction of free-surface waves by a slender ship. *Journal of Ship Research* 28(1):29–47.

Timman, R., and J. N. Newman. 1962. The coupled damping coefficients of symmetric ships. *Journal of Ship Research* 5(4):34–55.

Troesch, A. W. 1976. The diffraction potential for a slender ship moving through oblique waves. Ph.D. Diss., The University of Michigan.

Vugts, J. H. 1971. The hydrodynamic forces and ship motions in oblique waves. Research Centre TNO for Shipbuilding, Delft, Report No. 150S.

Wehausen, J. V. 1967. Initial value problem for the motion in an undulating sea of a body with fixed equilibrium position. *Journal of Engineering Mathematics* 1:1–19.

Wehausen, J. V., and E. V. Laitone. 1960. Surface waves. In *Handbuch der Physik*, 9:446–778, edited by S. Flugge. Berlin and New York: Springer-Verlag.

Yeung, R. W. 1982. The transient heaving motion of floating cylinders. *Journal of Engineering Mathematics* 16:97–119.